



**SYNTHESIS AND CHARACTERIZATION OF CARBAZOLE
DERIVATIVES FOR ORGANIC LIGHT-EMITTING
DIODE AND INDOLE DERIVATIVES FOR
DYE-SENSITIZED SOLAR CELL**

THITIMA SIRIROEM

**A THESIS SUBMITTED IN PARTIAL FULFILLMENT OF
THE REQUIREMENTS FOR THE DEGREE OF MASTER
OF SCIENCE MAJOR IN CHEMISTRY
FACULTY OF SCIENCE
UBON RATCHATHANI UNIVERSITY
ACADEMIC YEAR 2015
COPYRIGHT OF UBON RATCHATHANI UNIVERSITY**



UBON RATCHATHANI UNIVERSITY
THESIS APPROVAL
MASTER OF SCIENCE
MAJOR IN CHEMISTRY FACULTY OF SCIENCE

**TITLE SYNTHESIS AND CHARACTERIZATION OF CARBAZOLE
DERIVATIVES FOR ORGANIC LIGHT-EMITTING DIODE AND
INDOLE DERIVATIVES FOR DYE-SENSITIZED SOLAR CELL**

AUTHOR MISS THITIMA SIRIROEM

EXAMINATION COMMITTEE

ASST. PROF. DR. JARAY JARATJAROONPHONG	CHAIRPERSON
ASST. PROF. DR. TINNAGON KEAWIN	MEMBER
ASSOC. PROF. DR. SIRIPORN JUNGSUTTIWONG	MEMBER

ADVISOR

Tinnagon Keawin
.....
(ASST. PROF. DR. TINNAGON KEAWIN)

<i>Utith Inprasit</i> (ASSOC. PROF. DR. UTITH INPRASIT) DEAN, FACULTY OF SCIENCE	<i>A. Pongrat</i> (ASSOC. PROF. DR. ARIYAPORN PONGRAT) VICE PRESIDENT FOR ACADEMIC AFFAIRS
---	--

COPYRIGHT OF UBON RATCHATHANI UNIVERSITY
ACADEMIC YEAR 2015

ACKNOWLEDGEMENTS

In this thesis was carried out at Center for Organic Electronics and Alternative Energy (COEA). Firstly I would like to thank Asst. Prof. Dr. Tinnagon Keawin my advisor for excellent suggestion, NMR experiments, supervision and understanding throughout my research work.

I wish to express appreciation and thank to Prof. Dr. Vinich Promarak for allowing me to undertake this project, advice and guiding me in this thesis. I would also like to thank everyone in the electronics group who advice and instrumentation to my project at Ubon Ratchathani University. In particular, I would like to thank Assoc. Prof. Dr. Siriporn Jungsuttiwong for constructive comments and suggestion. Thanks so much to the many people who contributed their time and advice to me for sharing knowledge of chemistry. In particular, Ms. A-monrat Thangthong for synthesis of newly developed organic materials used in this work, Dr. Narid Prachumrak for fabrication of all OLEDs present in my work and guidance on the OLED knowledge and Miss Rattanawalee Rattanawan for molecular orbital calculation.

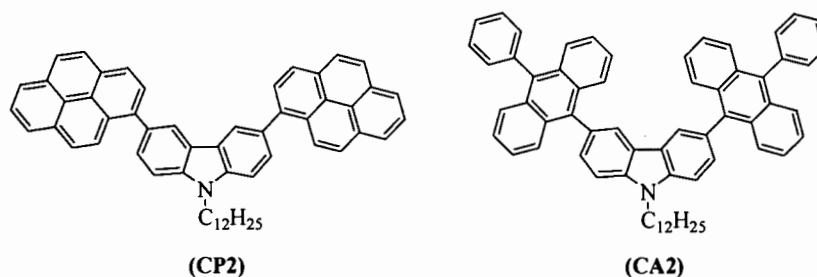
I want to acknowledge the Center of Excellence for Innovation in Chemistry (PERCH-CIC) for providing financial support for this work. I would like to thank Ubon Ratchathani University for instrumentation and place of research. Finally, I am heartfelt thanks to my family for their love, support, and encouragement during my study.

Titima Siriroem
Titima Siriroem
Researcher

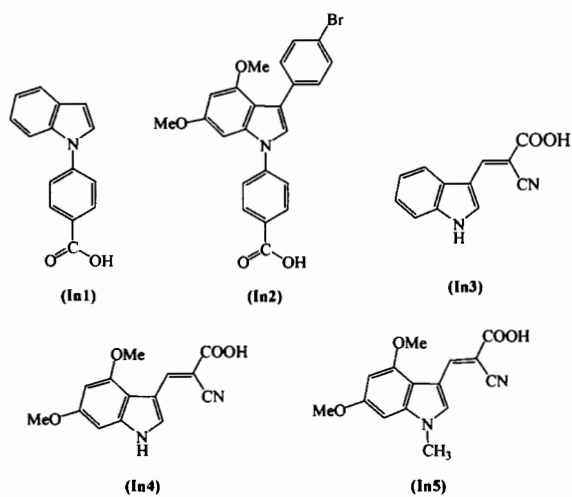
บทคัดย่อ

- เรื่อง : การสังเคราะห์และพิสจูจน์เอกลักษณะอนุพันธ์คาร์บาโซลสำหรับอุปกรณ์ไดโอดเรืองแสง สารอินทรีย์และอนุพันธ์อินโดลสำหรับอุปกรณ์เซลล์แสงอาทิตย์ชนิดสีย้อมไวแสง
- ผู้วิจัย : ธิติมา ศิริเริ่ม
- ชื่อปริญญา : วิทยาศาสตร์มหาบัณฑิต
- สาขาวิชา : เคมี
- อาจารย์ที่ปรึกษา : ผู้ช่วยศาสตราจารย์ ดร. ทินกร แก้วอินทร์
- คำสำคัญ : ไดโอดเรืองแสงอินทรีย์, สารส่งผ่านประจุ, สารเรืองแสง, ปฏิกริยาซุซูกิ, คrossover, อินโดล, เซลล์แสงอาทิตย์ชนิดสีย้อมไวแสง

ในงานวิจัยนี้ได้ทำการสังเคราะห์อนุพันธ์คาร์บาโซลที่มีหมู่ปิดท้ายด้วยโมเลกุลของไพรีน (CP2) และแอนทราซีน (CA2) โดยใช้ปฏิกิริยาโบรมิเนชัน และปฏิกิริยา Suzuki cross-coupling และพิสจูจน์เอกลักษณะด้วยเทคนิค $^1\text{H NMR}$, $^{13}\text{C-NMR}$, FT-IR, UV-Vis, fluorescence และ mass spectroscopy และ cyclic voltammetry โดย 9-dodecyl-3,6-di(pyren-1-yl)carbazole (CP2) และ 9-dodecyl-3,6-di(anthracen-1-yl)carbazole (CA2) ให้สเปกตรัมการคายแสงในช่วงสีน้ำเงินเข้มที่ 430 nm และ 442 nm และมีความเสถียรทางไฟฟ้าที่สูง สารเหล่านี้จึงน่าจะเป็นอีกทางเลือกหนึ่งสำหรับใช้เป็นสารเรืองแสงสีน้ำเงินในไดโอดเรืองแสงอินทรีย์



นอกจากนี้ยังได้ทำการสังเคราะห์อนุพันธ์อินโดลชนิดใหม่ **In1-In5** ที่โมเลกุลประกอบด้วยอนุพันธ์อินโดลเป็นหมู่ให้อิเล็กตรอน พันธะคู่หรือหมู่ฟินิลเป็นสายโซ่เชื่อมต่อและหมู่คาร์บอกซิลเป็นหมู่รับอิเล็กตรอนและยึดจับเพื่อใช้เป็นโมเลกุลสีย้อมไวแสงในเซลล์แสงอาทิตย์ชนิดสีย้อมไวแสง โมเลกุลเป้าหมายสังเคราะห์ได้จากปฏิกิริยา Ullman coupling, ปฏิกิริยาไฮโดรไลซิส, ปฏิกิริยา Knoevenagel condensation และ ปฏิกิริยา Vilsmeier-Haack โดยคาดหวังว่าโมเลกุลเป้าหมาย In1-In5 จะถูกนำไปใช้เป็นสีย้อมในเซลล์แสงอาทิตย์ชนิดสีย้อมไวแสงได้อย่างมีประสิทธิภาพ



สุดท้ายนี้โมเลกุลเป้าหมาย **In1-In5** ถูกพิสูจน์เอกลักษณ์โดยใช้เทคนิค $^1\text{H-NMR}$, $^{13}\text{C-NMR}$, FT-IR และ mass spectroscopy.

ABSTRACT

TITLE : SYNTHESIS AND CHARACTERIZATION OF CARBAZOLE DERIVATIVES FOR ORGANIC LIGHT-EMITTING DIODE AND INDOLE DERIVATIVES FOR DYE-SENSITIZED SOLAR CELL

AUTHOR : THITIMA SIRIROEM

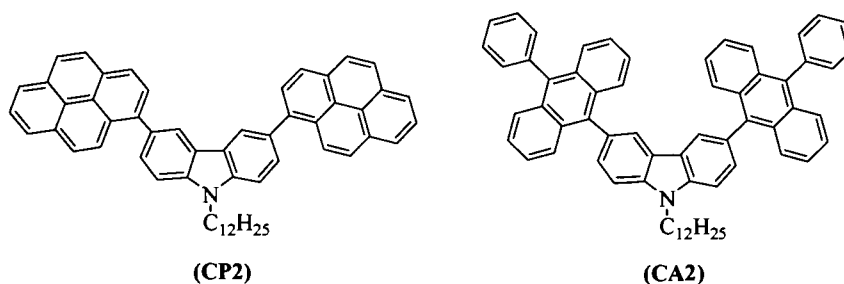
DEGREE : MASTER OF SCIENCE

MAJOR : CHEMISTRY

ADVISOR : ASST.PROF.TINNAGON KEAWIN, Ph.D.

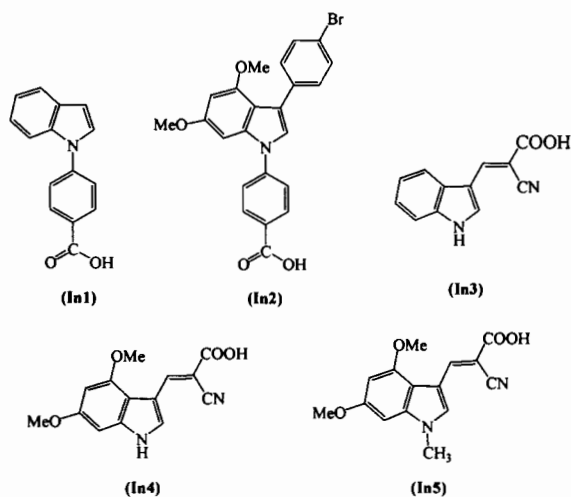
KEYWORDS : CARBAZOLE, ORGANIC LIGHT-EMITTING DIODES, SUZUKI CROSS-COUPPLING REACTION, INDOLE, DYE-SENSITIZED SOLAR CELL

In this research, carbazole derivatives end-capped with pyrene (**CP2**) and anthracene (**CA2**) have been synthesized using bromination and Suzuki cross-coupling reaction and characterized by ^1H NMR, ^{13}C -NMR, FT-IR, UV-Vis, fluorescence and mass spectroscopy and cyclic voltammetry. Compound 9-dodecyl-3,6-di(pyren-1-yl)carbazole (**CP2**) and 9-dodecyl-3,6-di(anthracen-1-yl)carbazole (**CA2**) showed the PL spectra in deep blue region at 430 nm and 442 nm and exhibited high electrochemical stability. These compounds could be alternative materials for using as blue light-emitters in organic light emitting diodes.



Moreover, a new series of indole derivatives **In1-In5**, containing indole derivatives as electron donating, double bond or phenyl group as π -spacer and carboxyl group as electron acceptor and anchor, for using as dye molecules in DSSCs were successfully synthesized. The target molecules were synthesized by using Ullman coupling, hydrolysis reaction, Knoevenagel condensation and Vilsmeier-

Haack reaction. The target compound **In1-In5** could be promising candidates for improvement of the performance dye of the DSSCs.



Finally, target molecules, **In1-In5** were characterized by using ¹H-NMR, ¹³C-NMR, FT-IR and mass spectroscopy.

CONTENTS

	PAGES
ACKNOWLEDGMENTS	I
THAI ABSTRACT	II
ENGLISH ABSTRACT	IV
CONTENTS	VI
LIST OF TABLES	VII
LIST OF FIGURES	VIII
LIST OF ABBREVIATIONS	XIII
CHAPTER 1 SYNTHESIS AND CHARACTERIZATION OF CARBAZOLE DERIVATIVES FOR ORGANIC LIGHT-EMITTING DIODE	
1.1 INTRODUCTION	1
1.2 RESULTS AND DISCUSSION	8
1.3 CONCLUSION	19
1.4 EXPERERIMENTAL	19
CHAPTER 2 SYNTHESIS AND CHARACTERIZATION OF INDOLE DERIVATIVES FOR DYE-SENSITIZED SOLAR CELL	
2.1 INTRODUCTION	24
2.2 RESULTS AND DISCUSSION	33
2.3 CONCLUSION	44
2.4 EXPERERIMENTAL	47
REFERENCES	57
APPENDICES	63
A ¹ H NMR, ¹³ C NMR and UV-Vis absorption spectrum of compounds	64
B Publication	82
VITAE	90

CONTENTS

	PAGES
ACKNOWLEDGMENTS	I
THAI ABSTRACT	II
ENGLISH ABSTRACT	IV
CONTENTS	VI
LIST OF TABLES	VII
LIST OF FIGURES	VIII
LIST OF ABBREVIATIONS	XIII
CHAPTER 1 SYNTHESIS AND CHARACTERIZATION OF CARBAZOLE DERIVATIVES FOR ORGANIC LIGHT-EMITTING DIODE	
1.1 INTRODUCTION	1
1.2 RESULTS AND DISCUSSION	8
1.3 CONCLUSION	19
1.4 EXPERERIMENTAL	19
CHAPTER 2 SYNTHESIS AND CHARACTERIZATION OF INDOLE DERIVATIVES FOR DYE-SENSITIZED SOLAR CELL	
2.1 INTRODUCTION	24
2.2 RESULTS AND DISCUSSION	33
2.3 CONCLUSION	44
2.4 EXPERERIMENTAL	47
REFERENCES	57
APPENDICES	63
A ¹ H NMR, ¹³ C NMR and UV-Vis absorption spectrum of compounds	64
B Publication	82
VITAE	90

LIST OF TABLES

TABLE		PAGES
1.1	Physical data of CP2 and CA2	15
1.2	Physical data of CP2 and CA2	18

LIST OF FIGURES (CONTINUED)

FIGURE		PAGES
1.1	Organic light emitting diodes (OLEDs) display applications	2
1.2	Organic light emitting diodes (OLEDs) structure	2
1.3	Working principle of OLEDs	3
1.4	Chemical structure of TCF	4
1.5	Structure of benzo[b]thien-2-yl derivatives	5
1.6	Structure of bis-(4-benzenesulfonyl-phenyl)-9-phenyl-9H-carbazoles	6
1.7	Structure of DPACz1, DPACz2 and DPACz3	6
1.8	Structure of DETPCZ and DECZDEP	7
1.9	The target molecules CP2 and CA2	8
1.10	Structure of CP2 and CA2	9
1.11	Retrosynthesis of carbazole CP2 and CA2	9
1.12	Synthesis of 9-dodecylcarbazole 2	10
1.13	Mechanisms of alkylation reaction of carbazole	10
1.14	Bromination of 9-dodecylcarbazole 2	11
1.15	Mechanisms of bromination of 9-dodecylcarbazole	11
1.16	Synthetic of target molecules CP2	12
1.17	The proposed mechanism of Suzuki coupling reaction	13
1.18	Synthetic of target molecules CA2	13
1.19	Normalized absorption spectra (left) and normalized emission spectra (right) in CH ₂ Cl ₂ of CP2 and CA2	15
1.20	Cyclic voltammograms of CP2 (left) and CA2 (right) in dry CH ₂ Cl ₂ with scan rate of 0.05 V/s and 0.1 M n-Bu ₄ NPF ₆ as electrolyte, muti scan.	16
1.21	Oxidation process of pyrene	17
1.22	The HOMO (bottom) and LUMO (top) orbitals of CP2 and CA2 calculated by DFT/B3LYP/6-31G(d,p) method	18

LIST OF FIGURES (CONTINUED)

FIGURE		PAGES
2.1	Dye-sensitized solar cells structure (DSSCs) structure	25
2.2	Working principle of DSSCs	26
2.3	Chemical structures of JK-24, JK-25 and JK-28 dyes	27
2.4	Chemical structures of 1P-PSP and 1N-PSP dyes	27
2.5	Chemical structures of CBZ, WD-5, and DTA dyes	28
2.6	Dye-organic synthesis included of benzo[<i>cd</i>]indole group	28
2.7	The structure of dyed molecules included of carbazole (MK75, MK79, MK80), indole (MK81-83) and indoline (MK84-86)	29
2.8	The structure of ID1-ID3 dye-sensitized molecules	30
2.9	Dye-organic synthesis	30
2.10	The synthesis of organic dyeing included of thiophene and <i>N</i> -methyl pyrrole as the connectors	31
2.11	structure of SD1 and SD2	32
2.12	structure of D1, D2 and D3	32
2.13	The target molecules In1-In5	33
2.14	Structure of In1-In5	34
2.15	Retrosynthesis of carbazole In1-In5	35
2.16	Synthesis of methyl 4-(indol-1-yl) benzoate 4	35
2.17	The proposed mechanism of Ullmann coupling reaction	36
2.18	Hydrolysis reaction of methyl 4-(indol-1-yl)benzoate 4	37
2.19	The proposed mechanism of hydrolysis reaction	37
2.20	Synthesis of methyl 4-(3-(4-bromophenyl)-4,6-dimethoxyindol-1-yl) benzoate 6	38
2.21	Hydrolysis reaction of methyl 4-(3-(4-bromophenyl)-4,6-dimethoxy indol-1-yl)benzoate 6	39
2.22	Knoevenagel reaction of indole-3-carbaldehyde 7	40

LIST OF FIGURES (CONTINUED)

FIGURE		PAGES
2.23	The proposed mechanism of Knoevenagal reaction	40
2.24	Vilsmeier–Haack reaction of 4,6-dimethoxyindole 8	41
2.25	The proposed mechanism of Vilsmeier–Haack reaction	42
2.26	Knoevenagal reaction of 3-formyl -4,6-dimethoxyindole 9	42
2.27	Methylation of 3-formyl -4,6-dimethoxyindole 9	43
2.28	Knoevenagal reaction of 3-formyl-4,6-dimethoxy- <i>N</i> -methylindol 10	44

LIST OF FIGURES (CONTINUED)

FIGURE		PAGES
A.1	The ^1H NMR (in CDCl_3) spectrum of 9-dodecylcarbazole 2	65
A.2	The ^{13}C NMR spectra of 9-dodecylcarbazole 2	65
A.3	The ^1H NMR (in CDCl_3) spectrum of 3,6-Dibromo-9-dodecylcarbazole	66
A.4	The ^{13}C NMR spectra of 3,6-Dibromo-9-dodecylcarbazole	66
A.5	The ^1H NMR (in CDCl_3) spectrum of CP2	67
A.6	The ^{13}C NMR spectra of CP2	67
A.7	The ^1H NMR (in CDCl_3) spectrum of CA2	68
A.8	The ^{13}C NMR spectra of CA2	68
A.9	The ^1H NMR (in CDCl_3) spectrum of methyl 4-(indol-1-yl)benzoate 4	69
A.10	The ^{13}C NMR spectra of methyl 4-(indol-1-yl)benzoate 4	69
A.11	The ^1H NMR (in CDCl_3) spectrum of methyl 4-(3-(4-bromophenyl)-4,6-dimethoxyindol-1-yl)benzoate 6	70
A.12	The ^{13}C NMR spectra of methyl 4-(3-(4-bromophenyl)-4,6-dimethoxyindol-1-yl)benzoate 6	70
A.13	The ^1H NMR (in CDCl_3) spectrum of In1	71
A.14	The ^{13}C NMR spectra of In1	71
A.15	The ^1H NMR (in CDCl_3) spectrum of In2	72
A.16	The ^{13}C NMR spectra of In2	72
A.17	The ^1H NMR (in CDCl_3) spectrum of In3	73
A.18	The ^{13}C NMR spectra of In3	73
A.19	The ^1H NMR (in CDCl_3) spectrum of 3-formyl-4,6-dimethoxyindole 9	74

LIST OF FIGURES (CONTINUED)

FIGURE		PAGES
A.20	The ^{13}C NMR spectra of 3-formyl -4,6-dimethoxyindole 9	74
A.21	The ^1H NMR (in CDCl_3) spectrum of In4	75
A.22	The ^{13}C NMR spectra of In4	75
A.23	The ^1H NMR (in CDCl_3) spectrum of 3-formyl-4,6-dimethoxy- <i>N</i> -methylindol 10	76
A.24	The ^{13}C NMR spectra of 3-formyl-4,6-dimethoxy- <i>N</i> -methylindol 10	76
A.25	The ^1H NMR (in CDCl_3) spectrum of In5	77
A.26	The ^{13}C NMR spectra of In5	77
A.27	UV-Vis absorption spectra of In1-In5 in DCM at 5×10^{-6} M.	78
A.28	UV-Vis absorption spectra of In1 in DCM at 5×10^{-6} M	78
A.29	UV-Vis absorption spectra of In2 in DCM at 5×10^{-6} M.	79
A.30	UV-Vis absorption spectra of In3 in DCM at 1×10^{-5} M.	79
A.31	UV-Vis absorption spectra of In4 in DCM at 5×10^{-6} M.	80
A.32	UV-Vis absorption spectra of In5 in DCM at 5×10^{-6} M	80

LIST OF ABBREVIATIONS

ABBREVIATION	FULL WORD
OLED	Organic light-emitting diode
LCD	Liquid crystal display
ITO	Indium tin oxide
HIL	Hole-injection layer
HIM	Hole-injection material
HTL	Hole-transporting layer
HTM	Hole-transporting material
EML	Emissive layer or emitting layer
ETL	Electron-transporting layer
ETM	Electron-transporting material
HOMO	Highest occupied molecular orbital
LUMO	Lowest unoccupied molecular orbital
EL	Electroluminescence
PL	Photoluminescence
TLC	Thin-layer chromatography
NMR	Nuclear magnetic resonance
¹ H-NMR	Proton nuclear magnetic resonance
¹³ C-NMR	Carbon nuclear magnetic resonance
FT-IR	Fourier transform Infrared
UV	Ultra-violet
CV	Cyclic voltammetry
DSC	Differential scanning calorimetry
δ	Chemical shift in ppm relative to tetramethylsilane
s	Singlet
d	Doublet
dd	Doublet of doublets

LIST OF ABBREVIATIONS (CONTINUED)

ABBREVIATION	FULL WORD
t	Triplet
ϵ	Molar absorption coefficient
eV	Electron volt
h	Hour/hours
rt	Room temperature
J	Coupling constant
MHz	Megahertz
V	Voltage
M	Molar concentration
μA	Microamperes
μm	Micrometer
nm	Nanometers
mmol	Milimoles
mol	Moles
ppm	Part per million
min	minutes
Ω	Ohm
DCM	Dichloromethane
THF	Tetrahydrofuran
$n\text{-Bu}_4\text{NPF}_6$	Tetrabutylammonium hexafluorophosphate
DFT	Density functional theory
ΔE_h	Hole energy barriers
ΔE_e	Electron energy barriers
EA	Electron affinity
E_g	Energy gap
E_{onset}	Energy onset

LIST OF ABBREVIATIONS (CONTINUED)

ABBREVIATION	FULL WORD
Φ_F	Fluorescent quantum yield
λ	Wavelength
λ_{abs}	Wavelength absorption
λ_{em}	Wavelength emission
λ_{max}	Wavelength maximum
λ_{onset}	Wavelength onset
λ_{el}	Wavelength electroluminescent
T_g	Glass transition temperature
T_c	Crystallization temperature
T_d	Decomposition temperature
T_m	Melting temperature

CHAPTER 1

SYNTHESIS AND CHARACTERIZATION OF CARBAZOLE DERIVATIVES FOR ORGANIC LIGHT-EMITTING DIODE

1.1 INTRODUCTION

1.1.1 Organic light emitting diodes (OLEDs)

In the former time, many exhibited technologies, for example, cathode ray tube (CRT), liquid crystal displays (LCDs), light emitting diodes (LEDs) were inducing to show in the market. However, there are lots of limitations of the displays such as bulkiness, low viewing angle, color purity, etc [1]. Furthermore, the current demand generation displays are the brightness reproduction, pure color, high resolution, light weight, thin screen, and decreasing of cost and low power consumption, which was set in these OLED devices.

Organic light-emitting diodes (OLEDs) are relatively technology for light sources in which the emissive electroluminescent layer is a film of organic compound that emits light in response to an electric current [2]. First proposed by Ching W. Tang in 1987 [3], OLEDs have attracted significant attention from the scientific community due to their optical potential properties for future flat-panel displays and lighting applications [2]. OLEDs have high potential electronic and optical properties, for example, low voltage driving, high brightness, ability of multicolor emission selected by emitting materials, easy large-area fabrication, and thin-film devices which they have no added backlight required for brightness of the screen [4]. According to the varieties of report on improving OLEDs properties, there are witness that is significant advancement related to brightness, multi- or full-color emission, and OLEDs endurance and thermal stability.

In addition, organic light emitting diodes are more attended recently because they have a wide range of display applications. The application of OLED technology is thin solid films of organic molecules that use electricity to generate light. There are various devices found consist of mobile phones, computer monitors, car radios, digital cameras and large TV screen, and etc [5]. The movable applications

help OLEDs high light output to read easily in sunlight, and it helps create brighter, especially wavy images in the devices. OLEDs using accompany with various prominent advantage included lower and better power used since it lacks of backlight effects and a faster reaction in view of its high speed. Also, the diodes are really lightweight and flexible. The OLEDs is the basis technology in the present time, but it tends to be the most needed in the future because of effective devices.



Figure 1.1 Organic light emitting diodes (OLEDs) display applications [6]

1.1.2 Organic light emitting diodes structure

The OLEDs structure consist of four part including substrate, anode, organic layers and cathode [7] as shown in **Figure 1.2**.

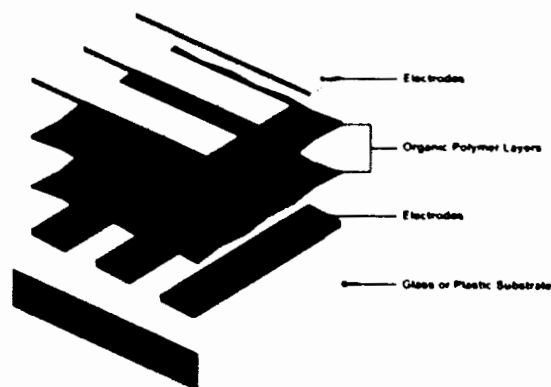


Figure 1.2 Organic light emitting diodes (OLEDs) structure [8]

1.1.2.1 Substrate layer–It supports OLED and is made up of transparent plastic or glass film.

1.1.2.2 Anode layer–It is a transparent layer that removes electrons. Indium tin oxide is commonly used as the anode material.

1.1.2.3 Organic layer–Layer formed of organic molecules or polymers

1) Conductive layer–Transports holes from anode made up of organic plastic. Polymer light-emitting diodes: PLED, also light-emitting polymers: LEP, are used in electroluminescent conductive polymer. Typical polymers used in PLED displays include derivatives of poly (*p*-phenylene vinylene) and polyfluorene.

2) Emissive layer–Transports electrons from the cathode layer. It is made up of organic plastic.

1.1.2.4 Cathode layer–Injects electrons. It may be transparent or not. Metals such as aluminium and calcium are often used in the cathode

1.1.3 Working principle of organic light emitting diodes

The working principle of OLEDs was shown in **Figure 1.3**. When electrical current is applied to the electrodes anode and cathode the charges and electron start moving in the device under the influence of the electric field. Electrons leave the cathode, giving electrons to emissive layer and electrons remove form conducting layer to anode, giving holes (h^+) at conducting layer. The holes jump to the emissive layer and recombine with the electrons. The recombination of this charges leads to the creation of a photon with a frequency given by the energy gap ($E = h\nu$) between the LUMO and HOMO levels of the emitting molecules. Therefore, the electrical power applied to the electrodes is transformed into light [2].

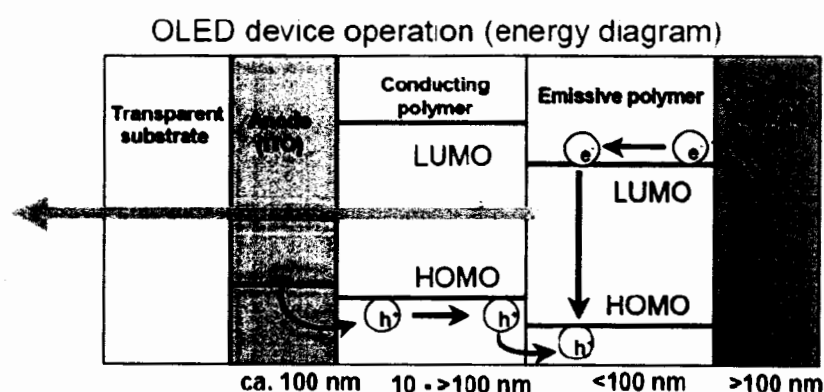


Figure 1.3 Working principle of OLEDs [9]

1.1.4 Literature reviews of OLEDs

In this part, the publications of synthesis and study optical properties of organic light emitting diodes would be described. For example:

In 2012, a highly fluorescent bis (4-diphenylaminophenyl) carbazole end-capped fluorine, TCF, was synthesized and characterized by D. Meunmart and co-workers. This material showed greater ability as a solution processed blue emitter and hole-transporter for OLEDs than commonly used NPB. High-efficiency deep-blue and Alq3-based green devices with luminance efficiencies and CIE coordinates of 0.93 cd/A, (0.16, 0.09), and 3.78 cd/A and (0.29, 0.45) were achieved, respectively. The use of the triphenylamine-carbazole substituent might be an effective method to prepare amorphous molecules with excellent electrochemical, thermal, and morphological stabilities for OLEDs by forming dendritic structures with other fluorescent or non-fluorescent core units [10].

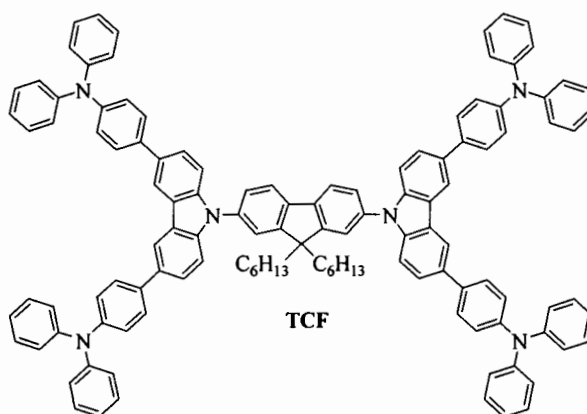


Figure 1.4 Chemical structure of TCF

In 2012, Sukrawee Pansay et al. [11] designed and synthesized four benzo[b]thien-2-yl derivatives **4a-4d** (Figure 1.5). The properties of **4a-4d** as a blue emissive layer (EML) in OLED were investigated. Under an applied voltage, the devices (**4b-d**) emitted a bright deep-blue light with maximum peaks (λ_{EL}) centered at 416, 428, and 436 nm, respectively. The electroluminescence (EL) spectra of all diodes matched their corresponding PL spectra indicating that the EL emission originates from the singlet-excited states of the EML materials. However, **4a** did not show any EL property in the device. This may be due to its very small, planar structure

leading to fluorescence quenching in the solid state. Carbazole **4d** bearing four benzo[b]thiophene substituents had the best EML properties among these four materials. The **4d**-based device exhibited a high maximum brightness of 582 cd m⁻² for blue OLED at 8.6 V, a turn-on voltage of 4.1 V.

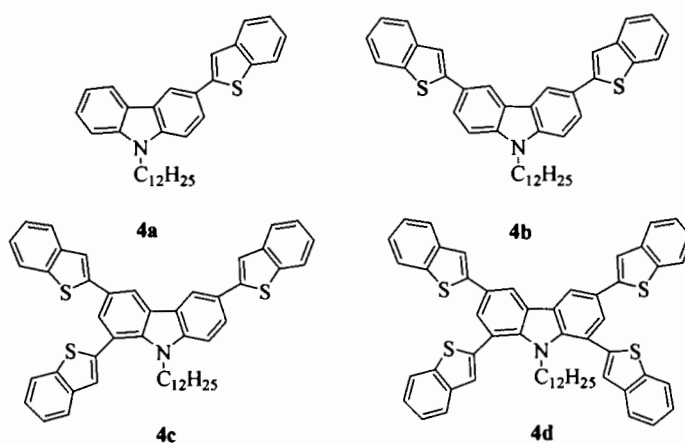


Figure 1.5 Structure of benzo[b]thien-2-yl derivatives.

In 2016, bis-(4-benzenesulfonyl-phenyl)-9-phenyl-9H-carbazoles were designed and synthesized by Bin Huang and co-workers [12]. The nondoped devices using 3,6-bis-(4-benzenesulfonyl-phenyl)-9-phenyl-9H-carbazoles **2a** and 2,7-bis-(4-benzenesulfonyl-phenyl)-9-phenyl-9H-carbazoles **2b** as the emitters show deep blue emission color with EL spectra peaks at 424 and 444 nm and the Commission Internationale de l'Eclairage (CIE) coordinates of (0.177, 0.117) and (0.160, 0.117), respectively. Furthermore, these materials based devices have high color-purity with small width at half-maximum (FWHM) of 65 and 73 nm, respectively. The results provide a novel approach for the design of deep blue emitter for high-color-purity nondoped OLEDs.

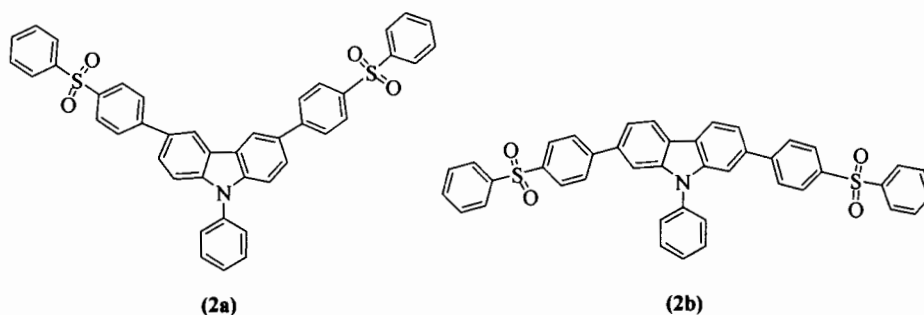


Figure 1.6 Structure of bis-(4-benzenesulfonyl-phenyl)-9-phenyl-9H-carbazoles.

In 2016, **DPACz1**, **DPACz2** and **DPACz3** were synthesized and characterized by Shahid Ameen *et al* [13]. Diphenylamine substituents at 1- or 1,8-positions of carbazoles show increasing of the band-gap compared with the previously reported 3,6- or 2,7-substituted ones. In addition, all materials indicated high triplet energy levels of 2.68, 2.60 and 2.45 eV, respectively. Based on suitable HOMO levels and high triplet energies, they were investigated for their potential as host materials for green phosphorescent OLEDs with the device configuration, [ITO/PEDOT:PSS/Emitting layer/TPBi/CsF/Al]. Moreover, the devices of all materials shown emitted typical green light with high luminance and had low turn-on voltages along with good luminous efficiencies. These results indicated the usefulness of new materials and kind of 1-/1,8-substitution of carbazole would open a new way of materials design.

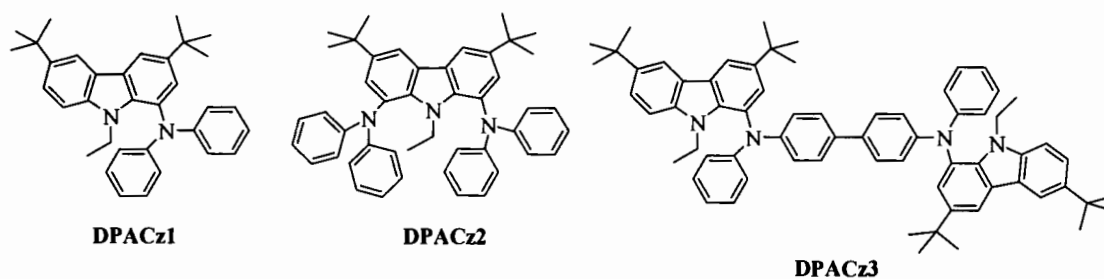


Figure 1.7 Structure of DPACz1, DPACz2 and DPACz3

In 2016, Shi H. et al [14] presented two novel phenylethene-carbazole derivatives containing dimesitylboron groups, 3-(dimesitylboryl)-9-ethyl-6-(1,2,2-triphenylvinyl)-9H-carbazole **DETPCZ** and 1,2-bis(6-(dimesitylboryl)-9-ethyl-9H-carbazol-3-yl)-1,2-diphenylethene **DECZDEP**. The electrochemical thermal and photophysical properties were reported. Both compounds show excellent thermal stability (T_d up to 254 °C) and high electrochemical stability. Moreover, the multi-layer EL devices illustrated the sky blue-green emitting EL with high maximum luminance and maximum luminance efficiency of 15,780 cd m⁻² and 6.90 cd A⁻¹ at CIE of (0.20, 0.28) and (0.23, 0.41), respectively. The results provide a novel way for the design and application of novel AIE-luminophores.

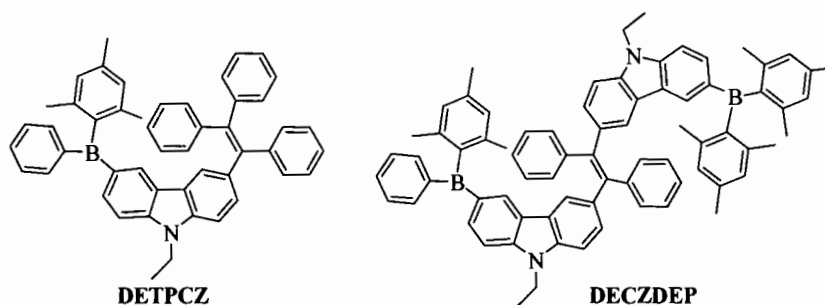


Figure 1.8 Structure of DETPCZ and DECZDEP

Due to a variety of organic materials of OLED have been reported. We are particularly interested in synthesizing organic compounds for OLEDs.

1.1.5 Aim of the thesis

Initially proposed by Ching W. Tang in 1987 [3], organic light-emitting diodes (**OLEDs**) have attracted significant attention from the scientific community due to their potential for future flat-panel displays and lighting applications [15]. Today, the developments of OLED technologies mainly focus on the optimization of device structures and on developing new emitting materials. Clearly, new materials emitting pure colors of red, green, and blue (**RGB**) with excellent emission efficiency and high stability, are the key point of OLED development for full-color flat displays. The performance of blue OLEDs is usually inferior to that of green and red OLEDs due to poor carrier injection into the emitters [16] and electroluminescent (**EL**)

properties of the blue OLEDs need to be improved. Therefore, one area of continuing research in this field is the pursuit of a stable-blue emitting material [17]. Although many fluorescent blue emitters have been reported such as pyrene derivatives [18], carbazole derivatives [19], anthracene derivatives [20], fluorene derivatives and aromatic hydrocarbons [21], there is still a clear need for further developments in terms of efficiency and color purity compared to red and green emitters.

In this research, we synthesize and characterize a series of emissive materials based on carbazole derivatives. In addition, we synthesize the following carbazole derivatives containing two pyrenyl and two anthracene endgroups of carbazole unit as core, whose chemical structure of target molecules, **CP2** and **CA2** are shown in **Figure 1.9**. They are used as light-emitting materials in OLEDs.

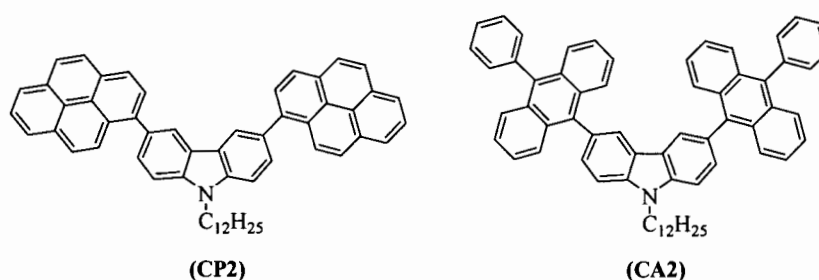


Figure 1.9 The target molecules **CP2** and **CA2**

Objectives of this research

- (1) To synthesize pyrene and anthracene-substituted carbazole derivatives as both emitting and hole-transporting materials for OLEDs.
- (2) To characterize and identify the target product during the synthesis steps
- (3) To study optical property and potential of the target molecules

1.2 RESULTS AND DISCUSSION

In this research, organic compounds, carbazole derivatives, were designed for studied OLEDs properties. The target molecules **CP2** and **CA2**, pyrene and anthracene-substituted carbazole derivatives, were designed synthesized, characterized and studied optical property. Structure of **CP2** and **CP1** are shown in **Figure 1.10**.

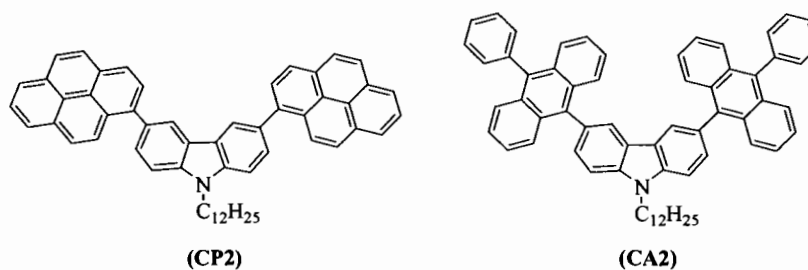


Figure 1.10 Structure of CP2 and CA2

1.2.1 Synthesis and characterization of CP2 and CA2

The target carbazole CP2 and CA2 were successfully synthesized by bromination and Suzuki cross coupling. The target carbazole were synthesized from Suzuki cross coupling of dibromocarbazole 3 with pyrene-1-boronic acid and 10-phenyl-9-anthraceneboronic acid. The dibromocarbazole 3 was synthesized alkylation of carbazole 1 with 1-bromododecane and following by bromination with *N*-bromosuccinamide (NBS) as shows in **Figure 1.11**.

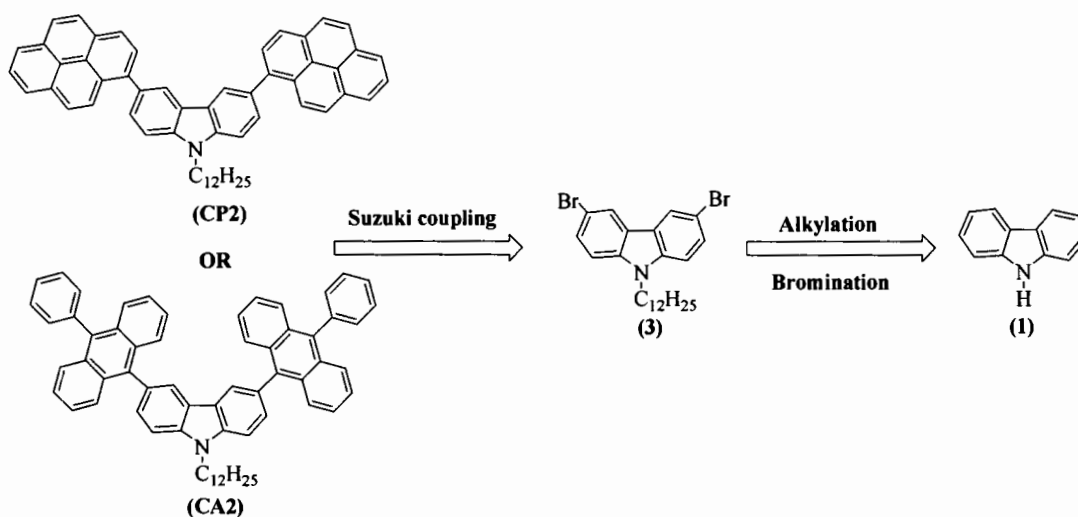


Figure 1.11 Retrosynthesis of carbazole CP2 and CA2

First step, 9-dodecylcarbazole 2 was synthesized by alkylation reaction at the N-position of carbazole 1 with 1-bromododecane. The treatment of carbazole with

sodium hydride (NaH) and 1-bromododecane in DMF at 0 °C to room temperature overnight gave 9-dodecylcarbazole **2** in 97% yield as shows in **Figure1.12**.

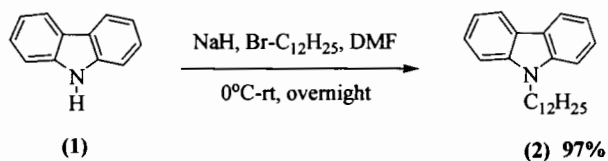


Figure1.12 Synthesis of 9-dodecylcarbazole 2

The 9-dodecylcarbazole **2** was confirmed by $^1\text{H-NMR}$ and $^{13}\text{C-NMR}$ [11]. $^1\text{H-NMR}$ spectra of 9-dodecylcarbazole **2** still show eight aryl proton in the same region of carbazole and shows new triplet peak of N-CH_2 - proton at $\delta = 4.36$ (2H) and peak of alkyl protons at $\delta = 1.96$ (2H), 1.41-1.37 (18H) and $\delta = 1.05$ (3H) ppm. Remarkable, the NH proton of carbazole was absented. Moreover, $^{13}\text{C-NMR}$ spectrum shows new signal of N-CH_2 - at $\delta = 43.2$ ppm and new ten peaks of 11 alkyl carbons. These results confirmed that product was compound **2**.

The mechanism of alkylation reaction was purposed *via* nucleophilic substitution reaction as shows in **Figure1.13**. Nitrogen anion intermediate [A] were generated by reaction of carbazole with hydride of NaH. Then, nitrogen anion attacked at C-1 position of 1-bromododecane to give 9-dodecylcarbazole **2**.

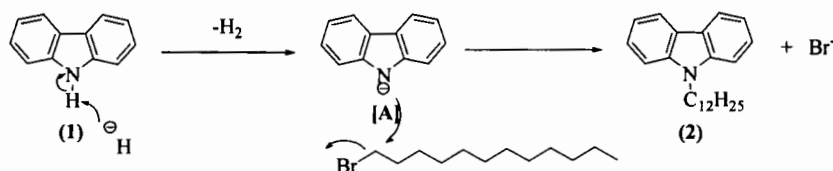


Figure 1.13 Mechanisms of alkylation reaction of carbazole

Next step, selective bromination of 9-dodecylcarbazole **2** at C-3 and C-6 position were investigated. The treatment of compound **2** with NBS in THF at room temperature for 3h afforded 3,6-dibromo-9-dodecylcarbazole **3** in 91% yields as shows in **Figure1.14**.

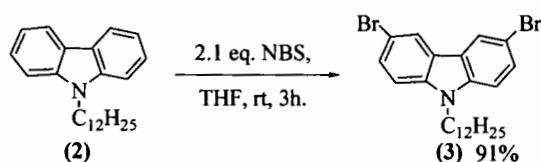


Figure 1.14 Bromination of 9-dodecylcarbazole 2

The compound **3** was confirmed by $^1\text{H-NMR}$ and $^{13}\text{C-NMR}$ [11]. $^1\text{H-NMR}$ spectra of 3,6-dibromo-9-dodecylcarbazole **3** shows six aromatic protons at $\delta = 8.15$ (2H), 7.55 (2H) and 7.29 (2H) and shows twenty five alkyl protons in the same region of dodecyl group. The absence of two protons of carbazole was believed that bromination on carbazole **2** was appeared. Moreover, $^{13}\text{C-NMR}$ spectrum shows CH aromatic carbon of carbazole only three signals at $\delta = 129.0$ (2 x CH), 123.5 (2 x CH), 123.3 (2 x CH). Therefore, NMR results confirm that two protons of carbazole were substituted by two bromine atoms. These results confirmed that product was compound **3**.

The mechanism of bromination was proposed *via* electrophilic aromatic substitution as shown in **Figure 1.15**. Firstly, carbon C-3 position of carbazole as a nucleophile attacked at bromine atom of *N*-bromosuccinimide to give carbazole intermediate **[B]**. The aromatization of intermediate **[B]** *via* deprotonation gave intermediate compound **[C]**. Then, bromination at C-6 position of carbazole **[C]** in the same mechanism gave intermediate **[D]** and 3,6-dibromo-9-dodecylcarbazole **3**, respectively.

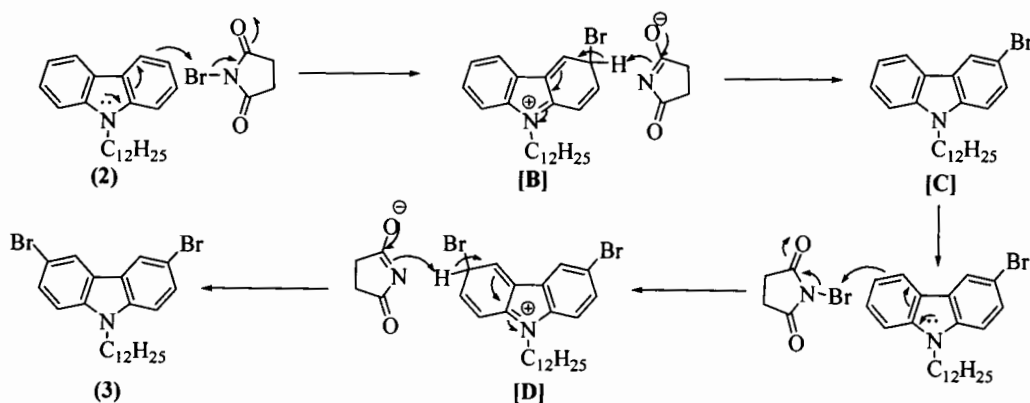


Figure 1.15 Mechanisms of bromination of 9-dodecylcarbazole (2)

Then, target molecules **CP2** was synthesized by Suzuki cross coupling reaction. The treatment of compound **3**, pyrene-1-boronic acid, Pd(PPh₃)₄ as the catalyst and aqueous Na₂CO₃ as the base in THF at reflux afforded target molecules **CP2** in 53 % yields as shows in **Figure1.16**.

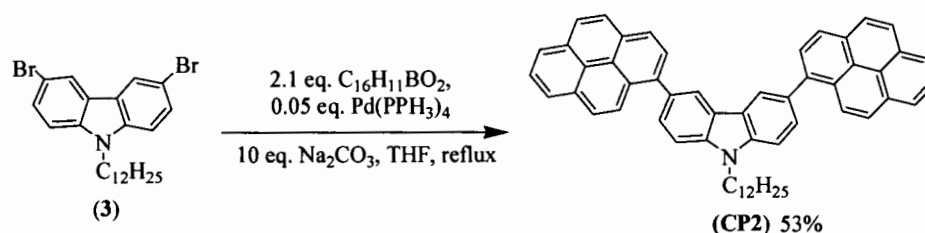


Figure 1.16 Synthetic of target molecules CP2

The target compound **CP2** was confirmed by ¹H-NMR and ¹³C-NMR. ¹H-NMR spectra of compound **CP2** show 24 aromatic protons (new more 18 aromatic protons from compound **3**) and show twenty five alkyl protons in the same region of dodecyl group. The increasing of new 18 aromatic protons were believe that bromine atom were substituted by pyrenyl group. In addition, ¹³C-NMR spectra shows new 18 CH aromatic carbons and new 14 C_q aromatic carbons of pyrenyl group. Therefore, NMR results confirm that two bromine atoms were substituted by two pyrenyl groups. Moreover, the high resolution mass spectrometry (MALDI-TOF) of compound **CP2** found 735.2981 (calcd for C₅₆H₄₉N: *m/z* 735.3865). These results confirmed that product was compound **CP2**.

The mechanism of Suzuki coupling reaction follows a three-step mechanism cycle, oxidative addition, transmetalation and reductive elimination as described in **Figure 1.16**. The oxidative addition at C-Br bond of compound **3** with Pd(0) gave organopaladium complex **[E]**. The reaction of complex **[E]** with Na₂CO₃ gave complex **[F]**. Transmetalation of complex **[F]** with organoboron species **[G]**, preparing from reaction of boronic acid and Na₂CO₃, gave complex **[H]**. Finally, reductive elimination of complex **[D]** gave molecules **[I]**. Then, Suzuki coupling reaction at C-6 position of carbazole **[I]** in the same mechanisms gave target compound **CP2**.

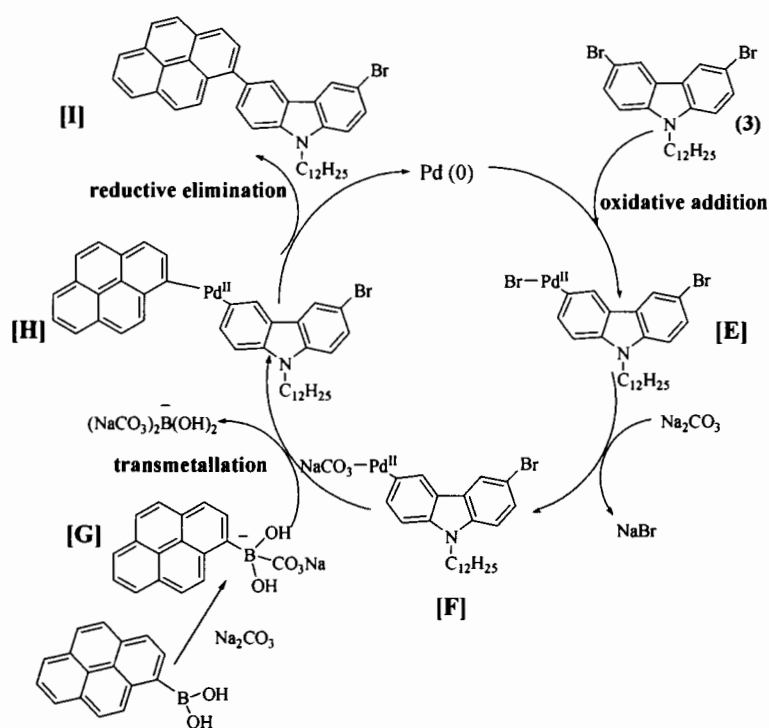


Figure 1.17 The proposed mechanism of Suzuki coupling reaction

Finally, the target molecules **CA2** was synthesized by Suzuki cross coupling reaction. The treatment of compound **3**, 10-phenyl-9-anthracene boronic acid, Pd(PPh₃)₄ as the catalyst and K^tOBu as the base in THF at reflux afforded target molecules **CA2** in 68 % yields as shows in **Figure 1.18**.

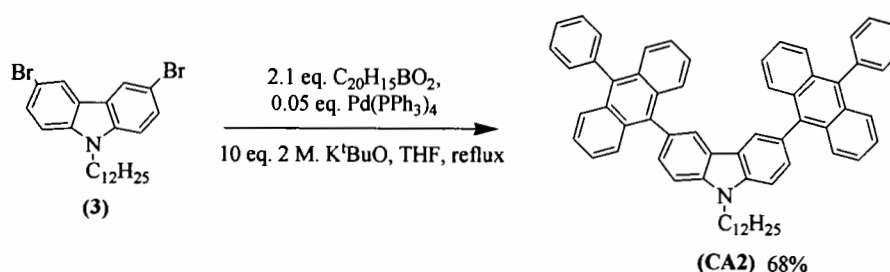


Figure 1.18 Synthetic of target molecules **CA2**

The target compound **CA2** was confirmed by ¹H-NMR and ¹³C-NMR. ¹H-NMR spectra of compound **CA2** shows 32 aromatic protons (new more 26 aromatic protons from compound **3**) and shows twenty five alkyl protons in the same region of

dodecyl group. The increasing of new 26 aromatic protons were believe that bromine atom were substituted by 10-phenyl-9-anthracenyl group. In addition, ^{13}C -NMR spectrum shows new 26 CH aromatic carbon and new 14 Cq aromatic carbon of 10-phenyl-9-anthracenyl group. Therefore, NMR results confirm that two bromine atoms were substituted by 10-phenyl-9-anthracenyl group. Moreover, the high resolution mass spectrometry (MALDI-TOF) of compound **CA2** found 839.3175 (calcd for $\text{C}_{64}\text{H}_{57}\text{N}$: m/z 839.4491). These results confirmed that product was compound **CA2**.

The mechanism of Suzuki coupling of compound **CA2** similar to mechanism of Suzuki coupling reaction as described in **Figure 1.17**.

1.2.2 Optical properties of **CP2** and **CA2**

The optical properties of the organic materials were investigated by UV-Vis and fluorescence spectrophotometer in dry dichloromethane (DCM). The UV-Vis absorption and photoluminescence spectra of the target molecules **CP2** and **CA2** were measured as shown in **Figure 1.19** and the corresponding data summarized in Table 1.1. In solution absorption spectra, the UV-Vis spectra of the target molecules **CP2** and **CA2** exhibited two major absorption bands. The first absorption band of compounds **CP2** and **CA2** were assigned in terms of the strong absorption band in the region of 200-275 nm corresponding to the π - π^* local electron transition of the carbazole moieties and the second absorption bands at longer wavelength around 350-400 nm corresponding to intermolecular charge transfer (ICT) transition between the carbazole and conjugated substituted dipylene and dianthracene. However, the substitution dipylene **CP2** to substituted anthracene **CA2** of carbazole increased the conjugation length of compounds resulting a red-shift and broad in absorption spectra. Therefore, the ICT of **CA2** was stronger than ICT of **CP2**.

These compounds in solution show fluoresce in the blue region (430–442 nm) with featureless photoluminescence (PL) spectra. The emission spectra display maxima at 430 and 442 nm, for **CP2** and **CA2**, respectively. From the substitution dipylene **CP2** to substituted anthracene **CA2**, the PL spectra also show a gradual red-shife, concomitant with the increasing conjugation length (**Figure 1.19**).

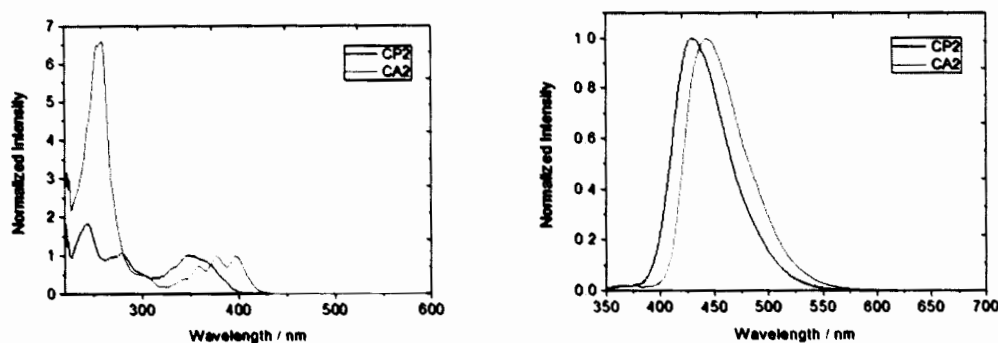


Figure 1.19 Normalized absorption spectra (left) and normalized emission spectra (right) in CH_2Cl_2 of CP2 and CA2

Table 1.1 Physical data of CP2 and CA2

Compound	$\lambda_{\text{abs}}(\log \epsilon)^{\text{a}}$ ($\text{nm M}^{-1}\text{cm}^{-1}$)	$\lambda_{\text{em}}^{\text{a}}$ (nm)	E_{g}^{b} (eV)
CP2	279 (5.37), 348 (2.35)	430	3.10
CA2	305 (3.93), 359 (4.09), 377 (4.24), 397 (4.23)	442	2.95

^a Measured in dilute CH_2Cl_2 solution.

^b Calculated from the absorption edge, $E_{\text{g}} = 1240$ per onset

The energy gaps (E_{g}) of the target molecules from the absorption edge were nearly identical (2.95-3.10 eV), despite the somewhat different molecular sizes and substance groups.

Conclusion of optical properties, compound CA2 has longer conjugate and stronger intermolecular charge transfer than CP2 from result of UV absorption spectra. Moreover, emission spectra conclude that compound CP2 and CA2 emit in the blue region but CA2 spectra showed peak shift of up to 12 nm from compound CP2.

1.2.3 Electrochemical properties of CP2 and CA2

The electrochemical properties of materials were performed using the cyclic voltammeter (CV). All measurements were made at room temperature on sample dissolved in freshly distilled dichloromethane and 0.1 M tetra-*n*-

butylammonium hexafluorophosphate ($n\text{-Bu}_4\text{NPF}_6$) as electrolyte. The solutions were degassed by bubbling with argon. A typical electrochemical cell consists of three electrodes; a glassy carbon working electrode, platinum wire counter electrode, and $\text{Ag}/\text{AgCl}/\text{NaCl}$ (Sat.) reference electrode, controlled by a potentiostat. The potential difference was applied between the working and counter. The third electrode was the reference electrode, through which no current flows, and from which the potentials of the other electrodes were measured. A part from the solutions, the solute in this work contained an electrolyte to decrease the resistivity.

The electrochemical stability of materials was performed by multiple-scan CV curves. The HOMO energy levels of materials were calculated from the oxidation onset potentials (E_{onset}) with empirical equation of $\text{HOMO} = - (4.44 + E_{\text{onset}})$ while LUMO energy levels were calculated by subtracting the E_g from HOMO levels.

Electrochemical behaviors of **CP2** and **CA2** investigated by cyclic voltammetry (CV), and resulting data are shown in **Figure 1.20**.

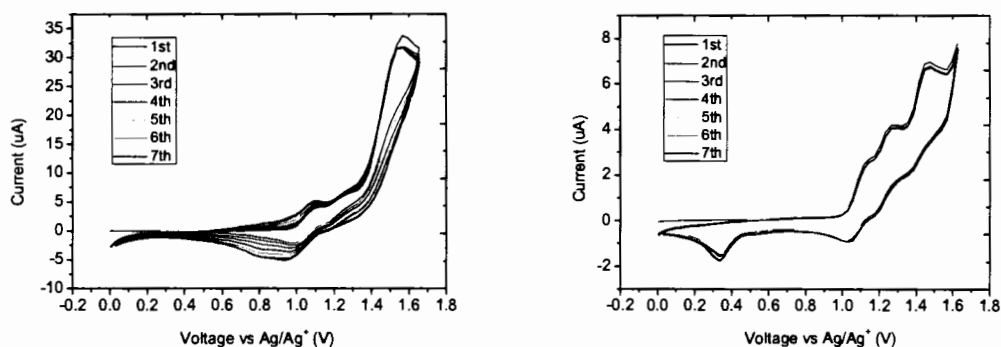


Figure 1.20 Cyclic voltammograms of **CP2** (left) and **CA2** (right) in dry CH_2Cl_2 with scan rate of 0.05 V/s and $0.1 \text{ M } n\text{-Bu}_4\text{NPF}_6$ as electrolyte, multi scan.

Multiple CV scans of **CA2** revealed identical CV curves with no additional peak at lower potentials on the cathodic scan (E_{pc}) being observed. This suggests no electrochemical coupling at either the carbazole or anthracene peripheries, indicating electrochemically stable molecules. However, the target molecule **CA2** more stable than target molecule **CP2**. The CV curve of **CP2** shows three irreversible oxidation processes. The first oxidation is assigned to the removal of electrons from the

carbazole moiety resulting in carbazole radical cations (CBZ.⁺). In all cases, during the cathodic scan additional peaks at lower potentials are observed, indicating electrochemical coupling reactions of the radical cations formed were taking place. As proposed in **Figure 1.21**, the generated CBZ.⁺ is stabilized by electron delocalization through 1,8-substituted electron rich pyrene rings to form a pyrene radical cation (Py.⁺) which is relatively less stable compared with the CBZ.⁺. The Py.⁺ readily undergoes a radical–radical dimerization coupling to form a stable neutral pyrene dimer as indicated by the presence of the cathodic peaks (Epc) around 0.61-0.94 V in their first CV scan and an increasing change in the CV curves under the repeated CV scans 10 **Figure 1.20**.

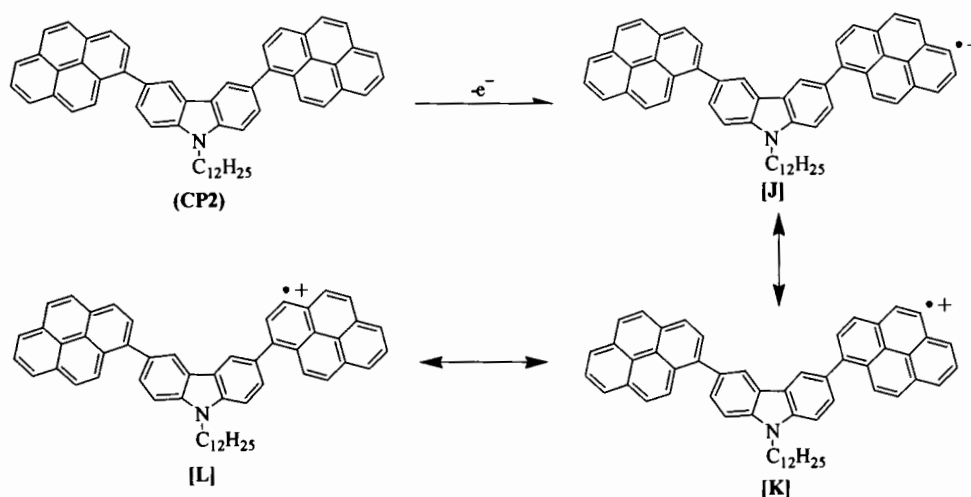


Figure 1.21 Oxidation process of pyrene

Moreover, they also showed similar wave in different scans, no distinct a slight shift of the CV curves. During in order oxidation cycle of all compounds, the oxidation progressively shifted to higher energy with increasing the aromatic unit. This might be the first example of pyrene and anthracene derivatives that undertake an electrochemical oxidation coupling reaction.

The HOMO energy levels of pyrene and anthracene derivatives were estimated to be -5.41 and -5.45 eV respectively. The LUMO energy levels of pyrene and anthracene derivatives were estimated to be -2.31 and -2.50 eV respectively (**Table 1.2**).

Table 1.2 Physical data of CP2 and CA2

Compound	E _g ^b (eV)	HOMO ^c (eV)	LUMO ^d (eV)
CP2	3.10	-5.41	-2.31
CA2	2.95	-5.45	-2.50

^b Calculated from the absorption edge, $E_g = 1240$ per onset

^c Estimated from $\text{HOMO} = -(4.44 + E_{\text{onset}}^{\text{ox}})$

^d Estimated from $\text{LUMO} = \text{HOMO} + E_g$

1.2.4 HOMO and LUMO frontier orbitals of CP2 and CA2

To gain insights into the geometrical and electronic properties of these multiple substituted carbazoles, quantum chemistry calculations were performed using the DFT/B3LYP/6-31G(d,p) method. The optimized structures of CP2 reveal that the attached pyrene units twist out of the plane of the carbazole forming bulky substituents around the carbazole. This would facilitate the formation of amorphous materials. In all cases CP2 and CA2, π -electrons in the HOMO orbitals delocalize only over the carbazole and two substituents at the 3,6-positions substituted carbazole backbone, whereas after light irradiation (LUMO), the excited electrons are delocalized largely over the pyrene and anthracene plane.

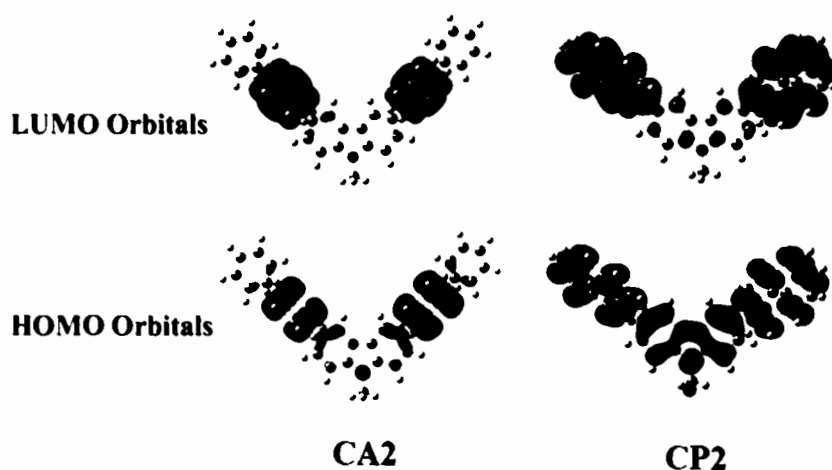
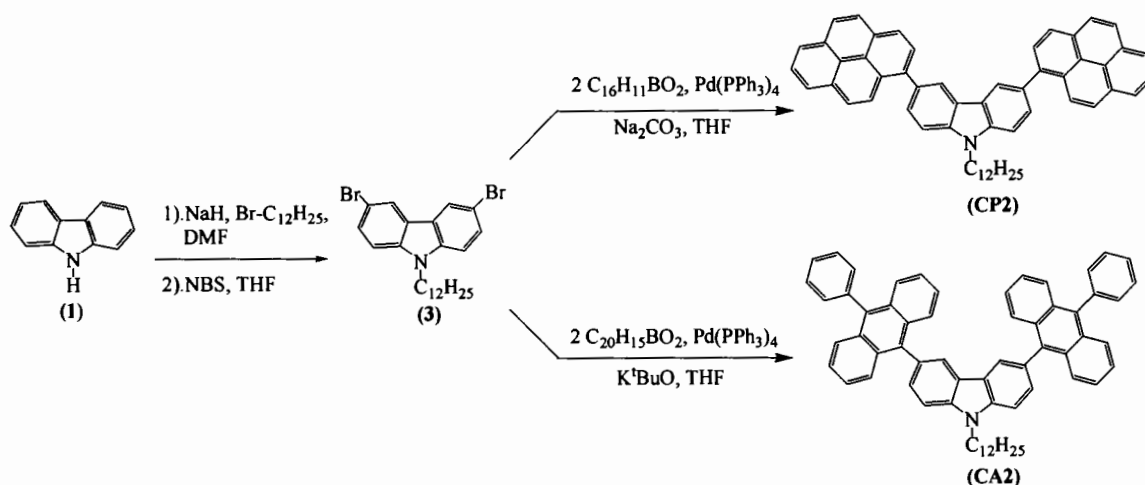


Figure 1.22 The HOMO (bottom) and LUMO (top) orbitals of CP2 and CA2 calculated by DFT/B3LYP/6-31G(d,p) method.

1.3 CONCLUSION

In conclusion, we have successfully synthesized pyrene and anthracene-substituted carbazole (**CP2**, **CA2**) by the Suzuki-cross coupling reaction of dibromo intermediates with pyrene-1-boronic acid and 10-phenyl-9-anthraceneboronic acid, respectively. The target molecules were characterized by using melting points, ^1H -NMR and ^{13}C -NMR spectroscopy, FT-IR spectroscopy and mass spectrometer.



The optical and electrochemical properties of both compounds can be tuned by varying the substituted on carbazole ring. The substitution dipyrene **CP2** to substituted anthracene **CA2** of carbazole increased the conjugation length of compounds resulting a red-shift and broad in absorption spectra. These compounds were emissive of blue light with high thermal stability which is potentially useful for applications in electroluminescent devices. Optimize structure and electron density of HOMO and LUMO have been performed by DFT/B3LYP/6-31G(d,p) method.

1.4 EXPERERIMENTAL

1.4.1 GENERAL EXPERIMENT

All solvents and reagents were purchased from Aldrich, Acros and Fluka received unless otherwise stated. Analytical thin-layer chromatography (TLC) was performed with Merck aluminium plates coated with silica gel 60 F₂₅₄. Column chromatography was carried out using gravity feed chromatography with Merck silica gel mesh, 60 Å. Where solvent mixtures are used, the portions are given by volume.

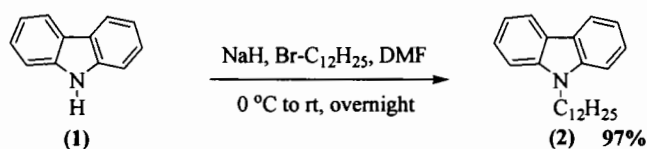
Melting points were measured by BUCHI 530 model in open capillary method and are uncorrected and reported in degree Celsius.

$^1\text{H-NMR}$ and $^{13}\text{C-NMR}$ spectra were recorded on a Bruker AVANCE 300 MHz spectrometer. Chemical shifts (δ) are reported relative to the residual solvent peak in part per million (ppm). Coupling constants (J) are given in Hertz (Hz). Multiplicities are quoted as singlet (s), broad (br), doublet (d), triplet (t), quartet (q), and multiplet (m).

The IR spectra were recorded on Perkin-Elmer FT-IR spectrum RXI spectrometer. The absorption peaks are quoted in wavenumber (cm^{-1}). MALDI-TOF mass spectra were recorded on Bruker Daltonics (Bremen, Germany) Autoflex II Matrix-Assisted Laser Desorption/Ionization-Time of Flight Mass Spectrometer (BIFEX) using α -cyano-4-hydroxycinnamic acid as matrix. UV-Vis spectra were recorded on a Perkin-Elmer UV Lambda 25 spectrometer.

The electrochemistry was performed using a AUTOLAB spectrometer. All measurements were made at room temperature on sample dissolved in freshly distilled dichloromethane, 0.1 M tetra-*n*-butylammonium hexafluorophosphate as electrolyte. The solutions were degassed by bubbling with argon. Dichloromethane was distilled from calcium hydride. A glassy carbon working electrode, platinum wire counter electrode, and a Ag/AgCl/NaCl (Sat.) reference electrode were used.

1.4.2 Synthesis of 9-Dodecylcarbazole (2)



To a solution of carbazole (10.1021 g, 59.80 mmol) in DMF (93 mL) was added NaH (2.3540g, 89.58 mmol) and then 1-bromododecane (15.0000 g, 89.70 mmol). The reaction mixture was stirred at 0 °C to rt for 20 h. Water (100 mL) was added and the mixture was extracted with ethyl acetate (50 mL x 3). The combined organic phases were washed with a dilute HCl solution (50 mL x 2), water (100 mL), and brine solution (50 mL), dried over anhydrous Na_2SO_4 , evaporated and purified by column chromatography to give a pale yellow viscous oil (19.7825 g, yield 97%) [11].

$C_{24}H_{33}N$;

1H -NMR (300 Hz, $CDCl_3$):

$\delta = 8.24$ (2H, d, $J = 7.8$ Hz), 7.79-7.49 (4H, m), 7.36 (2H, d, $J = 14.4$ Hz), 4.36 (2H, t, $J = 6.9$ Hz), 1.96 (2H, t, $J = 6.6$ Hz), 1.41-1.37 (18H, m) and 1.05 (3H, t, $J = 5.4$ Hz) ppm.

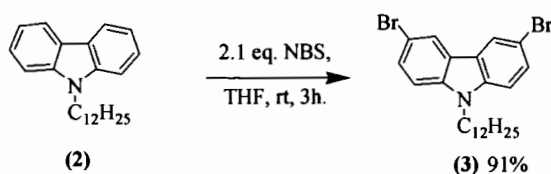
^{13}C -NMR (75 Hz, $CDCl_3$):

$\delta = 140.6$ (2 x Cq), 125.7 (2 x CH), 123.0 (2 x Cq), 120.5 (2 x CH), 118.8 (2 x CH), 108.8 (2 x CH), 43.2 (N- $\underline{C}H_2$), 32.1 (CH_2), 29.8 (2 x CH_2), 29.75 (CH_2), 29.7 (CH_2), 29.6 (CH_2), 29.5 (CH_2), 29.1 (CH_2), 27.4 (CH_2), 22.9 (CH_2), 14.3 (CH_3) ppm.

IR (KBr):

$\nu_{max} = 3052, 2922, 2851, 1597, 1484, 1451, 1324, 1152, 746, 720$ cm^{-1} .

1.4.3 Synthesis of 3,6-Dibromo-9-dodecylcarbazole(3)



In the flask, covered with aluminum foil, to a solution of 3-monobromo-9-dodecylcarbazolen **2** (0.5184 g, 1.54 mmol) in THF (15 mL) was added NBS (0.5772 g, 3.24 mmol) in small portions at 0°C. After stirred 0 °C to rt for 3 h, the reaction mixture was poured into water. The mixture was extracted with methylene chloride (20 mL x 3), washed with water (20 mL x 3), dried over anhydrous Na_2SO_4 , evaporated and purified by column chromatography to give a white pearl solid (0.6951 g, yield 91%). [11]

$C_{24}H_{31}Br_2N$; m.p. = 50-52 °C

1H -NMR (300 Hz, $CDCl_3$):

$\delta = 8.15$ (2H, s), 7.55 (2H, d, $J = 8.7$ Hz), 7.29 (2H, d, $J = 8.7$ Hz), 4.25 (2H, t, $J = 7.0$ Hz), 1.85 (2H, s), 1.30-1.21 (18H, m), 0.88 (3H, t, $J = 6.3$ Hz)

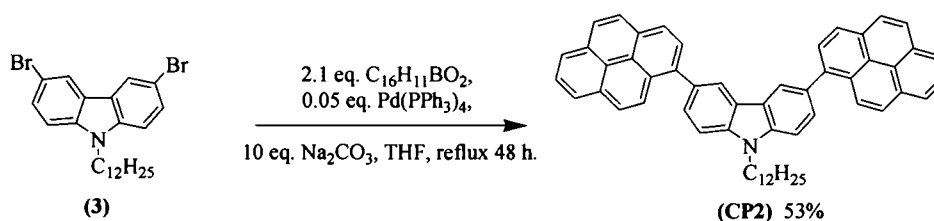
^{13}C -NMR (75 Hz, $CDCl_3$):

$\delta = 139.4$ (2 x Cq), 129.0 (2 x CH), 123.5 (2 x CH), 123.3 (2 x CH), 111.9 (2 x Cq), 110.4 (2 x CH), 43.4 (N-CH₂), 31.8 (CH), 29.6 (2 x CH), 29.5 (CH), 29.4 (CH), 29.3 (2 x CH), 28.8 (CH), 27.2 (CH), 22.7 (CH), 14.1 (CH₃) ppm.

IR (KBr):

$\nu_{\max} = 2950, 2918, 2848, 1592, 1469, 1289, 1224, 1057, 802, 720 \text{ cm}^{-1}$.

1.4.4 Synthesis of 9-Dodecyl-3,6-di(pyren-1-yl)carbazole (CP2)



To a stirred solution of 3,6-dibromo-9-dodecyl carbazole **3** (0.2000 g, 0.34 mmol) and Pd(PPh₃)₄ (0.0303 g, 0.02 mmol) in tetrahydrofuran (20 mL) were added pyrene-1-boronic acid (0.1759 g, 0.71 mmol) and an aqueous Na₂CO₃ solution (0.5576 g, 5.26 mmol). The mixture was refluxed for 48 h. After cooling, the mixture was extracted with dichloromethane (30 mL x 3), washed with water (30 mL x 3), dried over anhydrous, evaporated and purified by column chromatography to give a white pearl solids (0.2506 g, yield 53%).

C₅₆H₄₉N; m.p. = 170-173 °C

¹H-NMR (300 Hz, CDCl₃):

$\delta = 8.40$ (2H, s), 8.34 (2H, d, $J = 9.30$ Hz), 8.25 (2H, d, $J = 7.80$ Hz), 8.20-8.10 (10H, m), 8.06-7.97 (4H, m), 7.80 (2H, d, $J = 8.40$ Hz), 7.65 (2H, d, $J = 7.64$), 4.47 (2H, t, $J = 7.20$ Hz), 2.10 (2H, t, $J = 6.90$ Hz), 1.57-1.30 (18H, m) and 0.91 (3H, t, $J = 6.90$ Hz)

¹³C-NMR (75 Hz, CDCl₃):

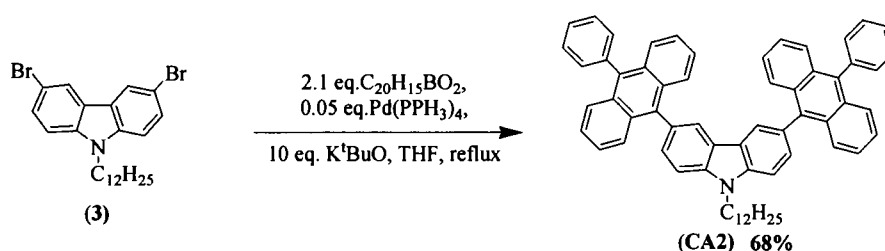
$\delta = 140.3$ (2 x Cq), 138.7 (2 x Cq), 132.1 (2 x Cq), 131.6 (2 x Cq), 131.1 (2 x Cq), 130.3 (2 x Cq), 128.9 (2 x Cq), 128.7 (2 x CH), 128.2 (2 x CH), 127.5 (2 x CH), 127.3 (2 x CH), 127.1 (2 x CH), 125.9 (2 x CH), 125.7 (2 x CH), 125.1 (2 x Cq), 125.0 (2 x Cq), 124.9 (2 x CH), 124.6 (4 x CH), 123.1 (2 x Cq), 122.5 (2 x CH), 108.7 (2 x CH), 43.6 (N-CH₂), 31.9 (CH₂), 29.7 (3 x CH₂), 29.6 (CH₂), 29.5 (CH₂), 29.4 (CH₂), 29.2 (CH₂), 27.5 (CH₂), 22.7 (CH₂), 14.1 (CH₃) ppm.

IR (KBr):

ν_{\max} = 3038, 2919, 2849, 1600, 1480, 1347, 1279, 1153, 849, 817 cm^{-1}

MALDI-TOF (m/z) calcd for $\text{C}_{56}\text{H}_{49}\text{N}$: 735.3865; found 735.2981 (M^+).

1.4.5 Synthesis of 9-Dodecyl-3,6-di(anthracen-1-yl)carbazole (CA2)



CHAPTER 2

SYNTHESIS AND CHARACTERIZATION OF INDOLE DERIVATIVES FOR DYE-SENSITIZED SOLAR CELL

2.1 INTRODUCTION

2.1.1 Dye-sensitized solar cells (DSSCs)

Actually, the capability of human is to extent dependently on the available energy sources. In the developing countries, energy consumption has reached a level of over 4×10^{18} J already in the present annual worldwide and it is foresighted to multiply swiftly accompany with the increasing of world population and demand of energy [22]. As to the rising energy demand and more reduced fossil fuel reserves, the damaged environment and the improved greenhouse effect, affected by the combustion of fossil fuels, can out of control [23]. In other words, if the demands of energy have a chance to use renewable energy sources, the cost of environment could be decreased. Yearly, the sun could provide energy 3×10^{24} J to the earth [24]. This is about 750000 times greater than the present consumption of global population. The expectation to absorb the sunlight and turn it into electric power or to generate chemical fuels, for example, hydrogen, is become reality in the last two decades. Colloids and nanocrystalline films of various semiconductor systems have been manipulated in form of transform the solar energy directly to be the chemical or electrical energy. The traditional photovoltaic which is based on the solid-state connection devices, such as crystalline or amorphous silicon, has exception of changing solar energy approximately 20% to become electricity efficiencies. To invent the photovoltaic, however, is extravagant because it has to use intensive high temperature energy and high vacuum processes.

In 1991, O'Regan and Gratzel distributed a progress of an option solar harvesting device, dye-sensitized solar cell (DSSCs), [25]. The device supplies 7% of altering a solar energy to electricity, based on a mesoscopic inorganic semiconductor. Then 2.5% of energy proficiency had been reached in this research field. Moreover, the some semiconductor surfaces such as TiO_2 or ZnO is stimulated by an optical

absorbing chromophore with properties of charge disunion that can absorb the solar light and its excited state inject electrons into the semiconductor [26].

2.1.2 Dye-sensitized solar cells structure

The dye-sensitized solar cell is a low-cost solar cell belonging to the group of thin film solar cells. It is based on a semiconductor formed between a photo-sensitized anode and an electrolyte, a photoelectrochemical system. Therefore, the DSSCs structure consist of 4 part including organic sensitizer coating, electrolyte solution, counter electrode and dye sensitizer [27] as shown in **Figure 2.1**.

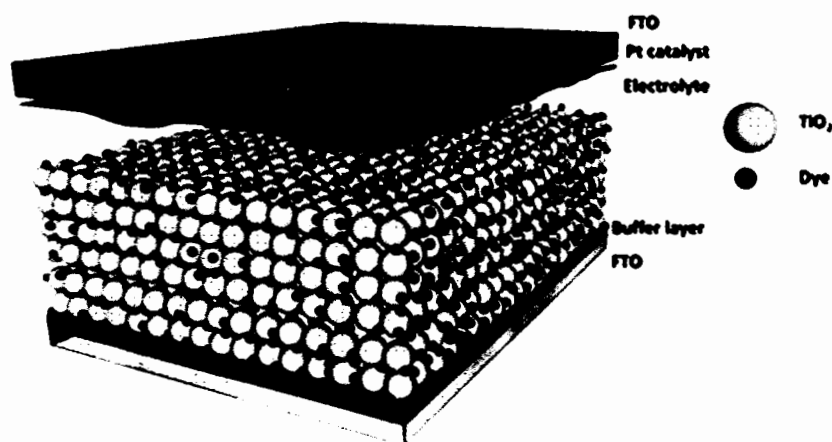


Figure 2.1 Dye-sensitized solar cells structure (DSSCs) structure [28]

2.1.2.1 Organic sensitizer coating with wide band gap semiconductor which is placed in contact with a redox electrolyte, the material of choice has been TiO_2 (anatase).

2.1.2.2 An electrolyte solution containing redox couple such as I^-/I_3^- , the regeneration of the sensitizer by iodide intercepts the recapture of the conduction band electron by the oxidized dye.

2.1.2.3 A counter electrode which is a platinized conductive glass substrate such as fluorine-doped tin oxide glass (FTO).

2.1.2.4 Dye sensitizer serve as the solar energy absorber in DSSC, whose proprieties will have much effect on the light harvesting efficiency and the overall photoelectric conversion efficiency. The ideal sensitizer for dye-sensitized solar cells should absorb all light below a threshold wavelength of about 920 nm. In addition, it

should be firmly grafted to the semiconductor oxide surface and inject electrons to the conduction band with a quantum yield of unity. Its redox potential should be sufficiently high that it can be regenerated rapidly via electron donation from the electrolyte or a hole conductor. Finally, it should be stable enough to sustain at least 10⁸ redox turnovers under illumination corresponding to about 20 years of exposure to natural light.

2.1.3 Principle of Dye-sensitized solar cells

The working principle of DSSCs was shown in **Figure 2.2**. Dye in dye-sensitized solar cells discharges electrons when hit by sunlight. Discharged electrons move toward a transparent anode (negative electrode) through titanium dioxide (titania particles). Electrons that have reached the transparent anode (negative electrode) move toward counter electrode (positive electrode) through an external circuit. Iodide electrolyte receives electrons from the positive electrode. Electrolyte provides received electrons to dye, thanks to the working of iodide ions. Dye received electrons returns to their original condition. Dye-sensitized solar cells generate power by repeating the cycle [29].

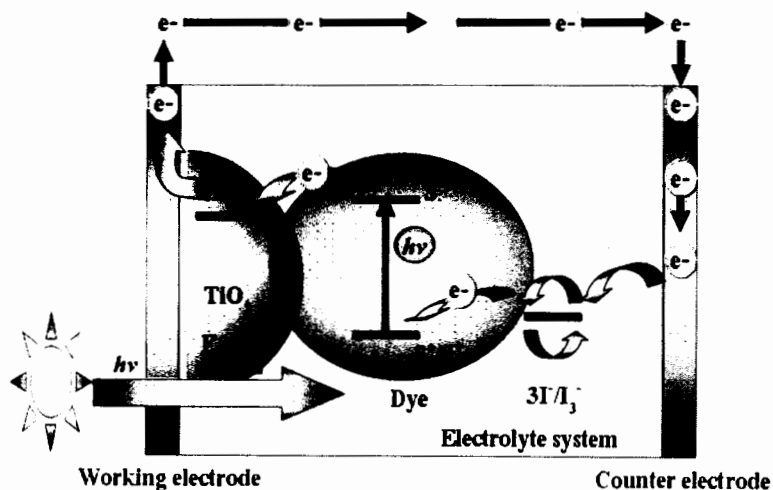


Figure 2.2 Working principle of DSSCs [30]

2.1.4 Literature reviews

In this part, the publications of synthesis and study optical properties of dye-sensitizer for DSSCs application would be described. For example:

In 2007, Kim, D et al. [31] investigated that the organic dyes (**JK-24**, **JK-25** and **JK-28**) containing *N*-(9,9-dimethylfluoren-2-yl)carbazole or *N*-(4-(2,2-diphenylvinyl)phenyl)carbazole as electron donor and cyanoacrylic acid as electron acceptor bridged by thiophene units, gave an overall conversion efficiency (η) of 3.87-5.15%. Although many structure frameworks such as coumarin, aniline and indoline have been employed as good electron donor unit, the small molecular organic dyes containing the *N*-substituted carbazole structural have been little explored for DSSCs.

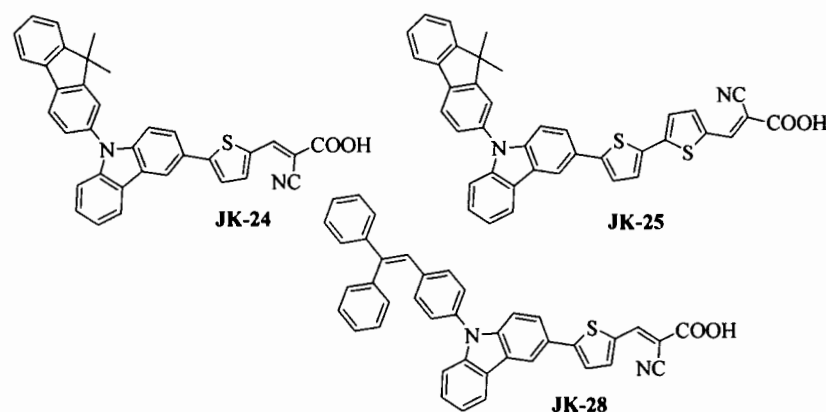


Figure 2.3 Chemical structures of JK-24, JK-25 and JK-28 dyes

In 2009, Chang, Y J. et al. [32] reported that the highly efficient and stable organic dyes (**1P-PSP** and **1N-PSP**) composed of triphenylamine or *N,N*-diphenylnaphthalen-1-amine moiety as the electron donor and cyanoacrylic acid moiety as the electron acceptor with an overall conversion efficiency of 5.25-7.08%.

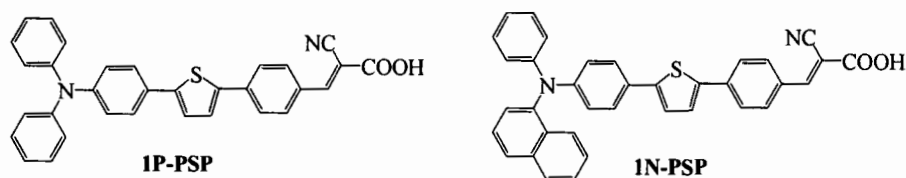


Figure 2.4 Chemical structures of 1P-PSP and 1N-PSP dyes

In 2012, Wan, Z. et al. [33] investigated that the organic dyes (**CBZ**, **WD-5**, and **DTA**) containing carbazole, phenothiazine or diphenylamine as electron donor and cyanoacrylic acid as electron acceptor bridged by phenyl units, gave an overall conversion efficiency of 1.77-2.03%.

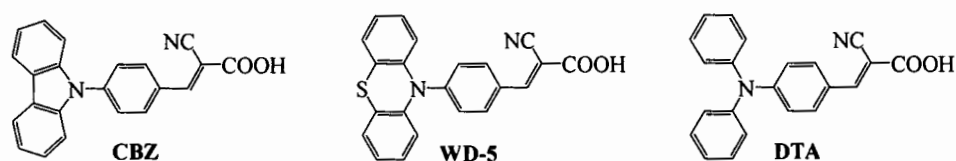


Figure 2.5 Chemical structures of **CBZ**, **WD-5**, and **DTA** dyes

In 2009, Jaejung, K. et al. [34] designed and synthesized organic dye benzo[*cd*]indole **JK51**. Firstly, benzoindole aldehyde **10JK** were synthesized from 2, 6, 7, 8-tetrahydro-1-phenylbenzo[*cd*]indole **1JK** via four steps reactions. Then aldehyde **10JK** were reacted with cyanoacetic acid and piperidine to gain the substance **JK51** as shown in **Figure 2.6**. The benzo[*cd*]indole **JK51** show conversion efficiency at 8.42%, short circuit at 17.43 mA/cm², open circuit voltage at 0.680 V, and fill factor at 0.71.

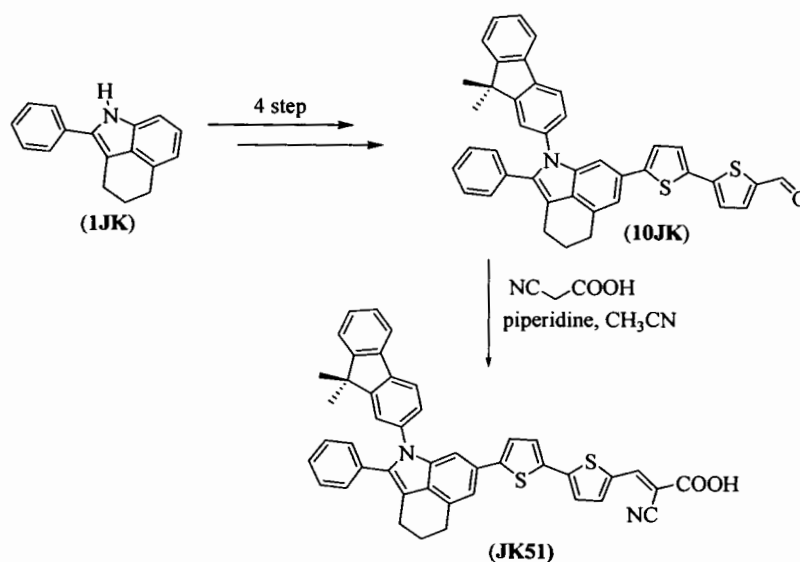


Figure 2.6 Dye-organic synthesis included of benzo[*cd*]indole group

In 2012, Shingo, K. et al. [35] synthesized new type of organic dyeing included of carbazole (MK75, MK79, MK80), indole (MK81-83), and indoline (MK84-86) as electron donors. These substances had cyanoacrylic acid which was electron acceptors and they were joined together with bi-3-*n*-hexylthiophene as shown in Figure 2.7. As for bringing this to study about conversion efficiency, carbazole MK75, MK79 and MK80 was valued from 5.1 to 5.4%, indole MK81-83 was valued between 3.5 to 3.9%, and indoline MK84-86 was valued from 3.0 to 3.7%.

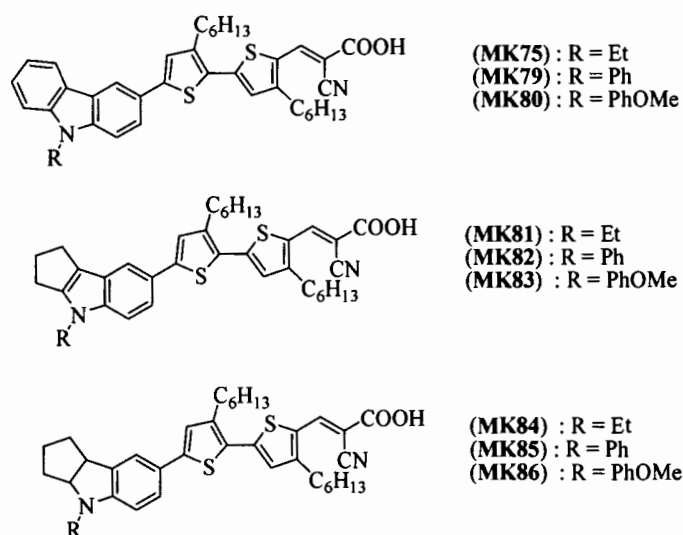


Figure 2.7 The structure of dye molecules included of carbazole (MK75, MK79, MK80), indole (MK81-83) and indoline (MK84-86)

In 2014, Gang, W. et al. [36] studied about the property of electricity and dye-sensitized which had a system of D- π -A in form of isoindigo group. The study was done by synthesizing ID1, ID2, and ID3 as shown in Figure 2.8. The finding indicated that ID1 had extended range of absorption and energy conversion efficiency (η). Moreover, ID1 was the utmost value at 3.33% under 100 mW/cm² simulated AM 1.5 G solar irradiation.

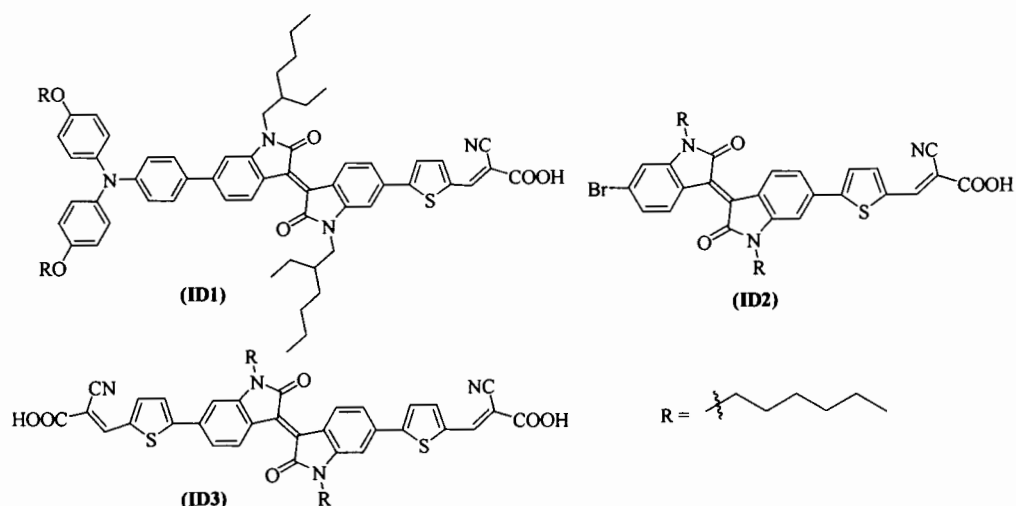


Figure 2.8 The structure of ID1-ID3 dye-sensitized molecules

In 2008, the efficiency and stability of organic dye **JK79**, improving working's quality of dye-sensitized solar cells, were studied by Kim, D. et al [37]. The improvement could be done by combining of bis-dimethylfluorenyl amino and indole group to target dye-sensitized molecule for increasing pi bond conjugation. The target molecule **JK79** was synthesized from indole substance **10JK**. The four reaction steps of compound **10JK** gave aldehyde **13JK**, and then it was reacted with cyanoacetic acid and piperidine to be Knoevenagel consideration to gain the target compound **JK79** as shown in **Figure 2.9**. The result of photo properties show that compound **JK79** gave short circuit at 13.62 mA/cm², open circuit voltage at 0.705 V, fill factor at 0.74 and conversion efficiency at 7.18%

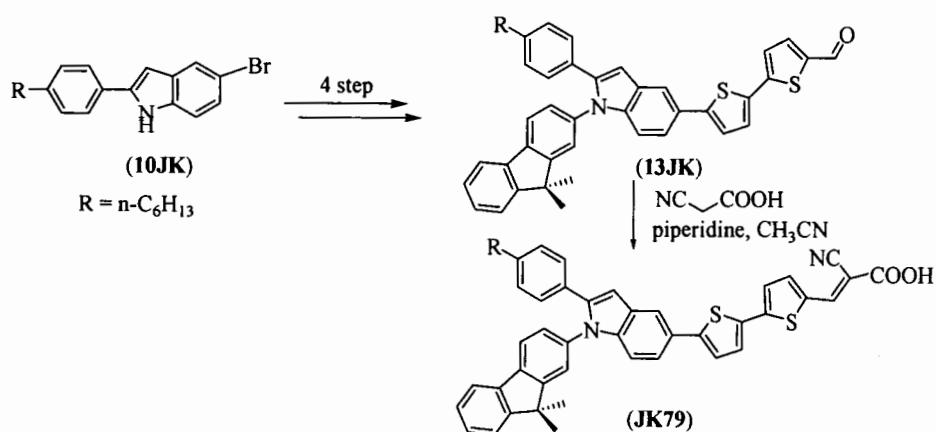


Figure 2.9 Dye-organic synthesis (8)

In 2013, Kim, B. H. et al. [38] synthesized organic dyeing (**DP-T**) and (**DP-P**) which included thiophene and *N*-methyl pyrrole as the connective between electron donors and electron acceptors respectively. The targets molecules were synthesized by Knoevenagel condensation of aldehyde (**1c**) and (**2d**) with cyanoacetic acid as shown in **Figure 2.10**. For bringing this to study about conversion efficiency, the result revealed that a thiophene derivative **DP-T** had the highest value as 3.53% and a methyl pyrrole derivative **DP-P** had the utmost value as 3.03%. It was clear that a thiophene derivative **DP-T** was more efficient than a methyl pyrrole derivative **DP-P**. This affected from thiophene captured and absorbed solar energy better than *N*-methyl pyrrole, so it was more conversion efficiency than *N*-methyl pyrrole.

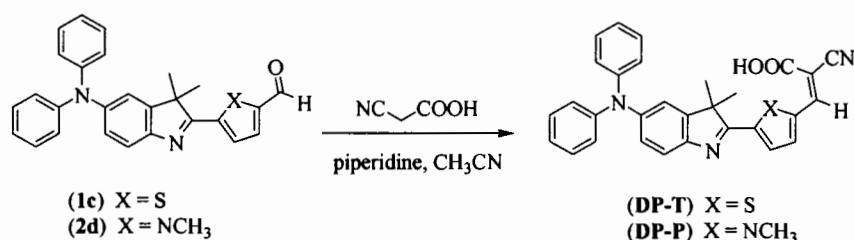


Figure 2.10 The synthesis of organic dyeing included of thiophene and *N*-methyl pyrrole as the connectors

In 2014, dye-sensitized type D-D- π -A, indole **SD1** and **SD2** (**Figure 2.11**), were synthesized and studied by Liu, X. et al [39]. The synthesis compounds included triphenylamine and indole as electron donors. The results of conversion efficiency indicated that the conversion efficiency (η) of dye-sensitized type **SD2** at 6.74% higher than the conversion efficiency (η) at 5.53% of **SD1**. It was believe that donated effective of SCN group of **SD2** stronger than H aton of **SD1**.

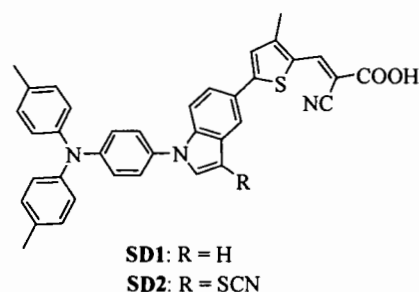


Figure 2.11 structure of SD1 and SD2

In 2015, new D- π -A type indole dye-sensitized **D1**, **D2** and **D3** (Figure 2.12), were synthesized and studied by BaBu, D. D. et al [40]. The target dyes included indole as electron donor and cyanoacetic acid, rhodanine-3-acetic acid and 4-aminobenzoic acid as electron acceptor, respectively. The dye **D1**, **D2** and **D3** gave conversion efficiency at 1.04, 0.35 and 1.18%. Interestingly, the absorption maximum red shifted in the order **D3**<**D**<**D2** but the device sensitized by **D3** displayed the highest efficiency.

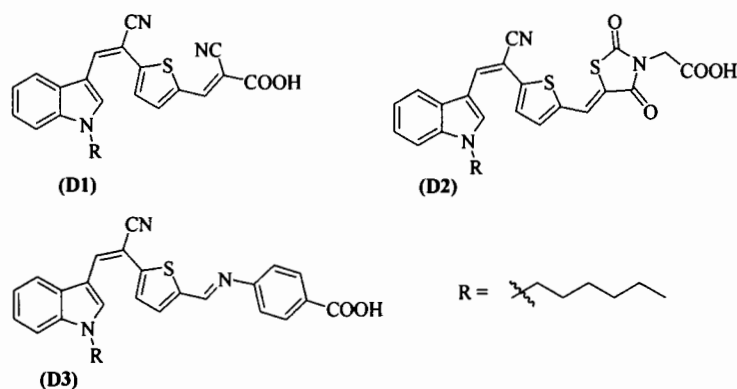


Figure 2.12 structure of D1, D2 and D3

2.1.5 Aim of the thesis

According to literature reviews, dye-sensitized molecule consist of major three parts [41]. The first part is electron donating group (D) which is electron rich function such as hetroaromatic group; carbazole, coumarins, triphenylamines and indolines. The second part is electron acceptor (A) which is electron withdrawing and polar group such as carboxyl group and sulfonyl group. The final part of dye is π -

spacer (π) which is conjugation linker between electron donating and electron acceptor group such as double bond and phenyl group.

In this research, we synthesized and characterized a new series of indole derivatives for dye-sensitized solar cells (DSSCs). The indole derivatives as electron donating group, containing double bond and phenyl group as π -spacer and benzoic and cyanoacetic acid group as electron acceptor, were designed, synthesized and characterized. The chemical structure of **In1-In5** are shown in **Figure 2.13**.

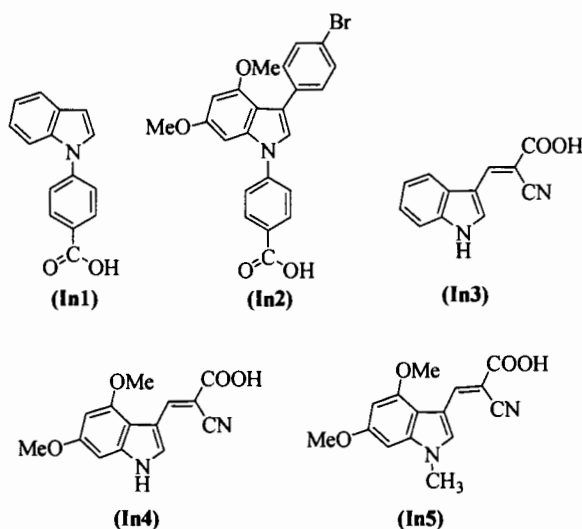


Figure 2.13 The target molecules **In1-In5**

2.1.5.1 Objectives of this research

To synthesize a series of aromatic or double bond and carboxyl-substituted indole derivatives as dye sensitizer for dye-sensitized solar cells.

To characterize and identify the target product during the synthesis steps.

2.2 RESULTS AND DISCUSSION

In this research, we synthesize and characterize a new series of dye-sensitized molecule for dye-sensitized solar cells (DSSCs) based on indole derivatives as electron donating group. Moreover, we designed and synthesized the following a indole containing double bond and phenyl group as π -spacer and benzoic and

cyanoacetic acid group as electron acceptor. The chemical structure of target molecules, **In1-In5**, are shown in **Figure 2.14**.

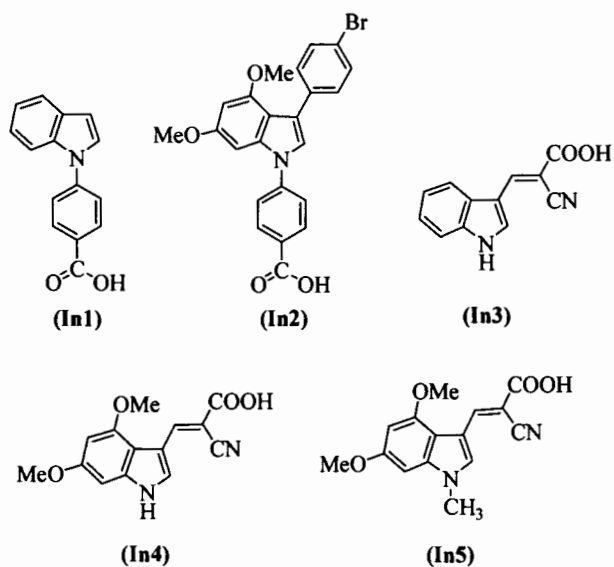


Figure 2.14 Structure of In1-In5

The target carbazole **In1-In5** were successfully synthesized by Ullman coupling, hydrolysis reaction and Knoevenagal condensation. The targets **In1** and **In2** were synthesized from Ullman coupling of indole with iodoarylester following by hydrolysis reaction. In addition, The indoles **In3-In5** was synthesized *via* Knoevenagal condensation of indolealdehyde with cyanoacetic acid as shows in **Figure 2.15**.

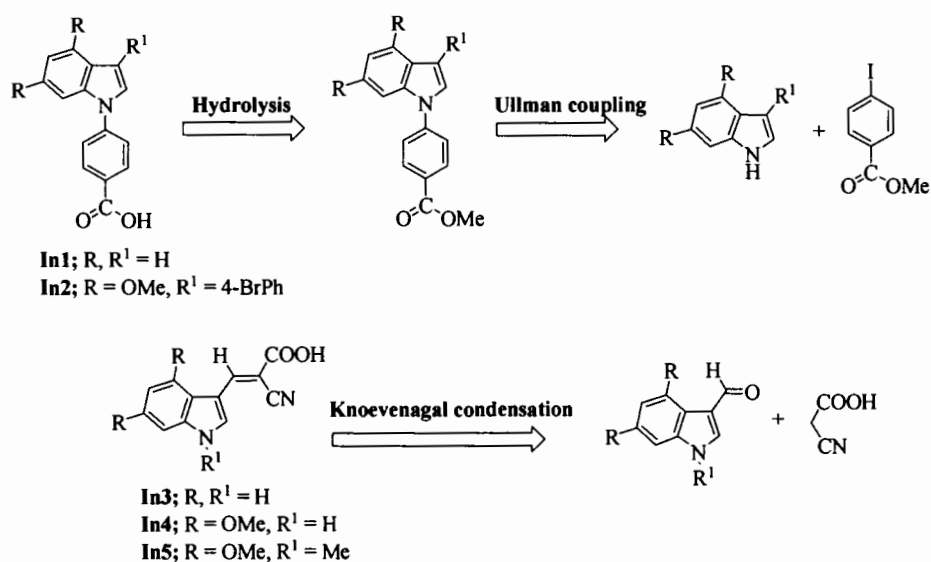


Figure 2.15 Retrosynthesis of carbazole In1-In5

2.2.1 Synthesis and characterization of 4-(indol-1-yl)benzoic acid (**In1**)

The target dye **In1**, containing indole as electron donating group, phenyl as π -spacer at *N*-position of indole and carboxyl group as electron acceptor was designed. The 4-(indol-1-yl)benzoic acid (**In1**) was successfully synthesized by Ullman coupling and hydrolysis reaction. First step, compound **4** was synthesized by Ullman coupling reaction of indole with methyl 4-iodobenzoate. The treatment of indole and methyl 4-iodobenzoate in the presence of copper iodide and trans-1,2-diaminocyclohexane as catalyst and K₃PO₄ as a base in toluene at reflux for 48 h led to compound **4** in 94% as show in **Figure 2.16**.

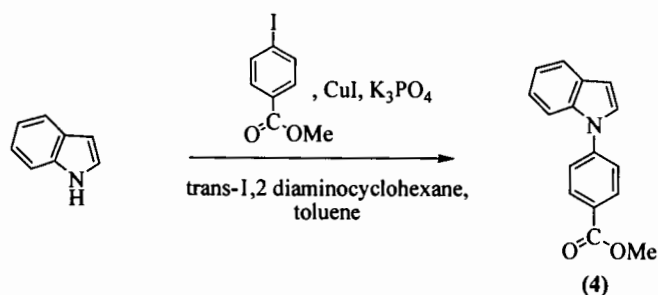


Figure 2.16 Synthesis of methyl 4-(indol-1-yl) benzoate 4

The compound **4** was confirmed by $^1\text{H-NMR}$ and $^{13}\text{C-NMR}$. $^1\text{H-NMR}$ spectra of compound **4** shows new peak of four protons of aryl group and the singlet peak of O-CH₃ protons at $\delta = 3.98$ (3H) ppm. Remarkable, the NH proton of indole was absented. Moreover, $^{13}\text{C-NMR}$ spectrum shows peck of C = O carbons at $\delta = 166.4$ ppm, new peak of six carbons of aryl carbon and new signal of O-CH₃- at $\delta = 52.2$ ppm. These results confirmed that product was methyl 4-(indol-1-yl) benzoate **4**.

The mechanism of Ullman coupling reaction follows a three-step mechanism cycle as described in **Figure 2.17**. The reaction of CuI, indole and K₃PO₄ afforded intermediate **[M]**. The oxidative addition at C-I bond of methyl 4-iodobenzoate with intermediate **[M]** gave organocopper complex **[N]**. Then, reductive elimination of complex **[N]** releases the coupling product **4** and the active CuI catalyst is regenerated.[42]

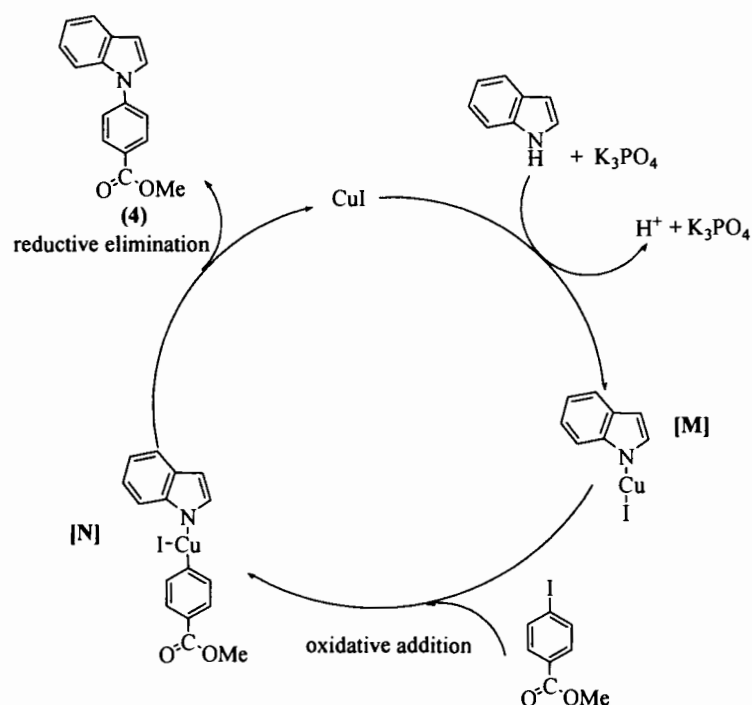


Figure 2.17 The proposed mechanism of Ullmann coupling reaction

Finally, the target molecule **In1** was synthesized by hydrolysis reaction. The treatment of methyl 4-(indol-1-yl)benzoate **4** and KOH as the base in THF and IPA at reflux for 2 h afforded target molecules **In1** in 64% yields as shows in **Figure 2.18**



Figure 2.18 Hydrolysis reaction of methyl 4-(indol-1-yl)benzoate 4

The compound **In1** was confirmed by $^1\text{H-NMR}$ and $^{13}\text{C-NMR}$. $^1\text{H-NMR}$ spectra of compound **In1** still show ten proton of aryl group but peak of O-CH_3 disappeared. Remarkable, $^{13}\text{C-NMR}$ spectrum of **In1** disappeared carbon peak of O-CH_3 group. Moreover, the high resolution mass spectrometry (MALDI-TOF) of compound **In1** found 237.1056 (calcd for $\text{C}_{15}\text{H}_{11}\text{NO}_2$: m/z 237.0790). These results confirmed that product was 4-(indol-1-yl) benzoic acid **In1**.

The mechanism of hydrolysis reaction was proposed *via* three-step as show in **Figure 2.19**[22]. First step, the hydroxide nucleophiles attacks at the electrophilic C=O of ester breaking the π bond and creating the intermediate **[O]**. The intermediate **[O]** collapses, reforming the C=O results in the loss of the leaving group the alkoxide, MeO^- , leading to the carboxylic acid. Finally, A very rapid equilibrium where the alkoxide, MeO^- functions as a base deprotonating the carboxylic acid, RCO_2H , (an acidic work up would allow the carboxylic acid **In1** to be obtained from the reaction).

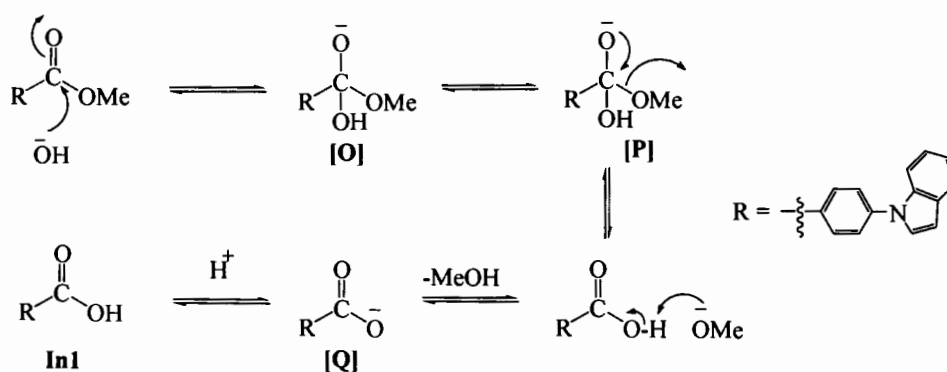


Figure 2.19 The proposed mechanism of hydrolysis reaction

2.2.2 Synthesis and characterization 4-(3-(4-bromophenyl)-4,6-dimethoxyindol-1-yl)benzoic acid (**In2**)

The target dye **In2**, containing 4,6-dimethoxyindole as electron donating group, phenyl as π -spacer at *N*-position of indole and carboxyl group as electron acceptor was designed. The 4-(3-(4-bromophenyl)-4,6-dimethoxyindol-1-yl) benzoic acid (**In2**) was synthesized *via* Ullman coupling and hydrolysis reaction similar to **In1** synthetic partway. First step, methyl 4-(3-(4-bromophenyl)-4,6-dimethoxyindol-1-yl) benzoate **6** was synthesized by Ullman coupling reaction of indole **5** with methyl 4-iodobenzoate. The treatment of indole **5** and methyl 4-iodobenzoate in the presence of copper iodide and *trans*-1,2-diaminocyclohexane as catalyst and K_3PO_4 as a base in toluene at reflux for 48 h led to ester **6** in 41% as show in **Figure 2.20**.

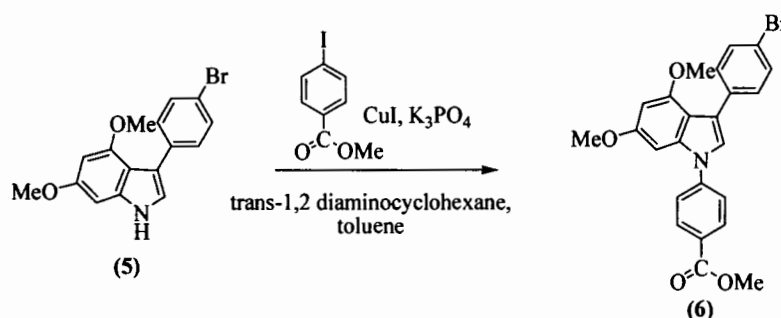


Figure 2.20 Synthesis of methyl 4-(3-(4-bromophenyl)-4,6-dimethoxyindol-1-yl) benzoate **6**

The compound **6** was confirmed by 1H -NMR and ^{13}C -NMR. 1H -NMR spectra of compound **6** show new peak of four protons of aryl group and new peak of three protons of O-CH₃ group. Remarkable, the N-H proton of indole **5** was absented. Moreover, ^{13}C -NMR spectrum shows peck of O=C carbons at $\delta = 166.3$ ppm, new peak of six carbons of aryl carbon and new peak of one carbon of O-CH₃ group. These results confirmed that product was of methyl 4-(3-(4-bromophenyl)-4,6-dimethoxyindol-1-yl)benzoate **6**.

The mechanism of Ullmann coupling of compound **6** similar to mechanism of Ullmann coupling of compound **4** as shown in **Figure 2.17**.

Finally, the target molecules **In2** was synthesized by hydrolysis reaction. The treatment of methyl 4-(3-(4-bromophenyl)-4,6-dimethoxyindol-1-yl)benzoate **6**

and KOH as the base in THF and IPA at reflux for 2 h afforded target molecules **In2** in 46% yields as shows in **Figure 2.21**.

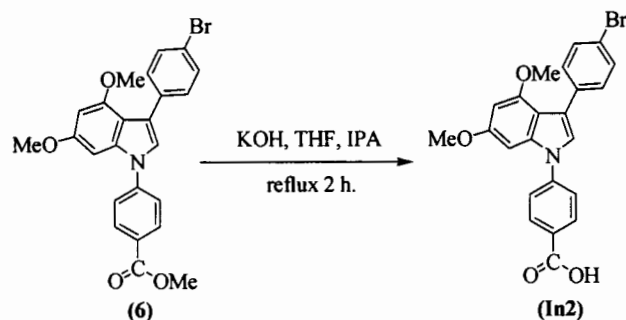


Figure 2.21 Hydrolysis reaction of methyl 4-(3-(4-bromophenyl)-4,6-dimethoxy indol-1-yl)benzoate 6

The compound **In2** was confirmed by $^1\text{H-NMR}$ and $^{13}\text{C-NMR}$. $^1\text{H-NMR}$ spectra of compound **In2** still show eleven protons of aryl group but proton of O-CH_3 reduced to six protons. Remarkable, $^{13}\text{C-NMR}$ spectrum of **In2** shown two carbon peak of O-CH_3 group. Moreover, the high resolution mass spectrometry (MALDI-TOF) of compound **In2** found 451.0924 (calcd for $\text{C}_{23}\text{H}_{18}\text{BrNO}_4$: m/z 451.0419). These results confirmed that product was 4-(3-(4-bromophenyl)-4,6-dimethoxyindol-1-yl) benzoic acid (**In2**).

The mechanism of hydrolysis of compound **6** similar to mechanism of hydrolysis of compound **4** as shown in **Figure 2.19**.

2.2.3 Synthesis and characterization of 2-cyano-3-(indol-3-yl)acrylic acid (**In3**)

The target dye **In3**, containing indole as electron donating group, double bond as π -spacer at C3-position of indole and cyanoacetic acid as electron acceptor was designed. The 2-cyano-3-(indol-3-yl)acrylic acid (**In3**) was easy synthesized by Knoevenagal condensation. The commercial indole-3-carbaldehyde **7** was reacted with cyanoacetic acid and piperidine in chloroform at reflux for 48 h led to 2-cyano-3-(indol-3-yl)acrylic acid **In3** in 24% as show in **Figure 2.22**.

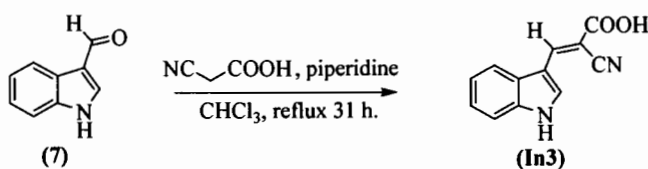


Figure 2.22 Knoevenagel reaction of indole-3-carbaldehyde 7

The 2-cyano-3-(indol-3-yl)acrylic acid **In3** was confirmed by $^1\text{H-NMR}$ and $^{13}\text{C-NMR}$. $^1\text{H-NMR}$ spectra of compound **In3** still show five protons of aryl and one proton of N-H group and new one proton peak of C=C-H group. Remarkable, the formyl proton (-CHO) of indole-3-carbaldehyde **7** was absent. In addition, $^{13}\text{C-NMR}$ spectrum shows new peak of carboxyl carbons (COOH) at $\delta = 165.9$ ppm, new peak of CN carbons at $\delta = 110.6$ ppm and new two carbon peak of alkene group. Moreover, the high resolution mass spectrometry (MALDI-TOF) of compound **In3** found 212.0361 (calcd for $\text{C}_{12}\text{H}_8\text{N}_2\text{O}_2$: m/z 212.0586). These results confirmed that product was 2-cyano-3-(indol-3-yl)acrylic acid (**In3**).

The mechanism of Knoevenagel reaction follows a step mechanism as described in **Figure 2.23**. [44]. In the first step, deprotonation of the cyanoacetic acid by piperidine afforded carbanion intermediate **[R]**. On the other hand, aldehyde **7** reacted with piperidine to give intermediate **[S]** and then release OH^- to give intermediate **[T]**. Next step, carbanion **[R]** attack at C=N of intermediate **[T]** gave intermediate **[U]**. Finally, elimination of piperidine afford target molecule **In3**.

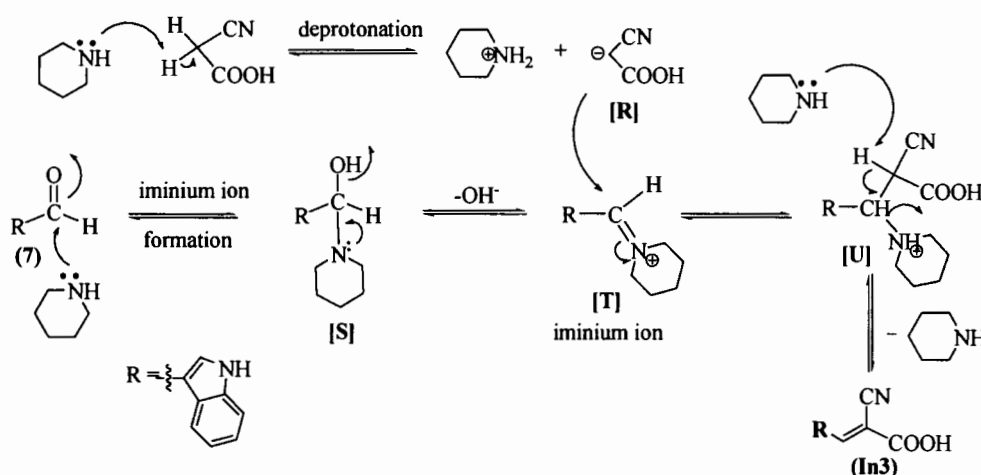


Figure 2.23 The proposed mechanism of Knoevenagel reaction

2.2.4 Synthesis and characterization of 2-cyano-3-(4,6-dimethoxyindol-3-yl)acrylic acid (**In4**)

The target dye **In4**, containing 4,6 dimethoxyindole as electron donating group, double bond as π -spacer at C3-position of indole and cyanoacetic acid as electron acceptor was designed. The 2-cyano-3-(4,6-dimethoxyindol-3-yl)acrylic acid (**In4**) was successfully synthesized by Vilsmeier–Haack reaction and Knoevenagel condensation. First step, aldehyde **9** was synthesized by Vilsmeier–Haack reaction of 4,6-dimethoxyindole **8** [45]. The treatment of compound **8** with phosphoryl chloride in *N,N*-dimethylformamide stirred at 0 °C to room temperature for 1 h led to compound **9** in 58% as show in **Figure 2.24**.

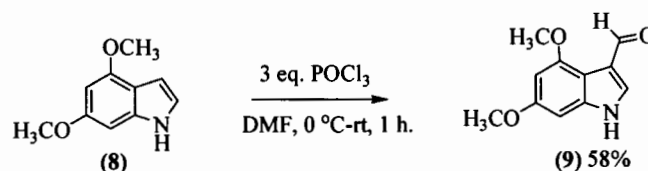


Figure 2.24 Vilsmeier–Haack reaction of 4,6-dimethoxyindole **8**

The compound **9** was confirmed by ¹H-NMR and ¹³C-NMR. ¹H-NMR spectra of compound **9** show new one peak proton of CHO group at 10.36 ppm, still show six protons of O-CH₃ and one peak of N-H proton but protons of aryl group reduced to three proton. Moreover, ¹³C-NMR spectrum shows new peck carbon of CHO group at $\delta = 188.3$ ppm and one C-H carbon peak was absented compare to ¹³C-NMR of starting material. These results confirmed that product was 3-formyl-4,6-dimethoxyindole **9**.

The mechanism of Vilsmeier–Haack reaction follows a step mechanism as described in **Figure 2.25**. In the first step, reaction of DMF and POCl₃ gave intermediate [**V**] and then then release PCl₂O₂⁻ afforded intermediate [**W**]. Next step, reaction C3 of indole **8** attack at C=N of intermediate [**W**] gave intermediate [**X**] and Cl⁻. Deprotonation of intermediate [**X**] gave intermediate [**Y**]. Finally, imminium hydrolysis of intermediate [**Y**] afford indole aldehyde [46] **9**.

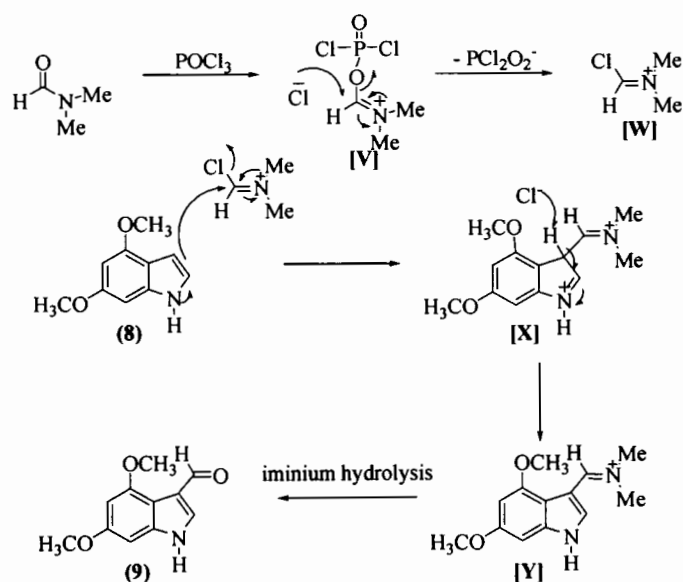


Figure 2.25 The proposed mechanism of Vilsmeier–Haack reaction

Finally, the target molecule **In4** was synthesized by Knoevenagel reaction. The 3-formyl-4,6-dimethoxyindole **9** reacted with cyanoacetic acid and piperidine in chloroform at reflux for 48 h led to 2-cyano-3-(4,6-dimethoxyindol-3-yl) acrylic acid **In4** in 27% as show in **Figure 2.26**.

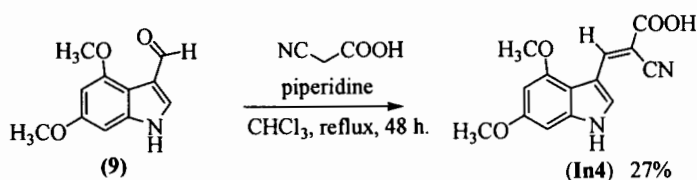


Figure 2.26 Knoevenagel reaction of 3-formyl -4,6-dimethoxyindole **9**

The 2-cyano-3-(4,6-dimethoxyindol-3-yl)acrylic acid **In4** was confirmed by ¹H-NMR and mass spectrometry. ¹H-NMR spectra of compound **In4** still show three protons of aryl, one protons of N-H group and new one proton peak of C=C-H group. Remarkable, the formyl proton (–CHO) of 3-formyl -4,6-dimethoxyindole **9** was not appeared. Moreover, the high resolution mass spectrometry (MALDI-TOF) of compound **In4** found 272.0978 (calcd for C₁₄H₁₂N₂O₄: *m/z* 272.0797). These results confirmed that product was 2-cyano-3-(4,6-dimethoxyindol-3-yl)acrylic acid **In4**.

The mechanism of Knoevenagel reaction of compound **In4** similar to mechanism of Knoevenagel reaction of compound **In3** as shown in **Figure 2.23**.

2.2.5 Synthesis and characterization of 2-cyano-3-(4,6-dimethoxy-*N*-methylindol-3-yl) acrylic acid (**In5**)

The target dye **In5**, containing 4,6-dimethoxy-*N*-methylindole as electron donating group, double bond as π -spacer at C3-position of indole and cyanoacetic acid as electron acceptor was designed. The 2-cyano-3-(4,6-dimethoxy-*N*-methylindol-3-yl)acrylic acid (**In5**) was successfully synthesized by methylation and Knoevenagel reaction. First step, 3-formyl-4,6-dimethoxyindole **9** was synthesized by methylation reaction at the *N*-position. Treatment of 3-formyl-4,6-dimethoxyindole **9** with sodium hydride (NaH) and methyl iodide in DMF for 1.5 h under N₂ gas gave 3-formyl-4,6-dimethoxy-*N*-methylindol **10** in 97% as show in **Figure 2.27**.

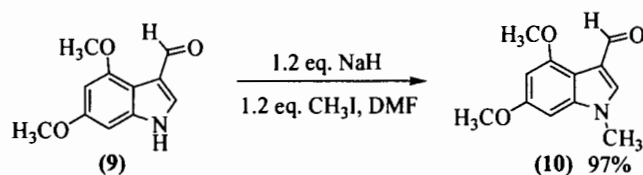


Figure 2.27 Methylation of 3-formyl -4,6-dimethoxyindole **9**

The 3-formyl-4,6-dimethoxy-*N*-methylindol **10** was confirmed by ¹H-NMR and ¹³C-NMR [25]. ¹H-NMR spectra of 9-dodecylcarbazole **2** still show proton of -CHO, aryl and OCH₃ group and shows new singlet peak of N-CH₃- proton at $\delta = 3.96$ ppm. Remarkable, NH proton of 3-formyl-4,6-dimethoxyindole **9** was absented. Moreover, ¹³C-NMR spectrum shows new signal of N-CH₃- at $\delta = 39.2$ ppm. These results confirmed that product was compound **10**.

The mechanism of methylation reaction of compound **10** similar to mechanism of alkylation reaction of carbazole **1** as shown in chapter 1 **Figure 1.13**.

Finally, the target molecules **In5** was synthesized by Knoevenagel reaction. The 3-formyl-4,6-dimethoxy-*N*-methylindol **10** reacted with cyanoacetic acid and piperidine in chloroform at reflux for 24 h led to 2-cyano-3-(4,6-dimethoxy-*N*-methylindol-3-yl)acrylic acid **In5** in 79% as show in **Figure 2.28**.

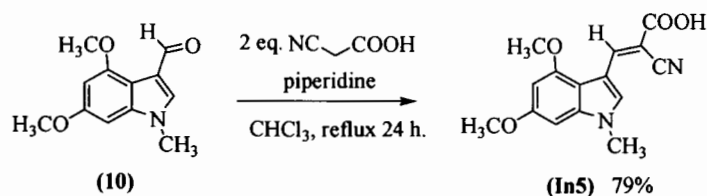


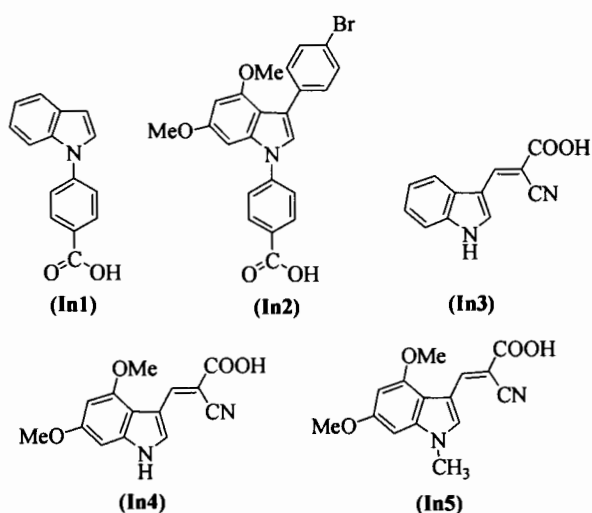
Figure 2.28 Knoevenagel reaction of 3-formyl-4,6-dimethoxy-*N*-methylindol 10

The 2-cyano-3-(4,6-dimethoxy-*N*-methylindol-3-yl) acrylic acid **In5** was confirmed by $^1\text{H-NMR}$ and $^{13}\text{C-NMR}$. $^1\text{H-NMR}$ spectra of compound **In5** still show three protons of aryl, three protons of N-CH_3 group, six protons of O-CH_3 and new one proton peak of C=C-H group. Remarkable, the formyl proton ($-\text{CHO}$) of 3-formyl-4,6-dimethoxy-*N*-methylindol **10** was not appeared. $^{13}\text{C-NMR}$ spectrum shows new peak of carboxyl carbons (COOH) at $\delta = 165.4$ ppm, new peak of CN carbons at $\delta = 114.5$ ppm and new two carbon peak of alkene group. Moreover, the high resolution mass spectrometry (MALDI-TOF) of compound **In5** found 286.1352 (calcd for $\text{C}_{15}\text{H}_{14}\text{N}_2\text{O}_4$: m/z 286.0954). These results confirmed that product was 2-cyano-3-(4,6-dimethoxy-*N*-methylindol-3-yl)acrylic acid **In5**.

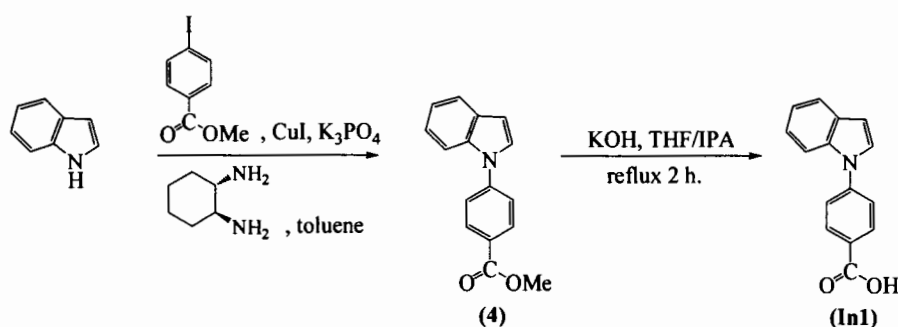
The mechanism of Knoevenagel reaction of compound **In5** similar to mechanism of Knoevenagel reaction of compound **In3** as shown in **Figure 2.23**.

2.3 CONCLUSION

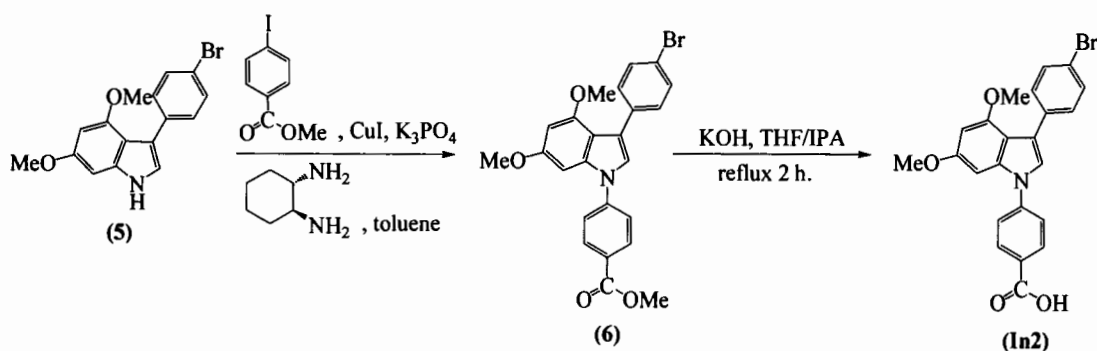
In this reserch, a new series of indole derivatives **In1-In5**, containing varies electron donating, π -spacer and electron acceptor, for using as dye molecules in DSSCs were successfully synthesized. The target molecules were synthesized by using Ullman coupling, hydrolysis reaction, Knoevenagel condensation and Vilsmeier-Haack reaction.



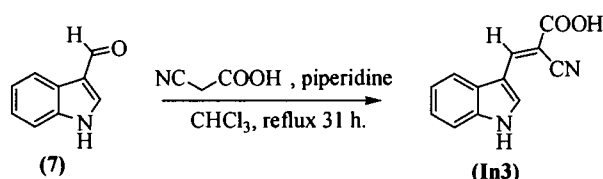
In the first, the target molecule **In1** was synthesized by Ullman coupling reaction of indole with methyl 4-iodobenzoate led to ester **4** in 94% and then hydrolysis of ester **4** with KOH to afforded 2-cyano-3-(indol-3-yl)acrylic acid **In1** in 64% yields.



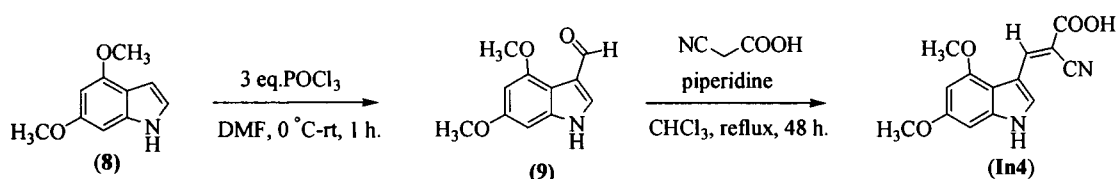
In the same way, the target molecule **In2** was synthesized by Ullman coupling reaction of 3-(4-bromophenyl)-4,6-dimethoxyindole **5** with methyl 4-iodobenzoate led to ester **6** in 41% and following by hydrolysis reaction of ester **6** with KOH afforded 4-(3-(4-bromophenyl)-4,6-dimethoxyindol-1-yl)benzoic acid **In2** in 46%.



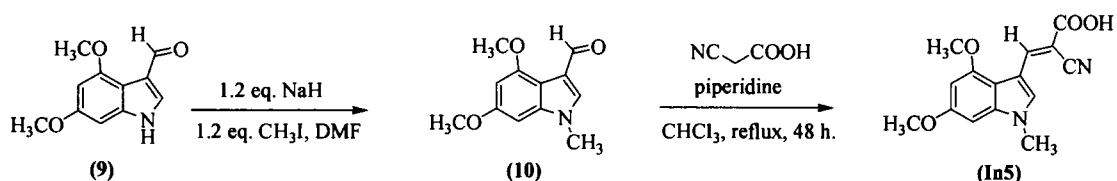
The target molecule **In3** was easily synthesized by Knoevenagel condensation. The commercial indole-3-carbaldehyde **7** was reacted with cyanoacetic acid led to 2-cyano-3-(indol-3-yl)acrylic acid **In3** in 24%.



The target molecule **In4** was successfully synthesized by Vilsmeier–Haack reaction and Knoevenagel condensation. First step, Vilsmeier–Haack reaction of 4,6-dimethoxyindole **8** led to aldehyde **9** in 58%. Next, Knoevenagel reaction of aldehyde **9** with cyanoacetic acid led to 2-cyano-3-(4,6-dimethoxyindol-3-yl)acrylic acid **In4** in 27%.



The final target molecule **In5** was successfully synthesized by methylation and Knoevenagel reaction. First step, methylation of aldehyde indole **9** gave 3-formyl-4,6-dimethoxy-*N*-methylindole **10** in 97%. Finally, Knoevenagel reaction of aldehyde **10** with cyanoacetic acid led to 2-cyano-3-(4,6-dimethoxy-*N*-methylindol-3-yl)acrylic acid **In5** in 79%.



All target molecules were characterized by using melting points, ¹H-NMR and ¹³C-NMR spectroscopy, FT-IR spectroscopy and mass spectrometer. Unfortunately we have no time for fabrication of solar cell all of them but we will complete it in the

future. Moreover, we believe that the target compound **In1-In5** are promising candidates for improvement of the performance of the DSSCs.

2.4 EXPERERIMENTAL

2.4.1 General experiment

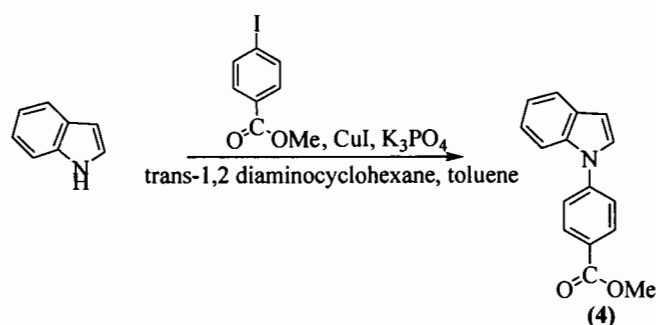
All solvents and reagents were purchased from Aldrich, Acros and Fluka received unless otherwise stated. Analytical thin-layer chromatography (TLC) was performed with Merck aluminium plates coated with silica gel 60 F₂₅₄. Column chromatography was carried out using gravity feed chromatography with Merck silica gel mesh, 60 Å. Where solvent mixtures are used, the portions are given by volume.

Melting points was measured by BUCHI 530 model in open capillary method and are uncorrected and reported in degree Celsius.

¹H and ¹³C NMR spectra were recorded on a Brüker AVANCE 300 MHz spectrometer. Chemical shifts (δ) are reported relative to the residual solvent peak in part per million (ppm). Coupling constants (J) are given in Hertz (Hz). Multiplicities are quoted as singlet (s), broad (br), doublet (d), triplet (t), quartet (q), and multiplet (m).

The IR spectra were recorded on Perkin-Elmer FT-IR spectrum RXI spectrometer. The absorption peaks are quoted in wavenumber (cm⁻¹). UV-Vis spectra were recorded on a Perkin-Elmer UV Lambda 25 spectrometer. MALDI-TOF mass spectra were recorded on Bruker Daltonics (Bremen, Germany) Autoflex II Matrix-Assisted Laser Desorption/Ionization-Time of Flight Mass Spectrometer (BIFEX) using α -cyano-4-hydroxycinnamic acid as matrix.

2.4.2 Synthesis of methyl 4-(indol-1-yl)benzoate



General Procedure of Ullman coupling:

A mixture of indole (0.1023 g, 0.8737 mmol), methyl 4-iodobenzoate (0.1908 g, 0.7281 mmol), CuI (0.0693 g, 0.3640 mmol), and K₃PO₄ (0.4636 g, 2.1843 mmol) in round bottom flask were added toluene (20 mL) and trans-1,2-diaminocyclohexane (0.0414 g, 0.3640 mmol). The mixture was degassed and stirred at reflux under N₂ for 48 h. After being cooled to room temperature, water (50 mL) was added and extracted with CH₂Cl₂ (50 mL x 3). The combined organic phases were washed with water (50 mL) and brine solution (70 mL), dried over MgSO₄ and evaporated under reduce pressure. Purification of crude reaction by column chromatography eluting with 1:3 v/v ethyl acetate/hexane gave methyl 4-(indol-1-yl)benzoate **4** (0.1719 g, 94%).

C₁₆H₁₃NO₂; m.p. = 50-52 °C

¹H-NMR (300 Hz, CDCl₃):

δ = 8.21 (d, 2H, ArH, *J* = 7.8 Hz), 7.72-7.55 (m, 4H, ArH), 7.39 (d, 1H, ArH, *J* = 2.4 Hz), 7.30-7.13 (m, 2H, ArH), 6.74 (d, 1H, ArH, *J* = 1.8 Hz), 3.98 (s, 3H, OCH₃) ppm.

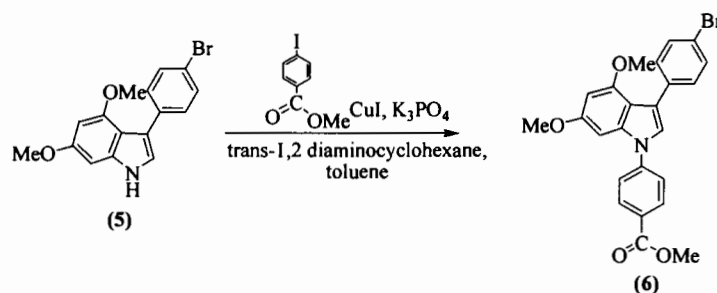
¹³C-NMR (75 Hz, CDCl₃):

δ = 166.4 (C=O), 143.8 (Cq), 135.5 (Cq), 131.3 (2 x CH), 129.8 (Cq), 127.6 (Cq), 127.4 (CH), 123.3 (2 x CH), 122.9 (CH), 121.4 (CH), 121.0 (CH), 110.6 (CH), 104.9 (CH), 52.2 (OCH₃) ppm.

IR (KBr):

ν_{max} = 3050, 2948, 1706, 1602, 1453, 1431, 1279, 1210, 1095, 745 cm⁻¹.

2.4.3 Synthesis of methyl 4-(3-(4-bromophenyl)-4,6-dimethoxyindol-1-yl)benzoate



According to general procedure of Ullman coupling, treatment of 3-(4-bromophenyl)-4,6-dimethoxyindole **5** (0.4000 g, 1.20 mmol), methyl 4-iodobenzoate (0.2629 g, 1.00 mmol), CuI (0.0094 g, 0.04 mmol), trans-1,2-diaminocyclohexane (0.0570 g, 0.50 mmol), K₃PO₄ (0.4473 g, 2.10 mmol) and toluene (40 mL) gave yellow oil methyl 4-(3-(4-bromophenyl)-4,6-dimethoxyindol-1-yl)benzoate **6** (0.1918 g, 41%).

C₂₄H₂₀BrNO₄;

¹H-NMR (300 Hz, CDCl₃):

δ = 8.21 (d, 2H, *J* = 8.1 Hz), 7.71-7.50 (m, 6H), 7.14 (s, 1H), 6.69 (s, 1H), 6.33 (s, 1H), 3.97 (s, 3H), 3.82 (s, 6H) ppm.

¹³C-NMR (75 Hz, CDCl₃):

δ = 166.3 (O=C), 158.4 (Cq), 155.0 (Cq), 143.5 (Cq), 138.0 (Cq), 136.7 (Cq), 134.3 (Cq), 131.3 (2 x CH), 131.1 (2 x CH), 130.7 (2 x CH), 128.1 (Cq), 123.8 (CH), 123.7 (2 x CH), 120.2 (Cq), 119.8 (Cq), 93.27 (CH), 86.6 (CH), 55.7 (OCH₃), 55.2 (OCH₃), 52.3 (OCH₃) ppm.

IR (KBr):

ν_{\max} = 2996, 2946, 2843, 1718, 1602, 1433, 1274, 1206, 1174, 1085, 730 cm⁻¹.

2.4.4 Synthesis of 4-(indol-1-yl)benzoic acid



General Procedure of Hydrolysis reaction:

Methyl 4-(indol-1-yl)benzoate **4** (0.1500 g, 0.5969 mmol) and KOH (0.0610 g, 1.1938 mmol) were dissolved in THF (10 mL) and IPA (10 mL). The reaction mixture was stirred at reflux for 2 h and monitored by TLC until it was complete. Acid H₃PO₄ 2M (50 mL) was added, and the reaction was extracted with DCM (20 mL x 2), washes with water (20 mL x 2) and bicine solution (20 mL x 2), and then dried over Na₂SO₄ anhydrous, followed by recrystallization by hexane/EtOH to give 4-(indol-1-yl)benzoic acid **In1** (0.0905 g, 64%).

C₁₅H₁₁NO₂; m.p. > 200 °C

¹H-NMR (300 Hz, CDCl₃):

δ = 8.29 (d, 2H, *J* = 8.1 Hz), 7.72 – 7.64 (m, 4H), 7.41 (d, 1H, *J* = 3.0 Hz), 7.31-7.19 (m, 2H), 6.75 (d, 1H, *J* = 2.4 Hz) ppm.

¹³C-NMR (75 Hz, CDCl₃):

δ = 169.9 (O=C), 144.5 (Cq), 135.4 (Cq), 132.0 (2 x CH), 129.9 (Cq), 127.3 (CH), 126.5 (Cq), 123.3 (2 x CH), 123.0 (CH), 121.4 (CH), 121.1 (CH), 110.6 (CH), 105.2 (CH) ppm.

IR (KBr):

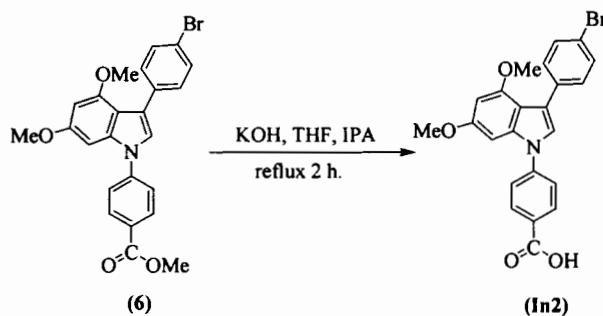
ν_{max} = 1666, 1599, 1452, 1426, 1315, 1291, 933, 822, 775, 721 cm⁻¹.

UV-vis spectroscopy (in CH₂Cl₂ at 5x10⁻⁶ M):

λ_{max} = 320 nm (ϵ = 1.11 x 10⁵ cm⁻¹ M⁻¹), 273 nm (ϵ = 9.20 x 10⁴ cm⁻¹ M⁻¹), 228 nm (ϵ = 1.27 x 10⁵ cm⁻¹ M⁻¹)

MALDI-TOF (*m/z*) calcd for C₁₅H₁₁NO₂: 237.0790; found 237.1056(M⁺).

2.4.5 Synthesis of 4-(3-(4-bromophenyl)-4,6-dimethoxyindol-1-yl)benzoic acid



According to general procedure of hydrolysis reaction, treatment of methyl 4-(3-(4-bromophenyl)-4,6-dimethoxyindol-1-yl) benzoate **6** (0.1227 g, 0.26 mmol), KOH (0.0268 g, 0.52 mmol), THF (10 mL) and IPA (10 mL) at reflux for 2 h gave 4-(3-(4-bromophenyl)-4,6-dimethoxyindol-1-yl) benzoic acid **In2** (0.0549 g, 46%).

$\text{C}_{23}\text{H}_{18}\text{BrNO}_4$; m.p. > 200°C

$^1\text{H-NMR}$ (300 Hz, CDCl_3):

δ = 8.29 (d, 2H, J = 8.4 Hz), 7.66 (d, 2H, J = 8.4 Hz), 7.51 (s, 4H), 7.16 (s, 1H), 6.72 (s, 1H), 6.35 (s, 1H), 3.84 (s, 3H), 3.83 (s, 3H) ppm.

$^{13}\text{C-NMR}$ (75 Hz, CDCl_3):

δ = 170.0 (O=C), 158.5 (Cq), 155.1 (Cq), 144.3 (Cq), 138.0 (Cq), 134.2 (Cq), 132.0 (2 x CH), 131.1 (2 x CH), 130.7 (2 x CH), 126.9 (Cq), 123.7 (2 x CH), 123.7 (Cq), 120.2 (Cq), 120.0 (Cq), 111.7 (Cq), 93.4 (CH), 86.7 (CH), 55.7 (OCH₃), 55.2 (OCH₃), ppm.

IR (KBr):

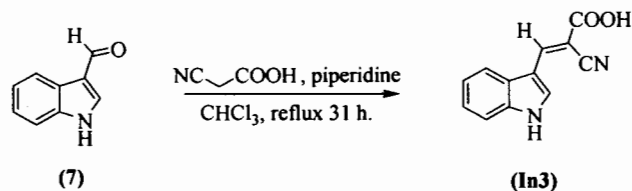
ν_{max} = 1689, 1594, 1429, 1318, 1293, 1240, 1208, 1174, 1083, 815, 769 cm^{-1} .

UV-vis spectroscopy (in CH_2Cl_2 at 5×10^{-6} M):

λ_{max} = 339 nm ($\epsilon = 3.50 \times 10^4 \text{ cm}^{-1} \text{ M}^{-1}$), 281 nm ($\epsilon = 7.28 \times 10^4 \text{ cm}^{-1} \text{ M}^{-1}$), 231 nm ($\epsilon = 1.07 \times 10^5 \text{ cm}^{-1} \text{ M}^{-1}$)

MALDI-TOF (m/z) calcd for $\text{C}_{23}\text{H}_{18}\text{BrNO}_4$: 451.0419; found 451.0924 (M^+).

2.4.6 Synthesis of 2-cyano-3-(indol-3-yl)acrylic acid



General Procedure of Knoevenagel condensation:

To solution of indole-3-carbaldehyde **7** (0.200 g, 1.38 mmol) and cyanoacetic acid (0.386 g, 4.54 mmol) in chloroform 20 mL was added piperidine (1 mL) and stirred at reflux for 48 h under N₂ gas. The mixture was extracted with ethyl acetate, washed with water, dried over MgSO₄ and evaporated under reduce pressure. The crude product was separated by column chromatography eluting with 1:9 v/v methanol/ethyl acetate to give 2-cyano-3-(indol-3-yl)acrylic acid **In3** (0.0696 g, 24%).

C₁₂H₈N₂O₂; m.p. > 200°C

¹H-NMR (300 Hz, CDCl₃):

δ = 8.61 (s, 1H), 8.55 (s, 1H), 7.81–7.78 (m, 1H), 7.54 (s, 1H), 7.48-7.46 (m, 1H), 7.29-7.22 (m, 2H) ppm.

¹³C-NMR (75 Hz, CDCl₃):

δ = 165.9 (O=C), 147.0 (CH), 136.3 (Cq), 131.5 (CH), 127.6 (Cq), 123.6 (CH), 122.1 (CH), 118.4 (Cq), 117.8 (CH), 112.4 (CH), 110.6 (CN), 93.3 (Cq) ppm.

IR (KBr):

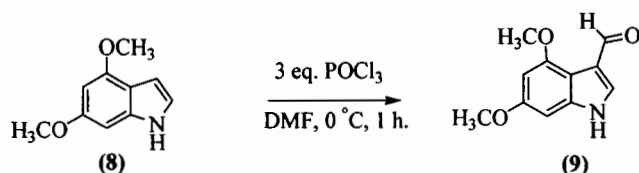
ν_{max} = 3296, 3063, 2925, 2208, 1606, 1398, 1113, 956, 742, 608 cm⁻¹.

UV-vis spectroscopy (in CH₂Cl₂ at 1x10⁻⁵ M):

λ_{max} = 389 nm (ε = 2.83 x 10⁴ cm⁻¹ M⁻¹), 276 nm (ε = 1.40 x 10⁴ cm⁻¹ M⁻¹), 229 nm (ε = 2.28 x 10⁴ cm⁻¹ M⁻¹)

MALDI-TOF (*m/z*) calcd for C₁₂H₈N₂O₂: 212.0586; found 212.0361 (M⁺).

2.4.7 Synthesis of 3-formyl -4,6-dimethoxyindole (9)



To a stirred and ice cooled solution of 4,6-dimethoxyindole **8** (0.5059 g, 2.86 mmol) in *N,N*-dimethylformamide (5 mL) was added dropwise an ice cooled solution of phosphoryl chloride (1.3159 g, 8.58 mmol) in *N,N*-dimethylformamide (5 mL). After stirred at 0 °C for 1 h, solution was allowed to come to room temperature and then was made strongly basic with 6 M sodium hydroxide solution (5 ml). The mixture was extracted with dichloromethane, washed with water, dried over MgSO₄ and evaporated under reduce pressure. The crude product was separated by column chromatography eluting with 3:2 v/v ethyl acetate/hexane to give 3-formyl -4,6-dimethoxyindole **9** (0.3391 g, 58%).

$C_{11}H_{11}NO_3$; m.p. = 148-153 °C

¹H-NMR (300 Hz, CDCl₃):

δ = 10.36 (s, 1H, CHO), 10.31 (brs, 1H, NH) 7.07 (t, 1H, ArH, J = 2.6 Hz), 6.56 (t, 1H, ArH, J = 2.6 Hz), 6.17 (s, 1H, ArH), 4.05 (s, 3H, OCH₃), 3.99 (s, 3H, OCH₃) ppm.

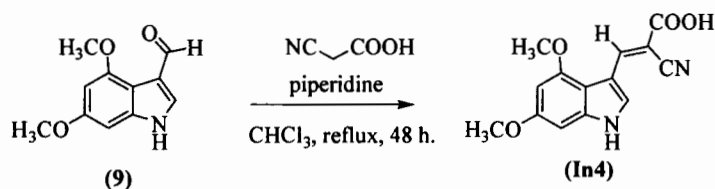
¹³C-NMR (75 Hz, CDCl₃):

δ = 188.3 (CHO), 163.1 (Cq), 160.2 (Cq), 136.7 (Cq), 122.7 (CH), 105.0 (Cq), 99.7 (Cq+CH), 86.8 (CH), 56.5 and 55.7 (2xOCH₃) ppm.

IR (KBr):

ν_{max} = 3368, 2850, 1630, 1500, 1218 cm⁻¹.

2.4.8 Synthesis of 2-cyano-3-(4,6-dimethoxyindol-3-yl)acrylic acid



According to general procedure of Knoevenagel condensation, treatment of 3-formyl-4,6-dimethoxyindole (**9**) (0.0819 g, 0.40 mmol), cyanoacetic acid (0.0683 g, 0.80 mmol) and piperidine (0.10 mL) in chloroform 20 mL gave 2-cyano-3-(4,6-dimethoxyindol-3-yl)acrylic acid **In4** (0.0290 g, 27%).

$\text{C}_{14}\text{H}_{12}\text{N}_2\text{O}_4$; m.p. = 171-174 °C

$^1\text{H-NMR}$ (300 Hz, $\text{CD}_3\text{OD} + \text{CDCl}_3$):

δ = 8.49 (s, 1H, NH), 7.80 (d, 1H, ArH, $J = 3.6$ Hz), 6.96 (d, 1H, ArH, $J = 3.6$ Hz), 6.37 (s, 1H, CH), 5.30 (s, 1H, CH), 4.16 (s, 3H, OCH_3), 4.05 (s, 3H, OCH_3) ppm.

IR (KBr):

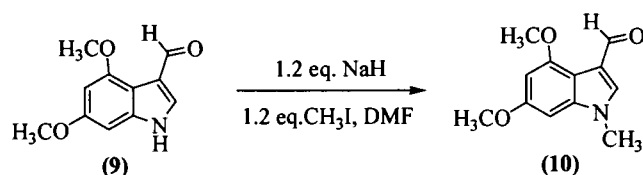
ν_{max} = 3100, 2921, 1633, 1603, 1264, 1070, 1050, 1032, 968, 719 cm^{-1} .

UV-vis spectroscopy (in CH_2Cl_2 at 5×10^{-6} M):

λ_{max} = 394 nm ($\epsilon = 4.90 \times 10^4 \text{ cm}^{-1} \text{ M}^{-1}$), 269 nm ($\epsilon = 2.24 \times 10^4 \text{ cm}^{-1} \text{ M}^{-1}$), 235 nm ($\epsilon = 2.08 \times 10^4 \text{ cm}^{-1} \text{ M}^{-1}$)

MALDI-TOF (m/z) calcd for $\text{C}_{14}\text{H}_{12}\text{N}_2\text{O}_4$: 272.0797; found 272.0978 (M^+).

2.4.9 Synthesis of 3-formyl-4,6-dimethoxy-*N*-methylindol



To a suspension of sodium hydride (NaH) (0.0145 g, 0.60 mmol) in *N,N*-dimethylformamide (DMF) 5 mL was added dropwise of 3-formyl-4,6-dimethoxyindole **9** (0.1022 g, 0.50 mmol) in DMF 5 mL. After stirred for 1 h, methyl iodide (0.0869 g, 0.60 mmol) was added into the reaction mixture and stirred for 1.5 h under N₂ gas. The mixture was neutralized with 6 M HCl, extracted with dichloromethane, washed with water, dried over MgSO₄ and evaporated under reduce pressure. The crude product was separated by column chromatography eluting with 1:4 v/v dichloromethane/hexane to give 3-formyl-4,6-dimethoxy-*N*-methylindol **10** (0.1055 g, 97%)

C₁₂H₁₃NO₃; m.p. = 100-106 °C

¹H-NMR (300 Hz, CDCl₃)

δ = 10.47 (s, 1H, CHO), 6.83 (d, 1H, H2, *J* = 3.0 Hz), 6.53 (d, 1H, H7, *J* = 3.0 Hz), 6.22 (s, 1H, H5), 4.05 (s, 3H, OCH₃), 4.01 (s, 3H, OCH₃), 3.96 (s, 3H, N-CH₃) ppm

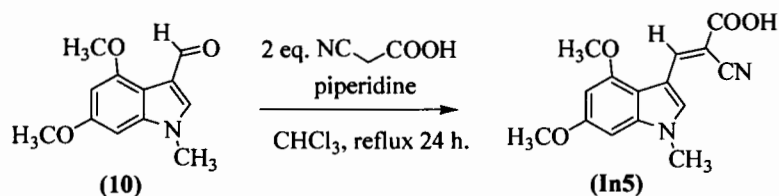
¹³C-NMR (75 Hz, CDCl₃)

δ = 188.0 (CHO), 165.0 (Cq), 159.2 (Cq₃), 130.3 (CH), 115.8 (Cq), 107.2 (Cq), 99.1 (CH), 87.9 (CH), 57.2 (OCH₃), 39.2 (NCH₃)

IR (KBr):

ν_{max} = 2944, 2921, 2848, 1653, 1561, 1514, 1459, 1362, 1246, 1207, 727 cm⁻¹.

2.4.10 Synthesis of 2-cyano-3-(4,6-dimethoxy-*N*-methylindol-3-yl)acrylic acid



According to general procedure of Knoevenagel condensation, treatment of 3-formyl-4,6-dimethoxy-*N*-methylindol (**10**) (0.7500 g, 3.43 mmol), cyanoacetic acid (0.582 g, 6.85 mmol) and piperidine (2.0 mL) in chloroform 20 mL gave 2-cyano-3-(4,6-dimethoxy-*N*-methylindol-3-yl)acrylic acid **In5** (0.770 g, 79%).

$C_{15}H_{14}N_2O_4$; m.p. = 170-174 °C

1H -NMR (300 Hz, $CDCl_3$)

δ = 8.55 (s, 1H, COOH), 6.61 (d, 1H, H-alkene, J = 3Hz), 6.27 (d, 1H, H2, J = 3Hz), 6.10 (s, H, H5), 3.78 (s, 3H, OCH₃), 3.76 (s, 3H, OCH₃), 3.65 (s, 3H, N-CH₃) ppm

^{13}C -NMR (75 Hz, $CDCl_3$)

δ = 165.4 (C=O), 157.8 (Cq), 157.7 (Cq), 149.0 (CH), 135.9 (Cq), 129.0 (Cq), 116.2 (Cq), 114.5 (CN), 103.7 (Cq), 100.2 (Cq), 98.8 (Cq), 87.1 (Cq), 55.2 (OCH₃), 55.1 (OCH₃), 36.8 (NCH₃).

IR (KBr)

ν_{max} = 2923, 2848, 1667, 1573, 1557, 1393, 1159, 1061, 1011, 708 cm^{-1} .

UV-vis spectroscopy (in CH_2Cl_2 at 5×10^{-6} M):

λ_{max} = 426 nm (ϵ = 5.30×10^4 $cm^{-1} M^{-1}$), 277 nm (ϵ = 7.90×10^4 $cm^{-1} M^{-1}$), 229 nm (ϵ = 1.36×10^5 $cm^{-1} M^{-1}$)

MALDI-TOF (m/z) calcd for $C_{15}H_{14}N_2O_4$: 286.0954; found 286.1352 (M^+).

REFERENCES

REFERENCES

- [1] McGehee, M. D. and Heeger, A. J. “Semiconducting (Conjugated) Polymers as Materials for Solid-State Lasers”, **Chemical Industry**. 12(22): 1655-1668; November, 2000.
- [2] Zissis, G. and Bertoldi, P. **Status Report on Organic Light Emitting Diodes (OLED)**. Luxembourg: European Union, 2014.
- [3] Tang, C.W. and Vanslyke, S.A. “Organic electroluminescent diodes”, **Applied Physics Letter**. 51(12): 913-915; July, 1987.
- [4] Wikipedia The Free Encyclopedia. “Organic light-emitting diode”, http://en.wikipedia.org/wiki/Organic_light-emitting_diode. April. 2014.
- [5] Karzazi, W. “Organic Light Emitting Diodes: Devices and applications”, **Journal of Materials and Environmental Science**. 5(1): 1-12, 2014.
- [6] KAPOOK. (2014). “ทำความรู้จัก OLED เทคโนโลยีจอภาพแห่งอนาคต”, <http://men.kapook.com/view54324.html>. March 20, 2014.
- [7] HOWSTUFFWORKS TECH. (2014). “How OLEDs Work http”, <http://electronics.howstuffworks.com/oled1.html>. March 20, 2014.
- [8] Techitive. “TV tech terms demystified, part two: Display types and technologies”, <http://www.techhive.com/article/2999888/smart-tv/tv-tech-terms-demystified-part-two-display-types-and-technologies.html>. April 18, 2014.
- [9] พิสิทธ์ราชมงคล. (2014). “จอ OLED”, <http://www.atom.rmutphysics.com/charud/invention/invention2/nanodisplay/nanodisplay5.html>. 18 April, 2014.
- [10] Meunmart, D. and et al. “Bis(4-diphenylaminophenyl)carbazole end-capped fluorene as solution-processed deep-blue light-emitting and hole-transporting materials for electroluminescent devices”, **Tetrahedron Lett**. 53(28): 3615–3618; July 2012.
- [11] Pansay, S and et al. “Multibromo-N-alkylcarbazoles: synthesis, characterization, and their benzo[b]thiophene derivatives”, **Tetrahedron Letters**. 53(34): 4568-4572; August, 2012.

REFERENCES (CONTINUED)

- [12] Huang B and et al. "Nondoped deep blue OLEDs based on Bis-(4-benzenesulfonyl-phenyl)-9-phenyl-9H-carbazoles", **Journal of Luminescence**. 172: 7–13; April, 2016.
- [13] Ameen, S. and et al. "Diphenylaminocarbazoles by 1,8-functionalization of carbazole Materials and application to phosphorescent organic light-emitting diodes", **Dyes and Pigments**. 24: 35-44; January, 2016.
- [14] Shi, H. and et al. "Two novel phenylethene-carbazole derivatives containing dimesitylboron groups: Aggregation-induced emission and electroluminescence properties", **Dyes and Pigments**. 128: 304-313; May, 2016.
- [15] Geffroy, B., Roy, le P. and Prat, C. "Organic light-emitting diode (OLED) technology: materials, devices and display technologies", **Polymer International**. 55(6): 572-582; June, 2016.
- [16] Grice, A. W. and et al. "High brightness and efficiency blue light-emitting polymer diodes", **Applied Physics Letters**. 73(5): 629; May, 1998.
- [17] Thangthong, A. M. and et al. "Synthesis, Properties and Applications of Biphenyl Functionalized 9,9-Bis (4-diphenylaminophenyl) fluorenes as ifunctional Materials for Organic Electroluminescent Devices", **European Journal of Organic Chemistry**. (27): 5263-5274; September, 2012.
- [18] Kumchoo, T. and et al. "Dipyrenylcarbazole Derivatives for Blue Organic Light-Emitting Diodes", **Chemistry–An Asian Journal**. 5(10): 2162-2167; October, 2010.
- [19] Yang, Z. and et al. "Blue-light-emitting carbazole derivates with high thermal stability", **Optical Materials**. 32(2): 398–401; December, 2009.
- [20] Wee, K.-R. and et al. "Asymmetric anthracene-based blue host materials: synthesis and electroluminescence properties of 9-(2-naphthyl)-10-arylanthracenes", **Journal of Materials Chemistry**. 21(4): 1115-1123; November, 2011.

REFERENCES (CONTINUED)

- [21] Qin, T. and et al. "Core, Shell, and Surface-Optimized Dendrimers for Blue Light-Emitting Diodes", **Journal of the American Chemical Society**. 133(5): 1301-1303; January, 2011.
- [22] Gratzel, M. "Mesoscopic solar cells for electricity and hydrogen production from sunlight", **Chem. Lett.** 34(1): 8-13, 2005.
- [23] O'Regan, B. and Gratzel, M. "A low-cost, high-efficiency solar cell based on dye sensitized colloidal TiO₂ films", **Nature**. 353(6346): 737-740; 1991.
- [24] Bard, A. J. "Design of semiconductor photoelectrochemical systems for solar energy conversion", **J. Phys. Chem.** 86(2): 172-177; January, 1982.
- [25] Bignozzi, C. A. and et al. "Molecular and supramolecular sensitization of nanocrystalline wide band-gap semiconductors with mononuclear and polynuclear metal complexes", **Chem. Soc. Rev.** 29(2): 87-96; January , 2000.
- [26] Matsumura, M. and et al. "Dye Sensitization and Surface Structures of Semiconductor Electrodes", **Ind. Eng. Chem. Prod. Res. Dev.** 19(3): 415-421; September , 1980.
- [27] Graetzel, M and O'Regan B. "Dye Sensitized Solar Cells", **Smart. Sustainable. Solar**. <http://gcell.com/dye-sensitized-solar-cells>. March 20, 2016.
- [28] Tate, P. (2014). "The Technologies and Performance of Solar Shingles and Transparent Solar Glass", Originally prepared as a degree requirement for the UIC Master of Energy Engineering program. March 10, 2015
- [29] Gratzel, M. "Solar energy conversion by dye-sensitized photovoltaic cells", **Inorg. Chem.** 44(20): 6841-6851; September , 2005.
- [30] KOCHPRADIST, P. **Synthesis and characterization of novel-r-a type organic dyes**. Doctor' s Thesis: Ubon ratchathain University, 2013.
- [31] Kim, D. and et al. "Molecular engineering of organic dyes containing N-aryl carbazole moiety for solar cell", **Tetrahedron**. 63(9): 1913-1922; February , 2007.

REFERENCES (CONTINUED)

- [32] Chang, Y. J. and et al. "Dye-sensitized solar cell utilizing organic dyads containing triarylene conjugates", **Tetrahedron**. 65(24): 4726-4734; June, 2009.
- [33] Wanand, Z. et al. "Influence of different arylamine electron donors in organic sensitizers for dye-sensitized solar cells", **Dyes Pigments**. 95(1): 41-46; October, 2012.
- [34] Kim, D. and et al. "Efficient organic sensitizers containing benzo [cd] indole: Effect of molecular isomerization for photovoltaic properties", **Journal of Photochemistry and Photobiology A: Chemistry**. 201: 102-110; January, 2009.
- [35] Shingo K. and et al. "Organic dyes with oligo-n-hexylthiophene for dye-sensitized solar cells: Relation between chemical structure of donor and photovoltaic performance", **Dyes and Pigments**. 92(3): 1250-1256; March, 2012.
- [36] Gang, W. and et al. "Series of D- π -A system based on isoindigo dyes for DSSC: Synthesis, electrochemical and photovoltaic properties", **Synthetic Metals**. 187: 17-23; January, 2014.
- [37] Kim, D. and et al. "Molecular engineering of organic sensitizers containing indole moiety for dye-sensitized solar cells", **Tetrahedron**. 64(45): 10417-10424; November, 2008.
- [38] Kim, B. H. and et al. "New N-methyl pyrrole and thiophene based D- π -A systems for dye-sensitized solar cells", **Dyes and Pigments**. 96(2): 313-318; February, 2013.
- [39] Liu X. et al. "Novel D-D- π -A organic dyes based on triphenylamine and indole-derivatives for high performance dye-sensitized solar cells", **Journal of Power Sources**. 248: 400-406; February, 2014.
- [40] BaBu, D. D. and et al. "New D- π -A type indole based chromogens for DSSC: Design, synthesis and performance studies", **Dyes and Pigments**. 112: 183-191; January, 2015.

REFERENCES (CONTINUED)

- [41] Tian, H. and et al. "Effect of different electron donating groups on the performance of dye-sensitized solar cells", **Dyes and Pigments**. 84(1): 62-68; January, 2010.
- [42] Sperotto, E. and et al. "The mechanism of the modified Ullmann reaction", **Dalton Trans.** 39(43): 10338–10351; October, 2010.
- [43] Hunt, I. "Department of Chemistry Hydrolysis of Esters", <http://www.chem.ucalgary.ca/courses/350/Carey5th/Ch20/ch20-3-3-1.html>. June 20, 2014.
- [44] Menegatti, R. "Green Chemistry–Aspects for the Knoevenagel Reaction", <http://www.intechopen.com/books/green-chemistry-environmentally-benign-approaches/greenchemistry-aspects-for-knoevenagel-reaction>. March 16, 2012
- [45] Rijskiewicz, E. E. and Silverstein, R. M. "N-Methyl-2-pyrrolealdehyde and N-Methyl-2-hydroxymethylpyrrole", **J. Am. Chem. Soc.** 76(22): 5802-5803; November, 1954.
- [46] Keawin, T. **Synthesis of endoperoxide of anthracene derivatives and their biological activities and chemistry of 4,6-dimethoxyindole derivatives photooxidation and nitration**. Doctor's Thesis: Mahidol University, 2005.

APPENDICES

APPENDICES A

^1H NMR, ^{13}C NMR and UV-Vis absorption spectrum of compounds

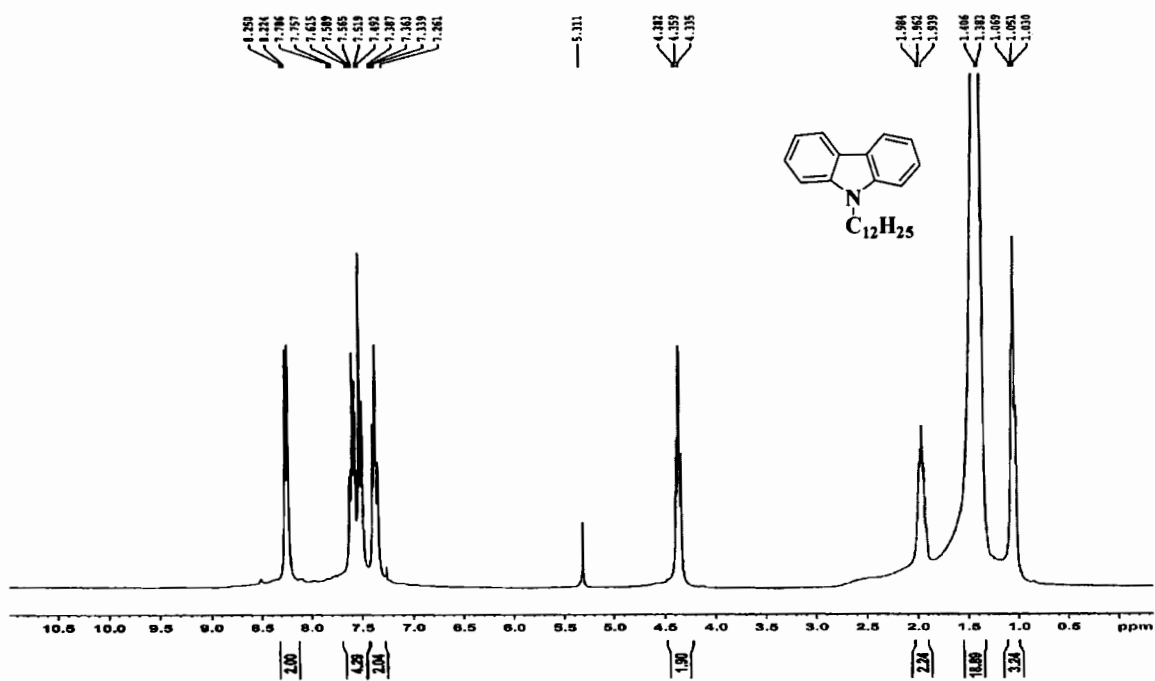


Figure A.1 The ¹H NMR (in CDCl₃) spectrum of 9-dodecylcarbazole 2

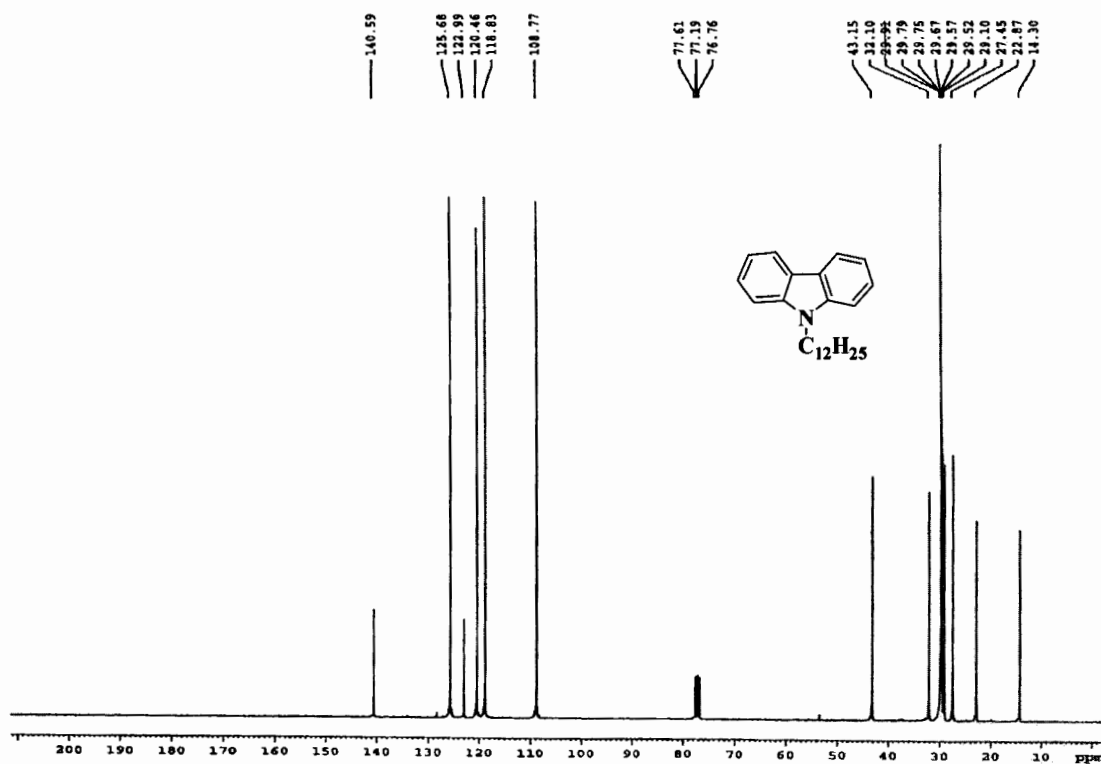


Figure A.2 The ¹³C NMR spectra of 9-dodecylcarbazole 2

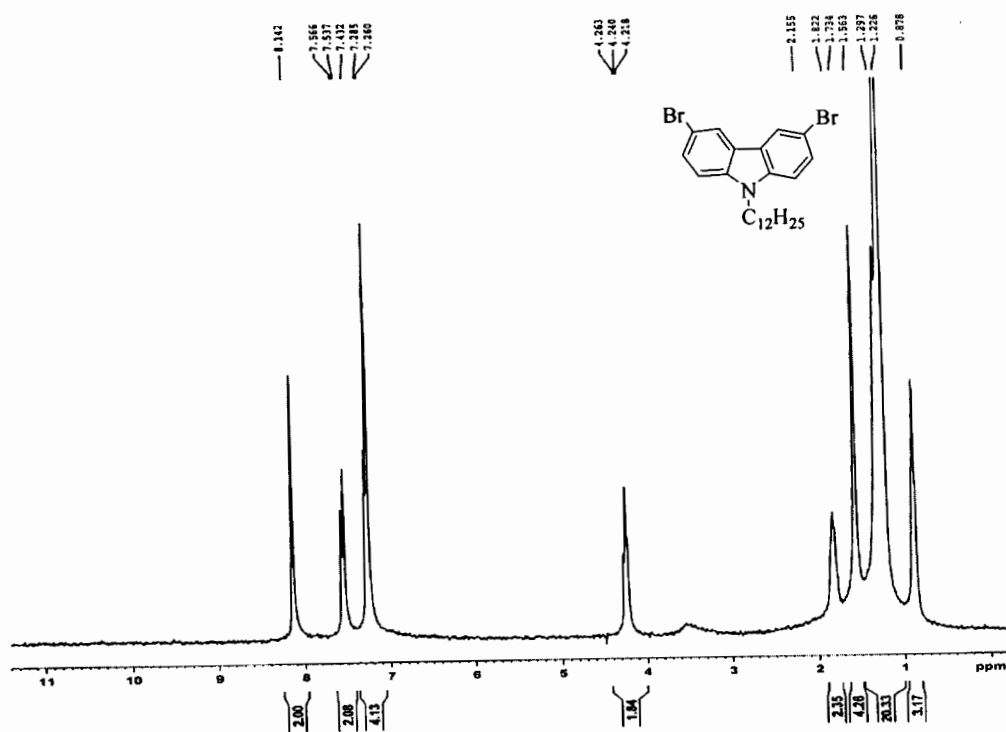


Figure A.3 The ^1H NMR (in CDCl_3) spectrum of 3,6-Dibromo-9-dodecylcarbazole

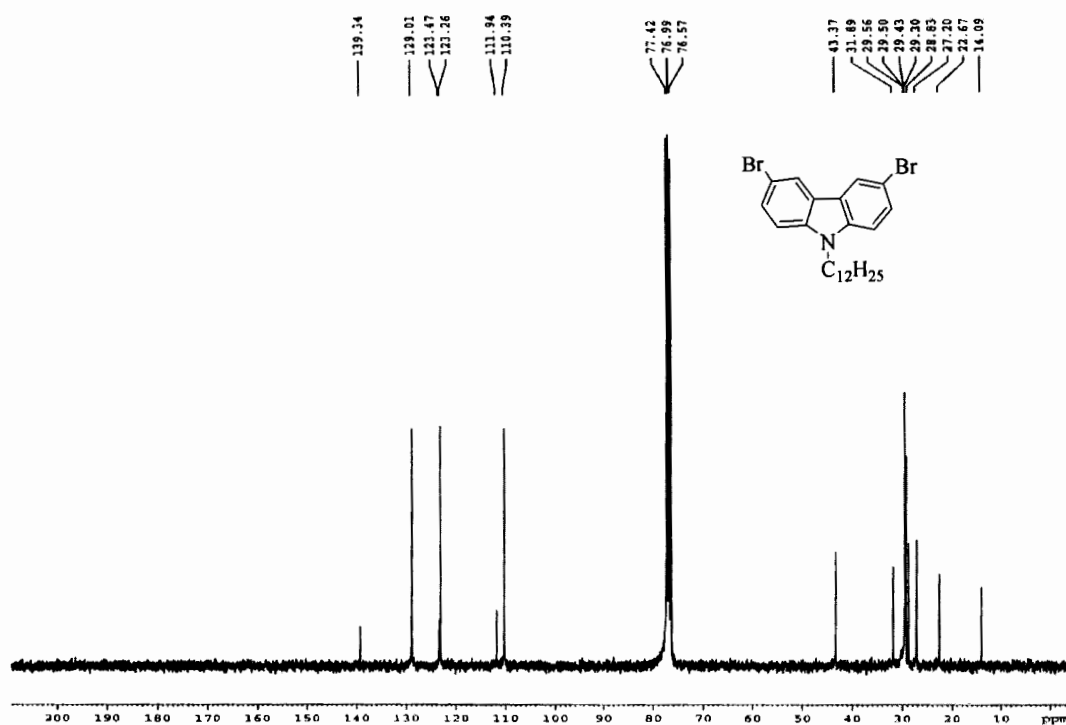


Figure A.4 The ^{13}C NMR spectra of 3,6-Dibromo-9-dodecylcarbazole

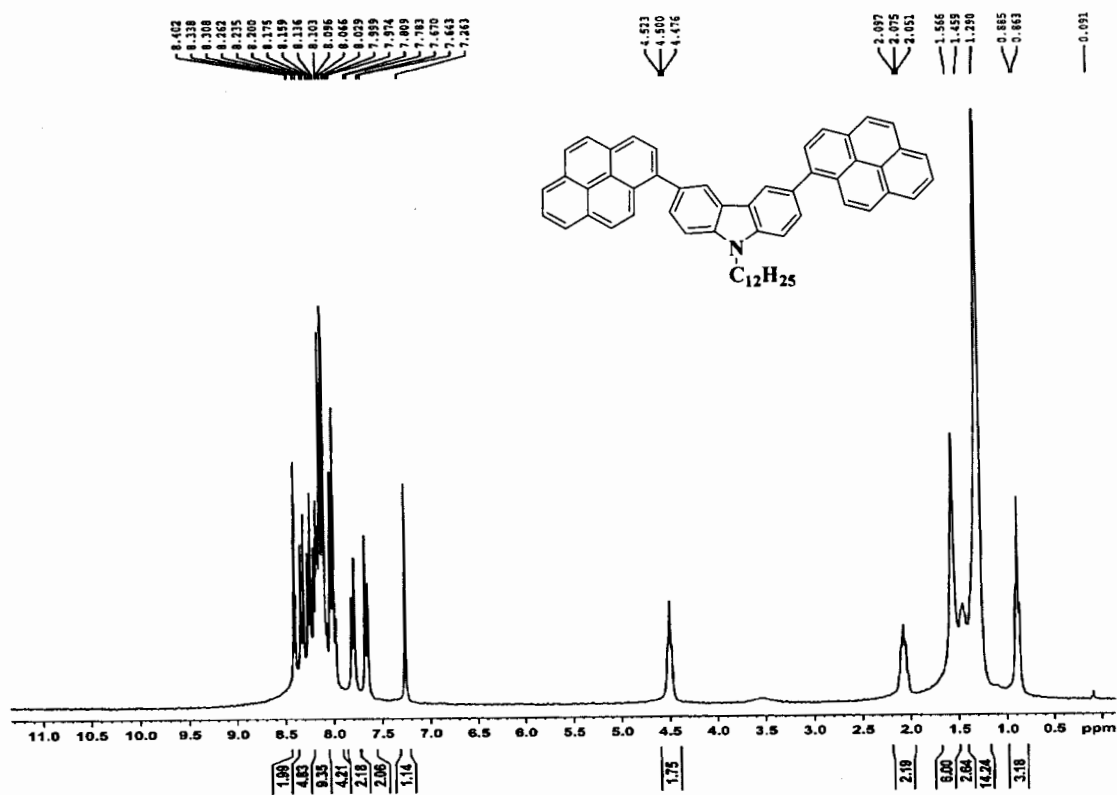


Figure A.5 The ^1H NMR (in CDCl_3) spectrum of CP2

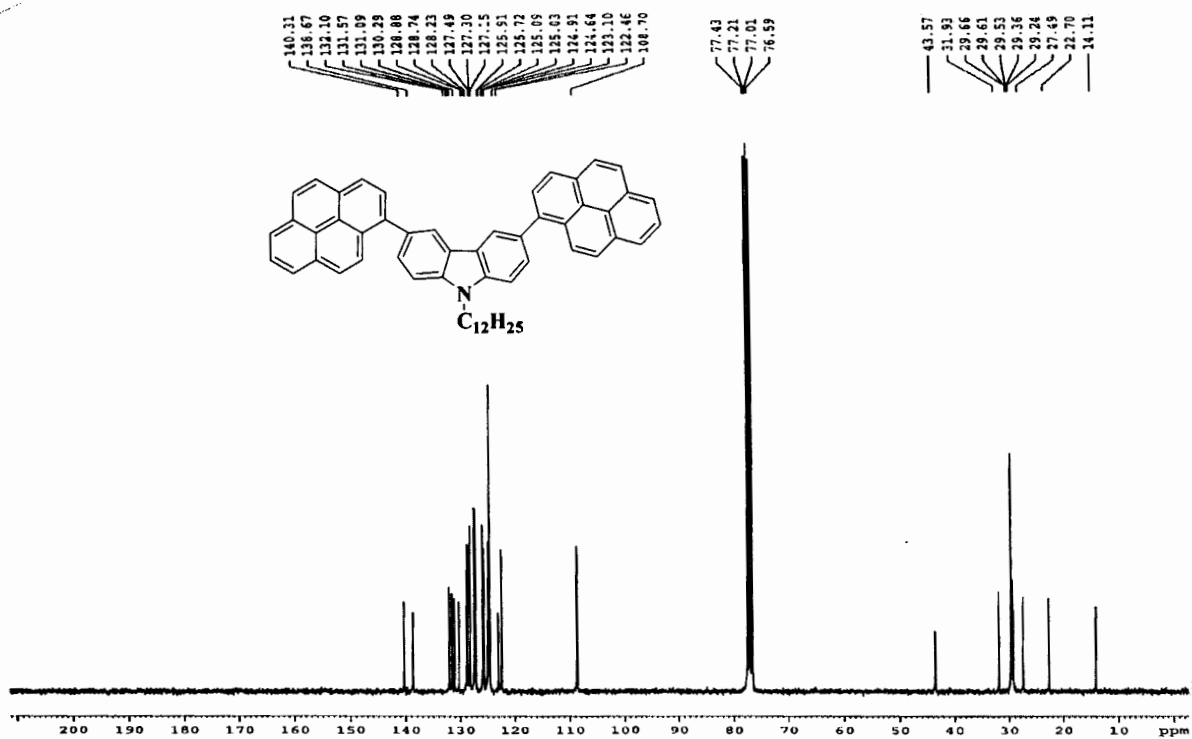


Figure A.6 The ^{13}C NMR spectra of CP2

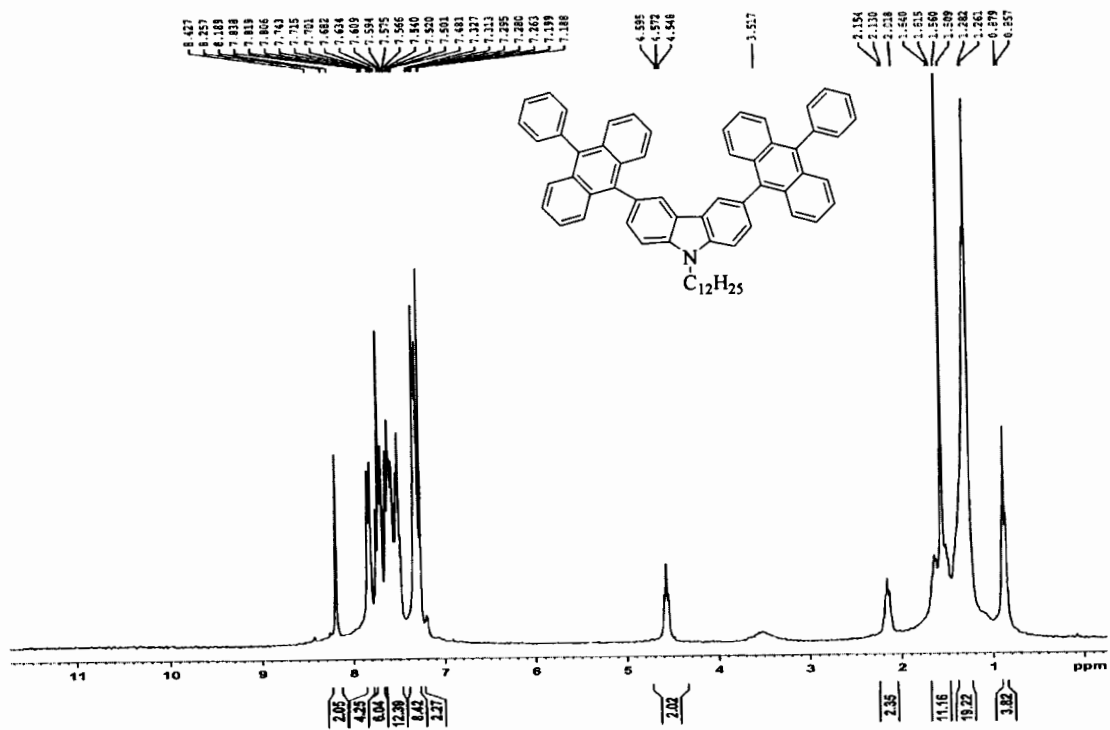


Figure A.7 The ^1H NMR (in CDCl_3) spectrum of CA2

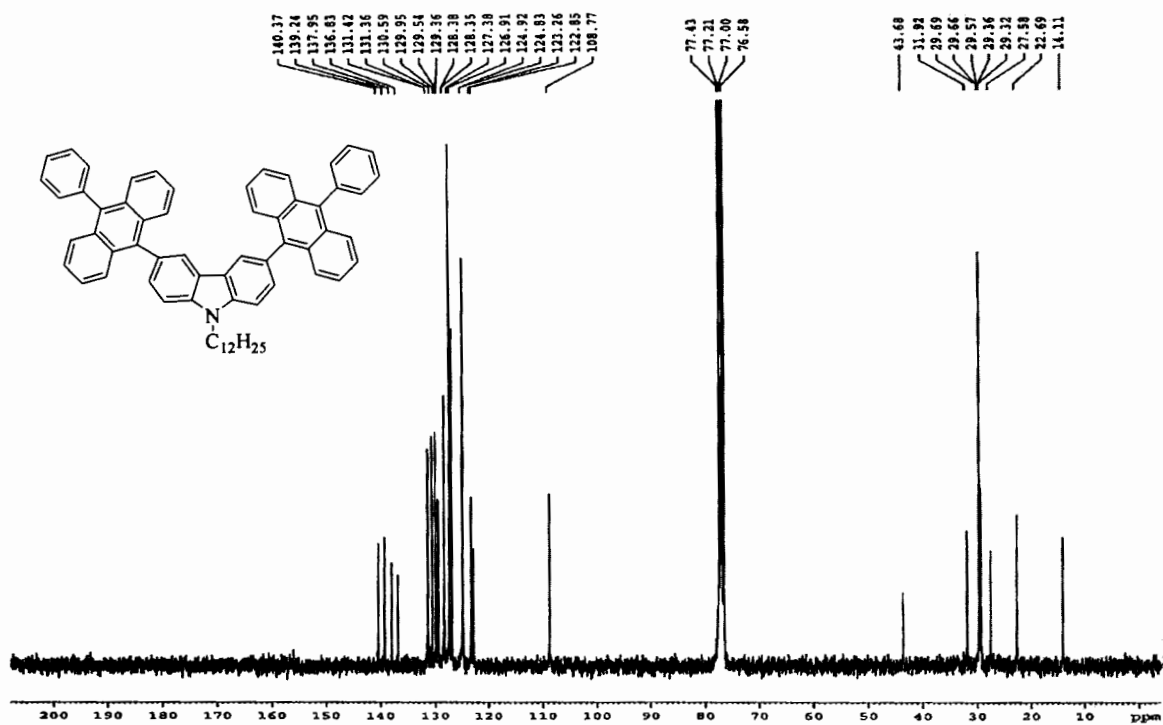


Figure A.8 The ^{13}C NMR spectra of CA2

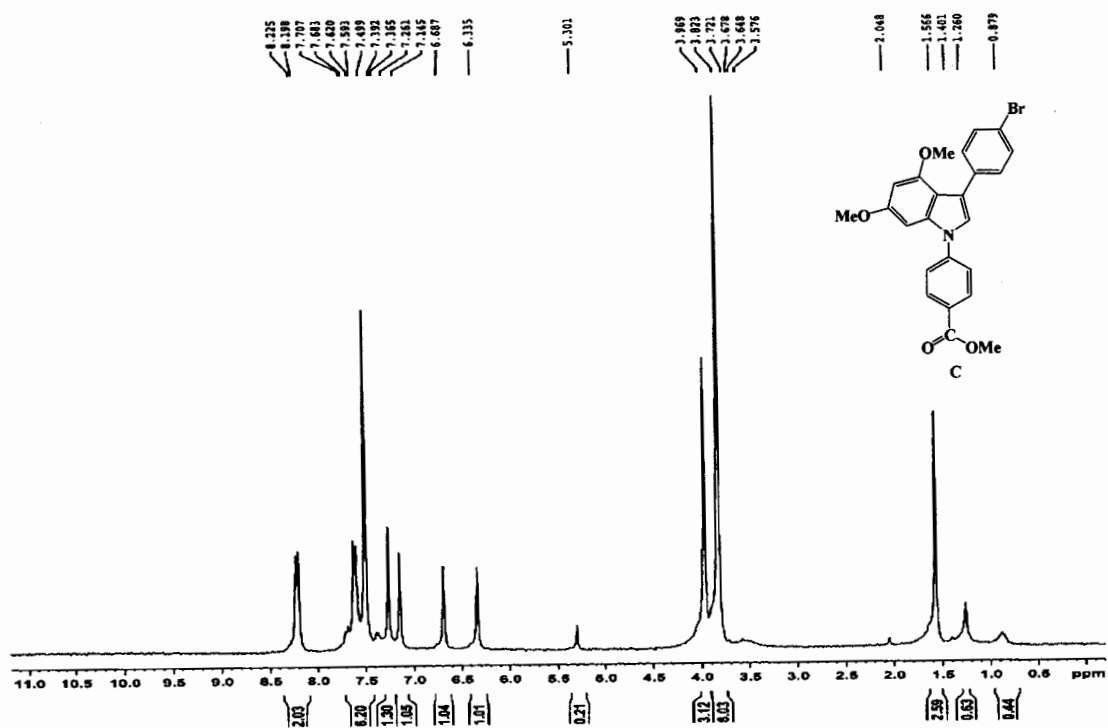


Figure A.11 The ¹H NMR (in CDCl₃) spectrum of methyl 4-(3-(4-bromophenyl)-4,6-dimethoxyindol-1-yl)benzoate 6

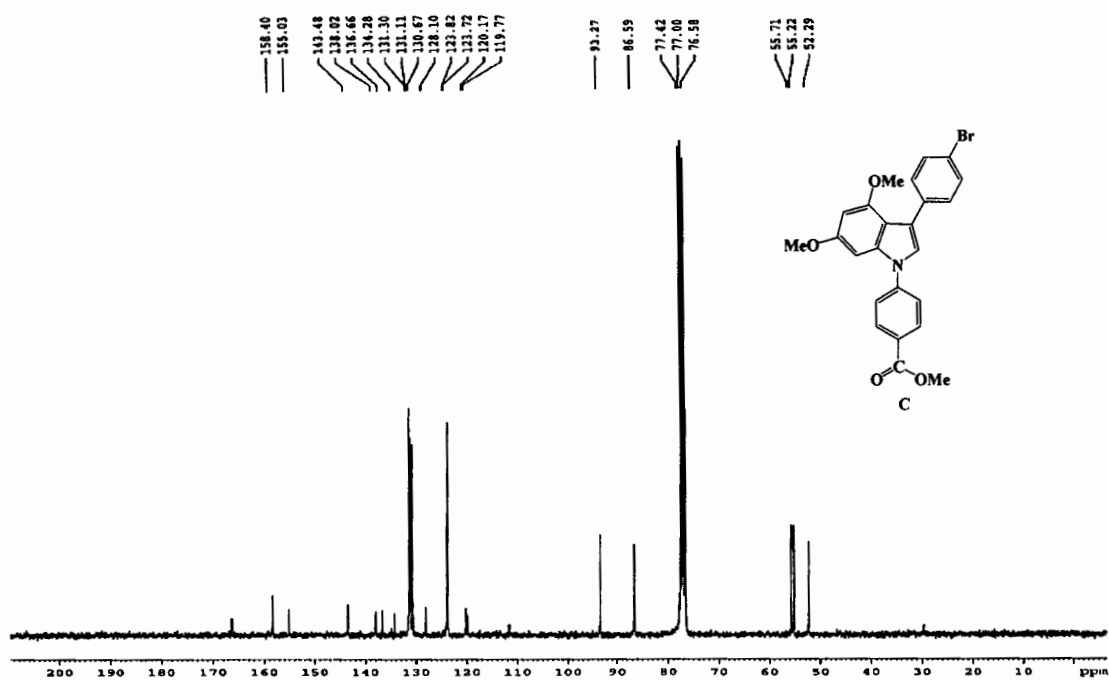


Figure A.12 The ¹³C NMR spectra of methyl 4-(3-(4-bromophenyl)-4,6-dimethoxyindol-1-yl)benzoate 6

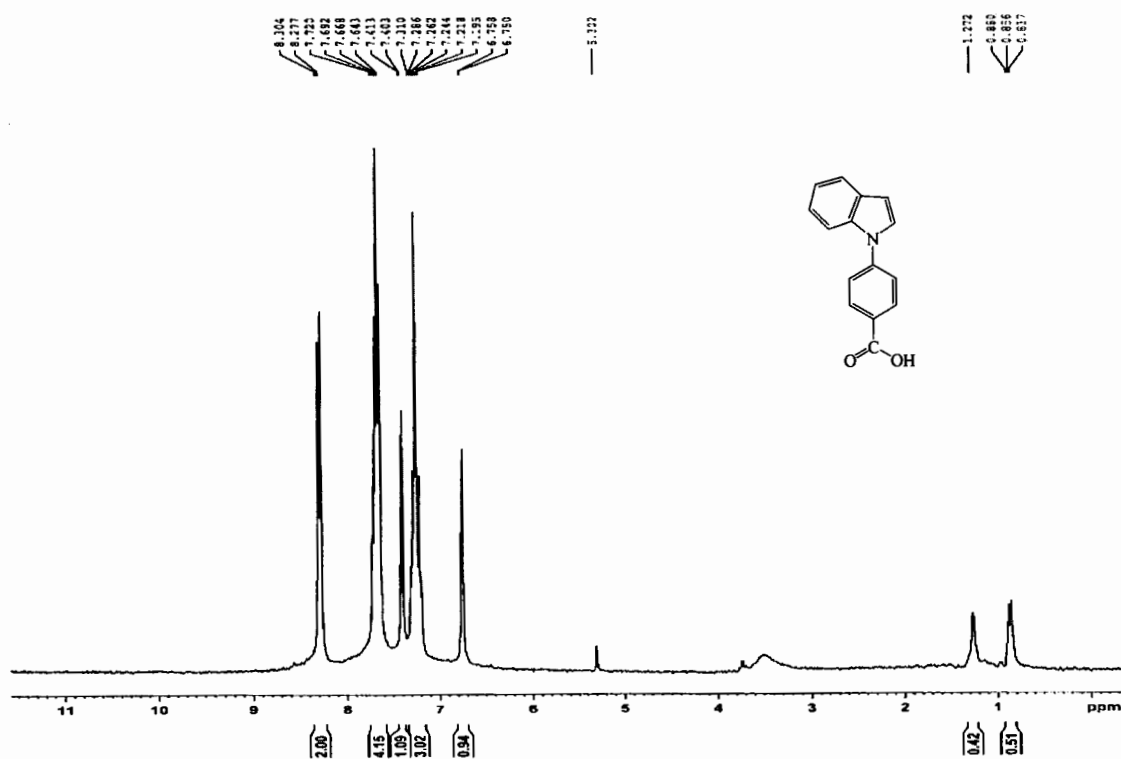


Figure A.13 The ^1H NMR (in CDCl_3) spectrum of In1

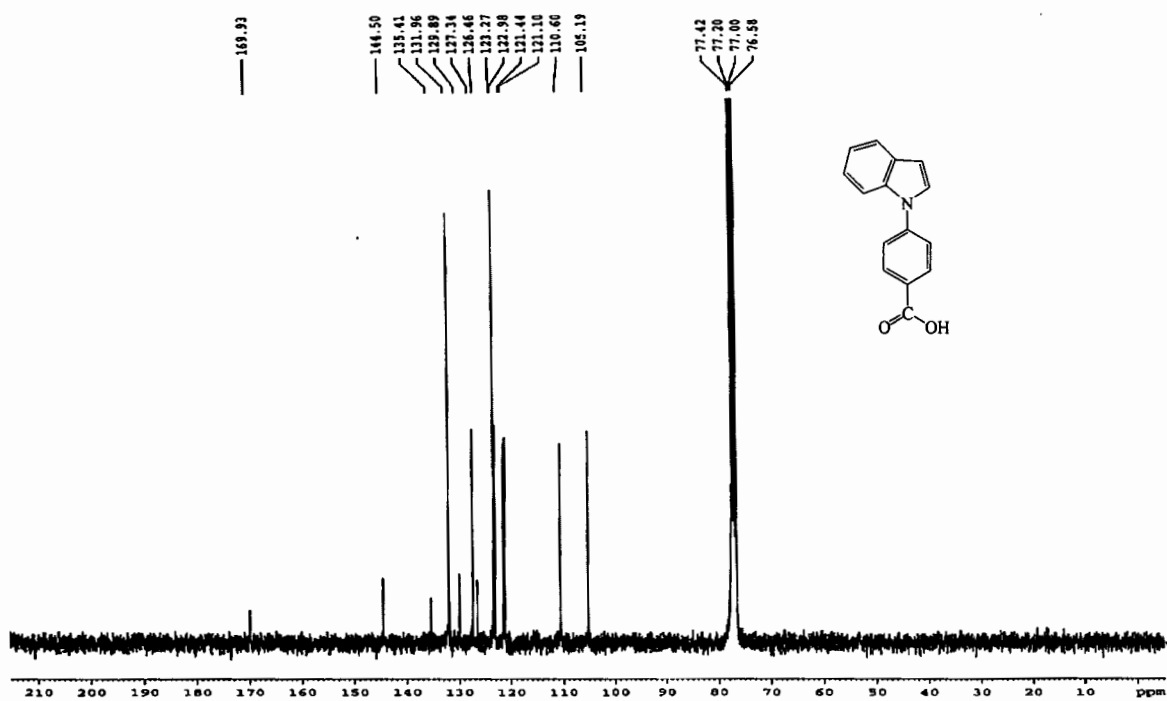


Figure A.14 The ^{13}C NMR spectra of In1

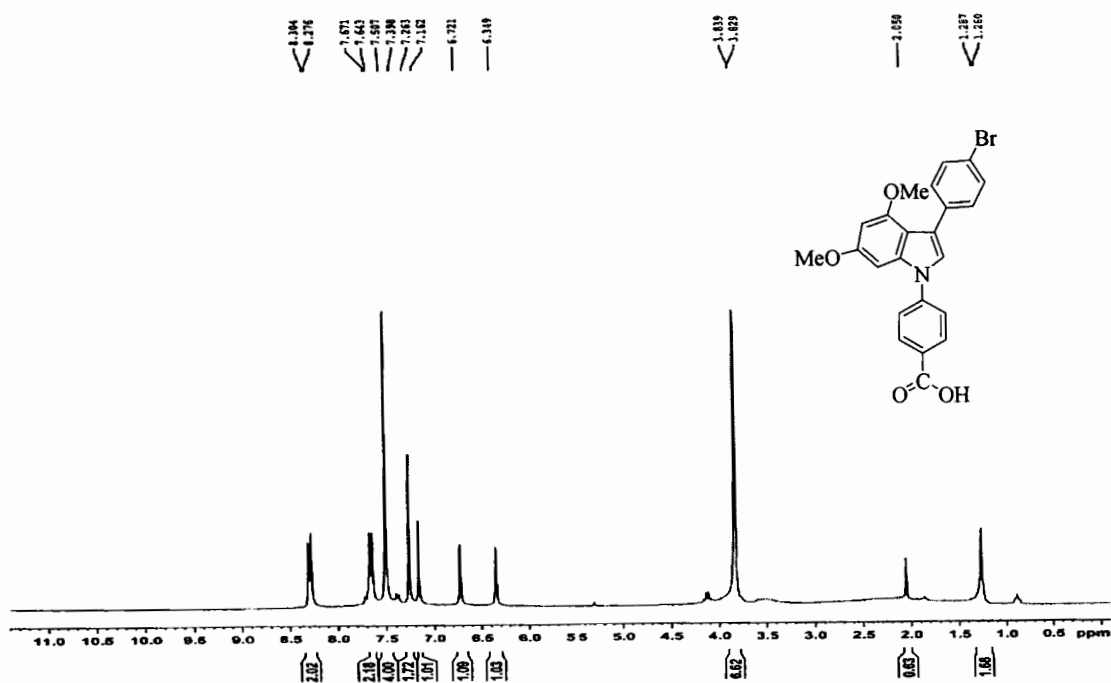


Figure A.15 The $^1\text{H NMR}$ (in CDCl_3) spectrum of In2

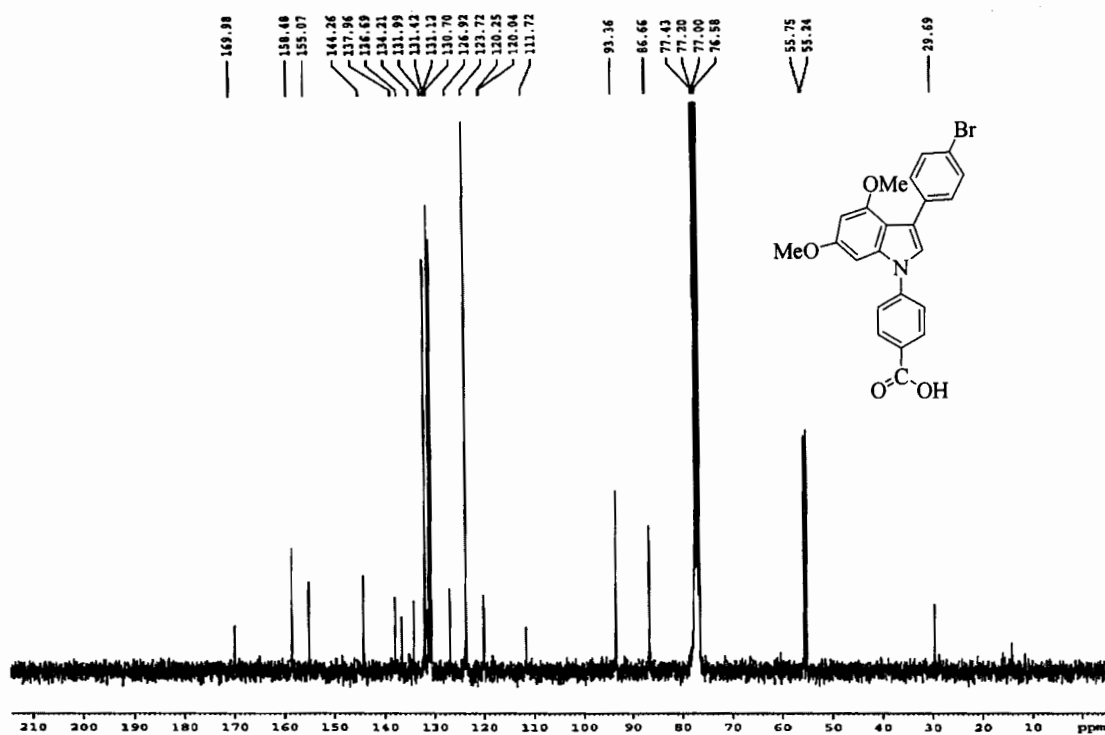


Figure A.16 The $^{13}\text{C NMR}$ spectra of In2

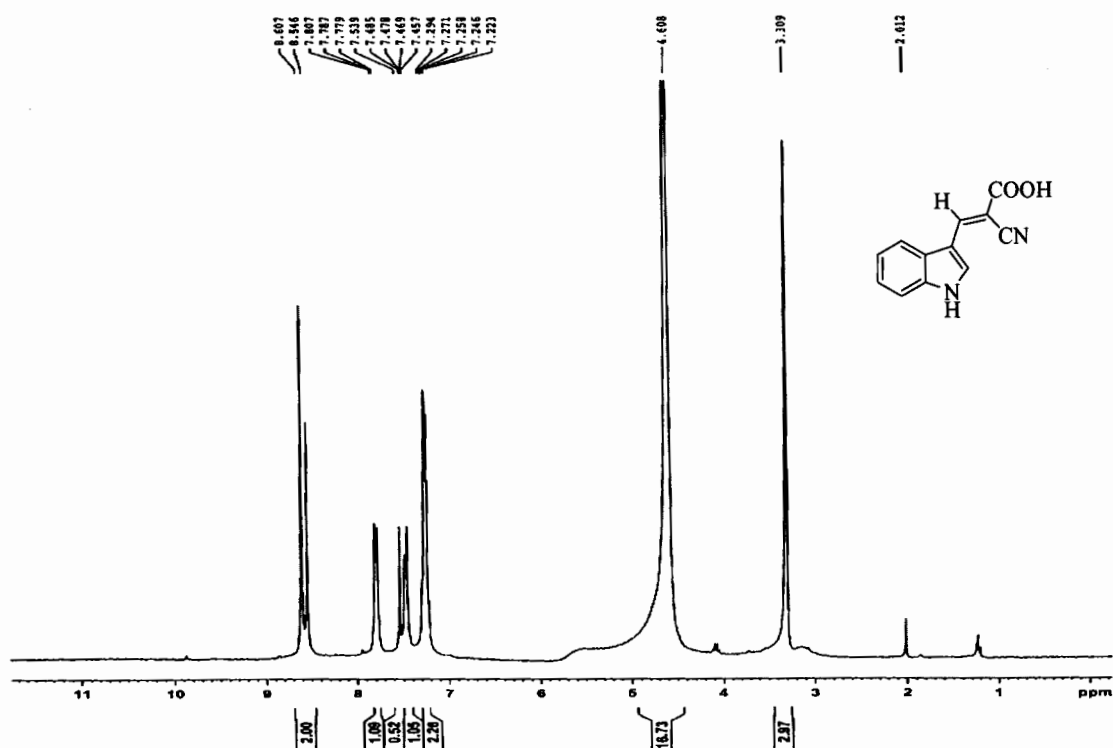


Figure A.17 The ^1H NMR (in CDCl_3) spectrum of In3

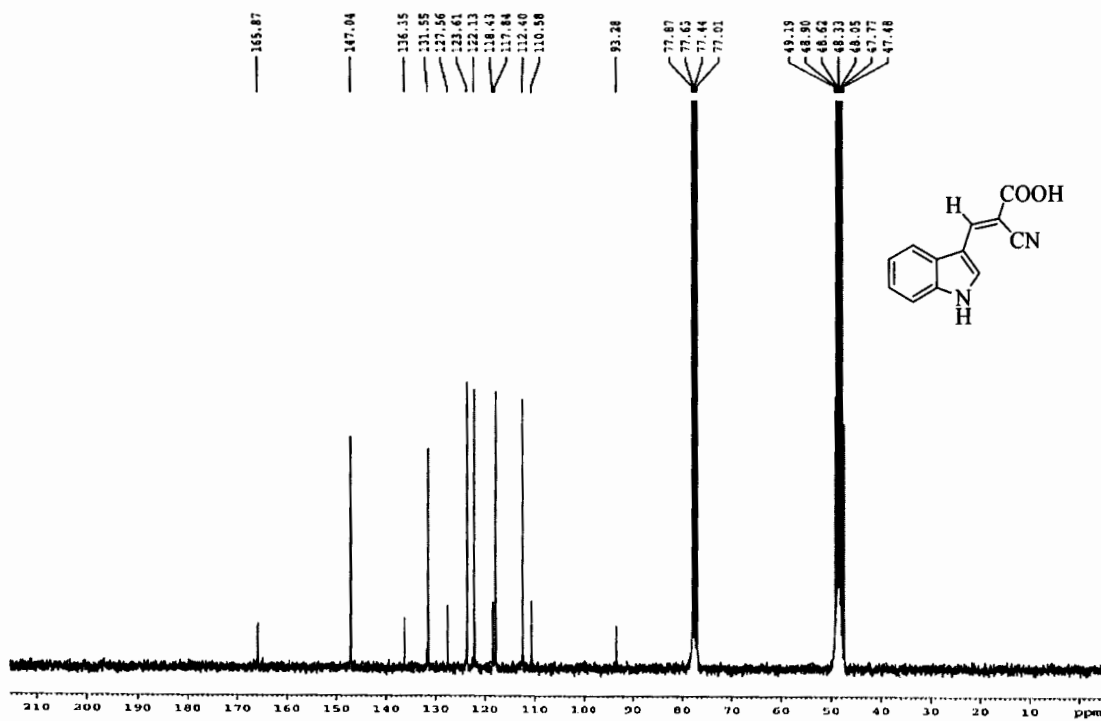


Figure A.18 The ^{13}C NMR spectra of In3

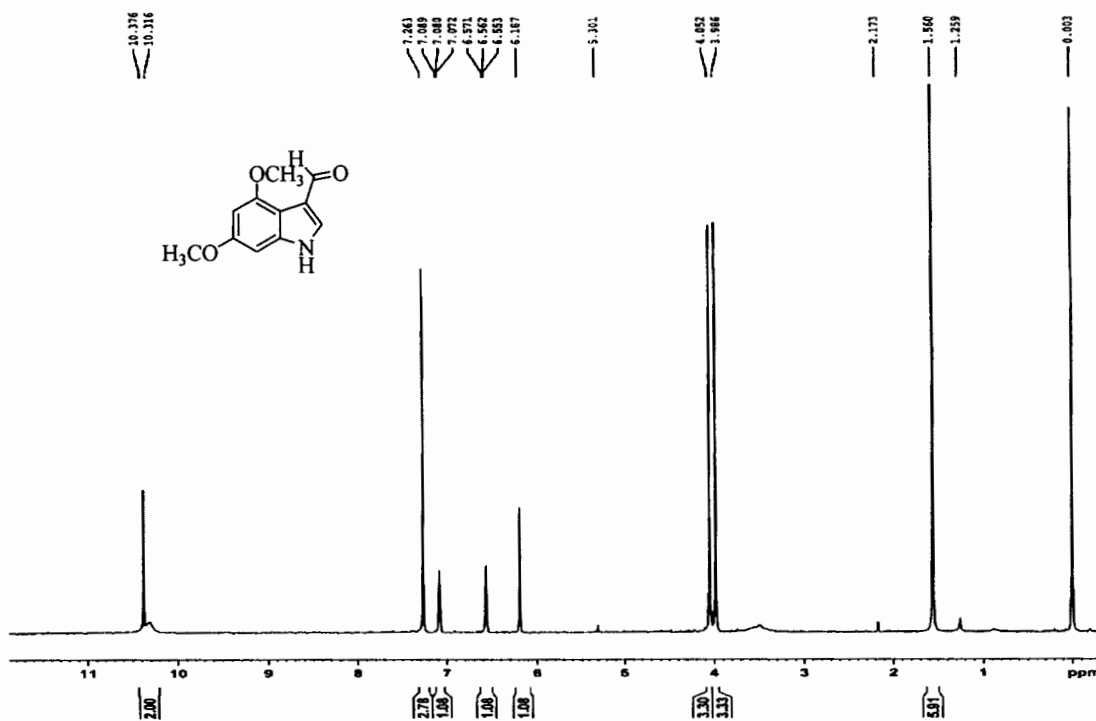


Figure A.19 The ^1H NMR (in CDCl_3) spectrum of 3-formyl-4,6-dimethoxyindole 9

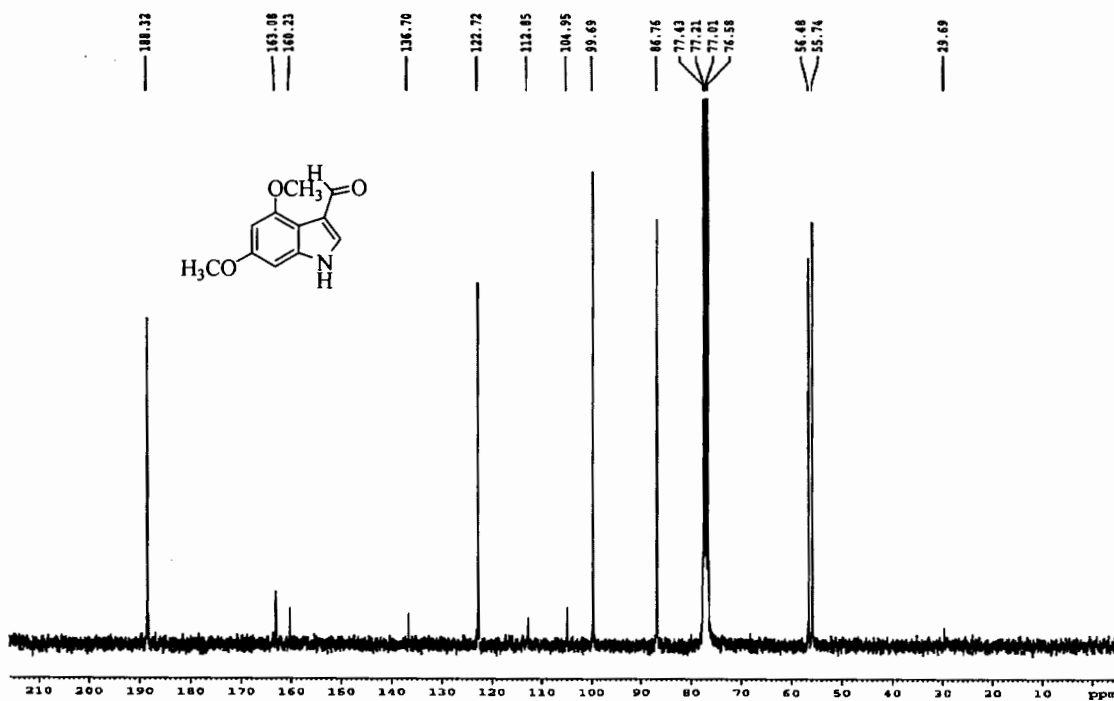


Figure A.20 The ^{13}C NMR spectra of 3-formyl-4,6-dimethoxyindole 9

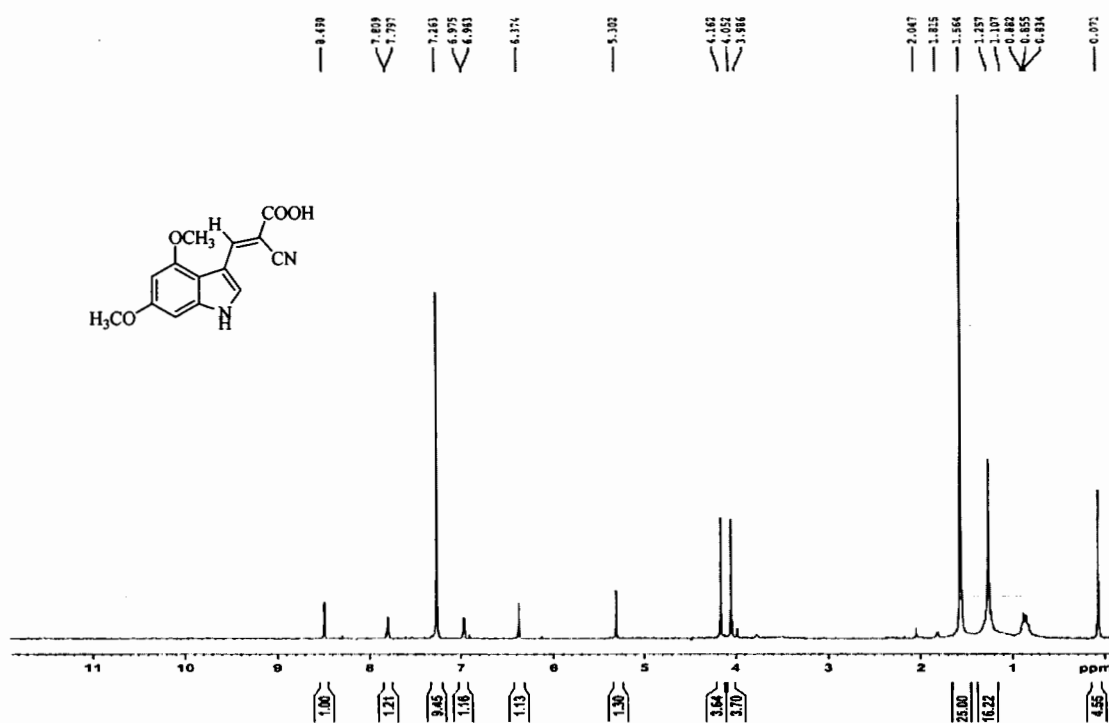


Figure A.21 The ¹H NMR (in CDCl₃) spectrum of In4

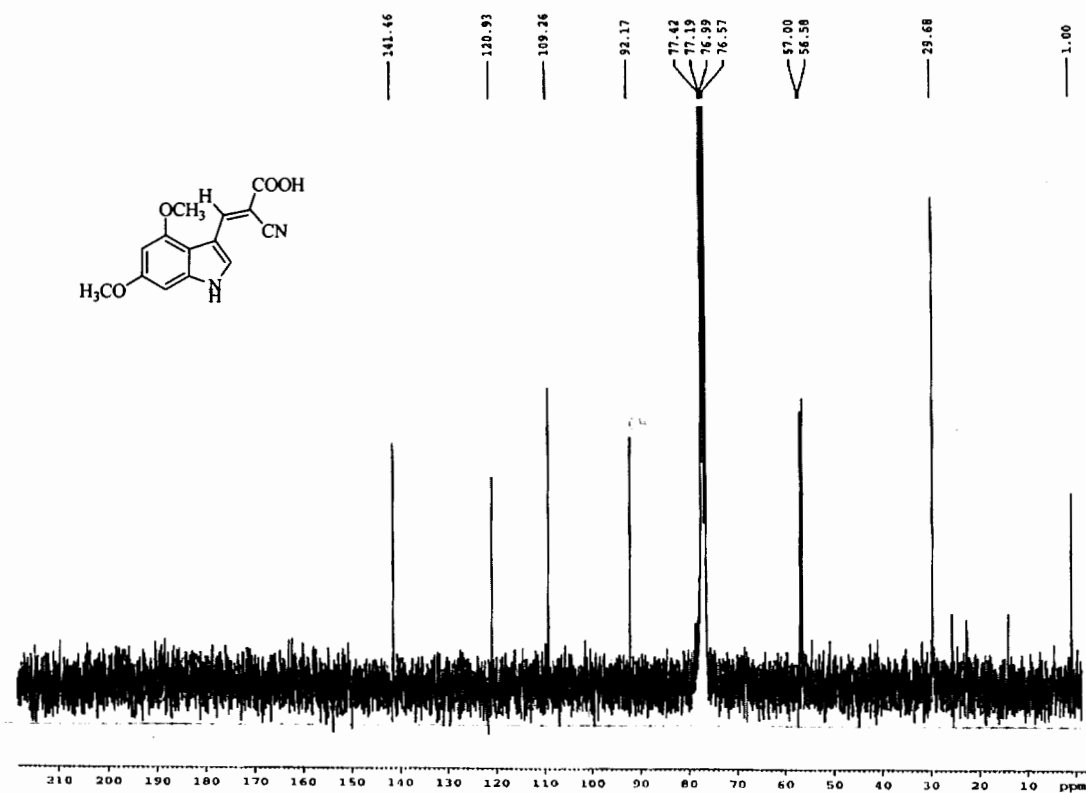


Figure A.22 The ¹³C NMR spectra of In4

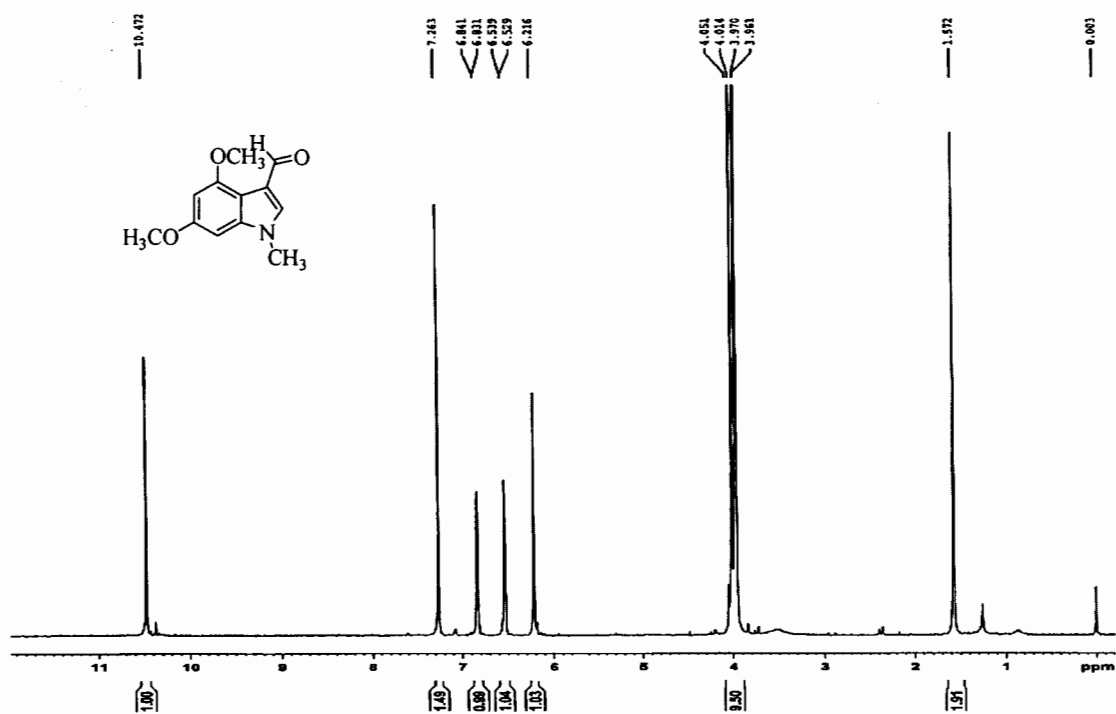


Figure A.23 The ^1H NMR (in CDCl_3) spectrum of 3-formyl-4,6-dimethoxy-*N*-methylindol 10

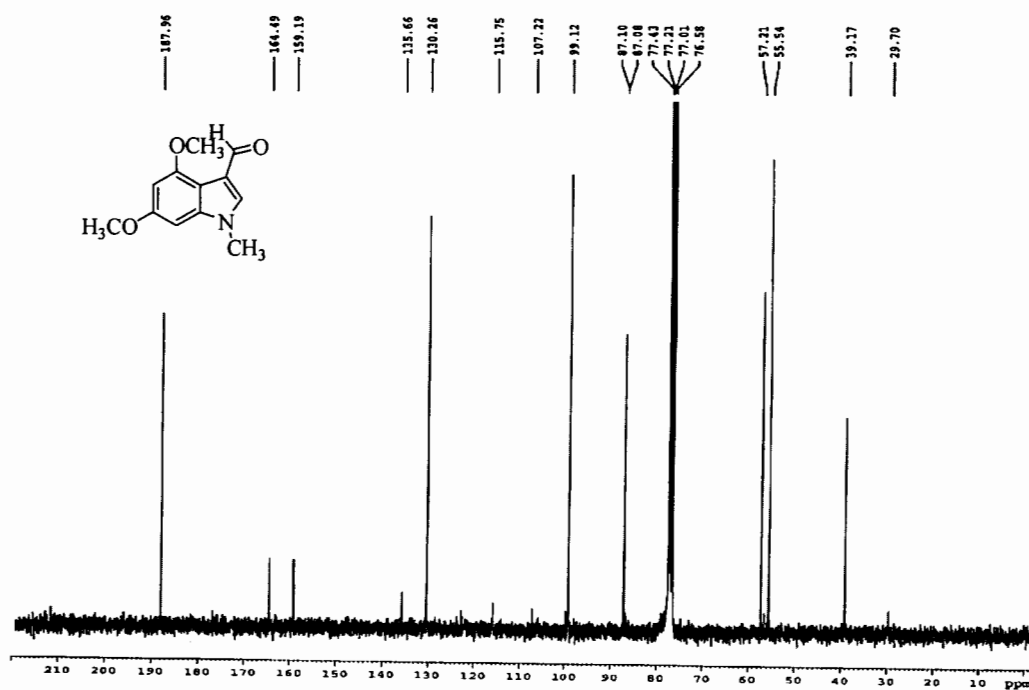


Figure A.24 The ^{13}C NMR spectra of 3-formyl-4,6-dimethoxy-*N*-methylindol 10

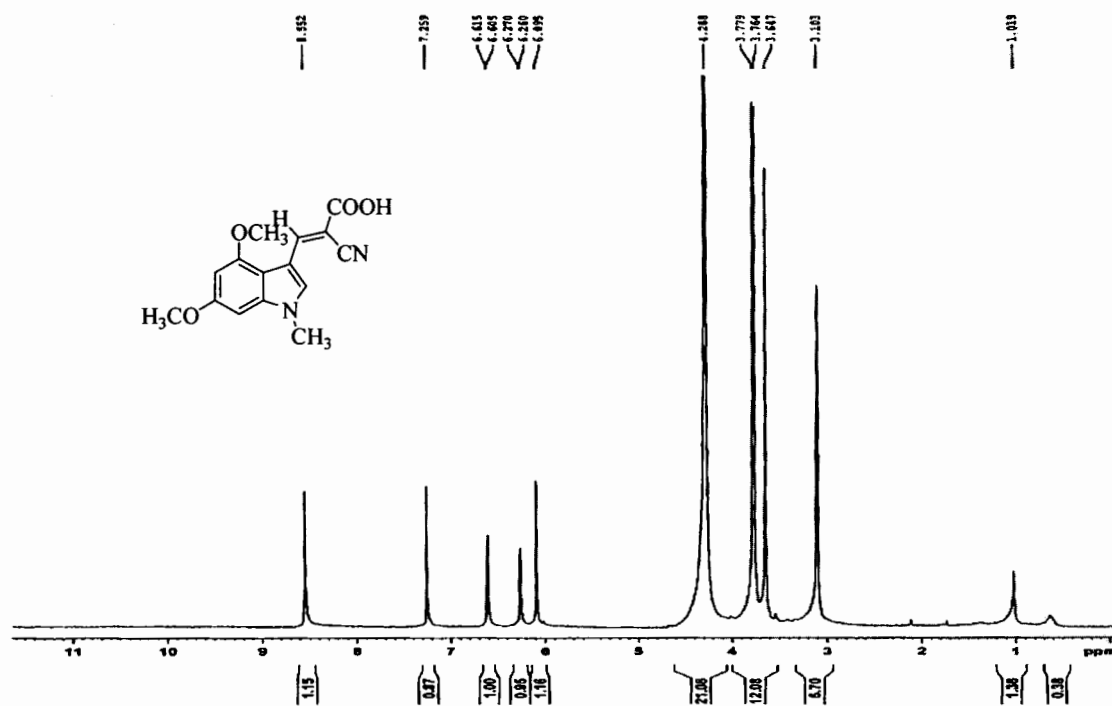


Figure A.25 The ¹H NMR (in CDCl₃) spectrum of In5

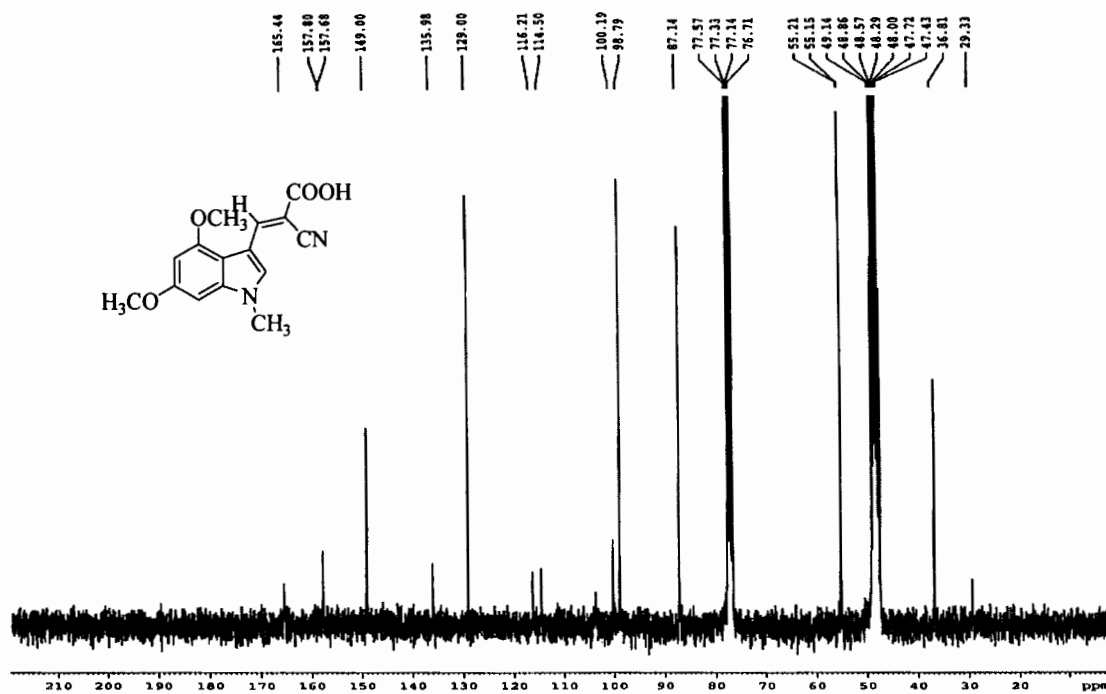


Figure A.26 The ¹³C NMR spectra of In5

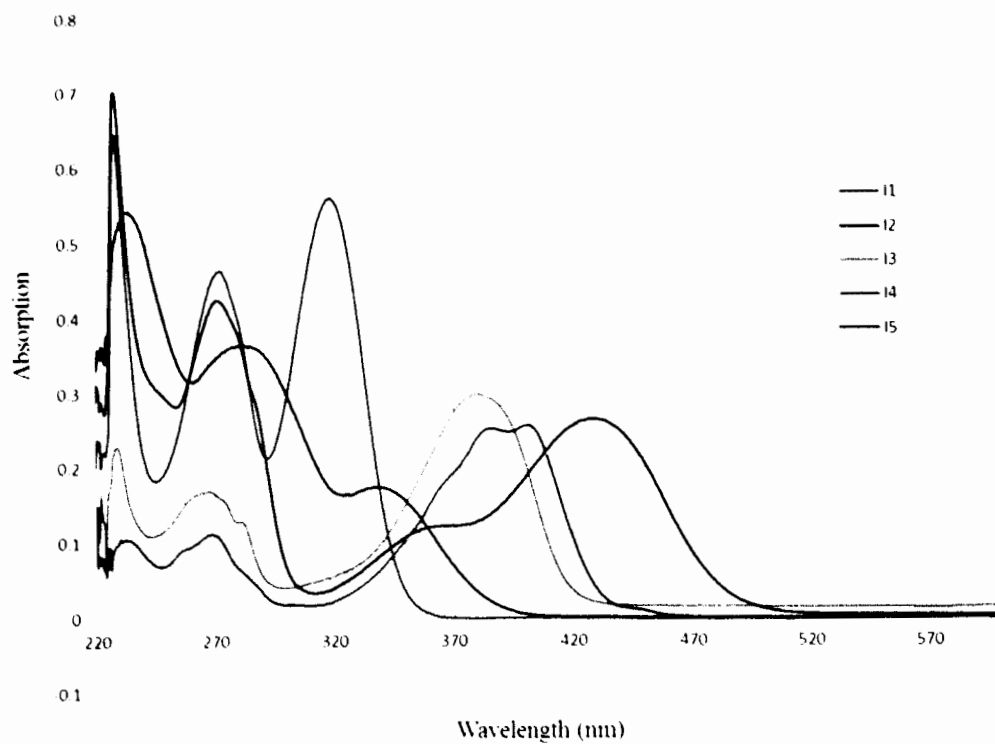


Figure A.27 UV-Vis absorption spectra of In1-In5 in DCM at 5×10^{-6} M.

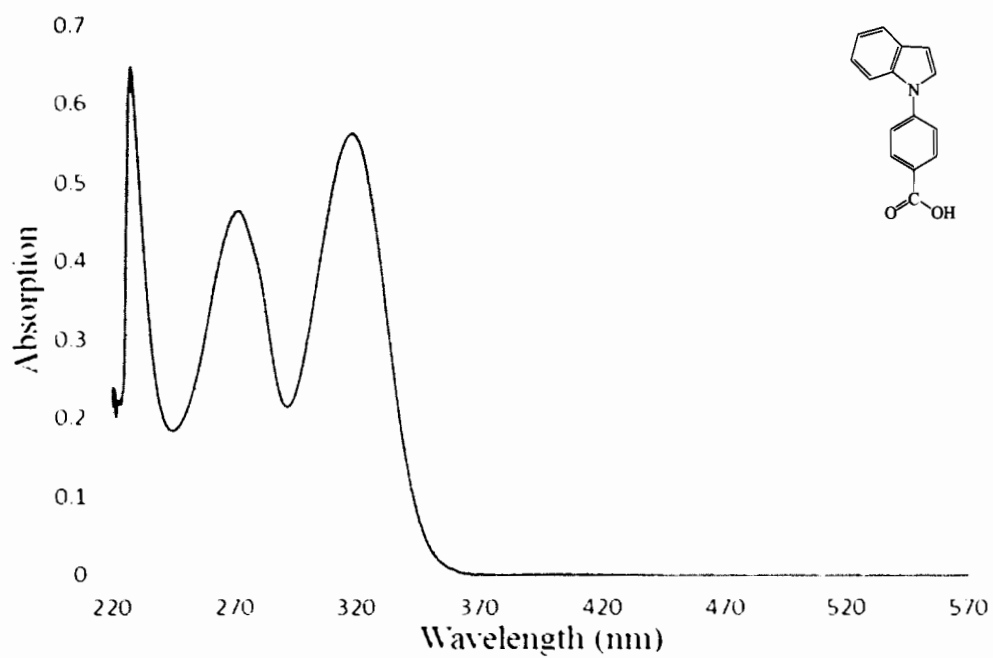


Figure A.28 UV-Vis absorption spectra of In1 in DCM at 5×10^{-6} M.

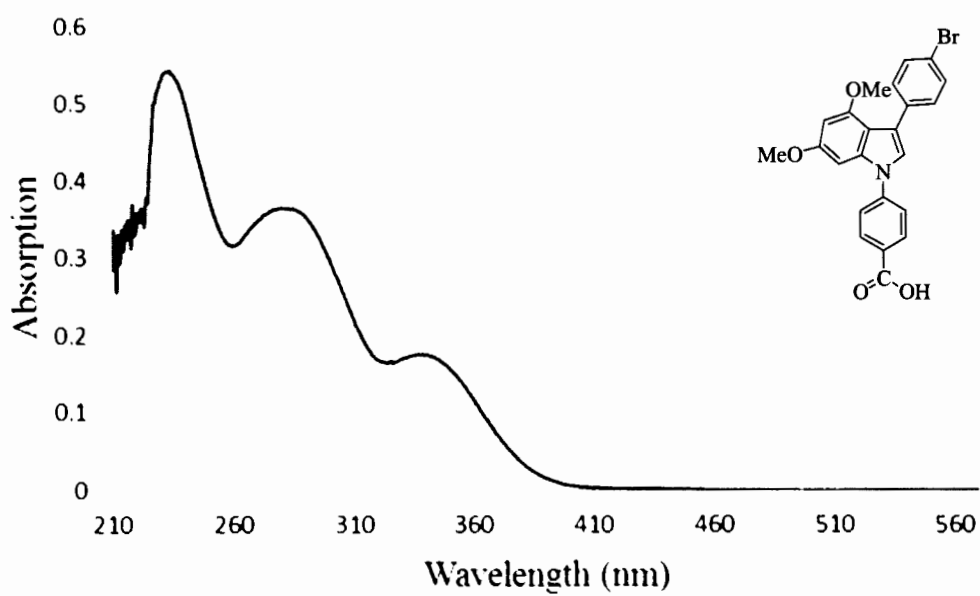


Figure A.29 UV-Vis absorption spectra of In2 in DCM at 5×10^{-6} M.

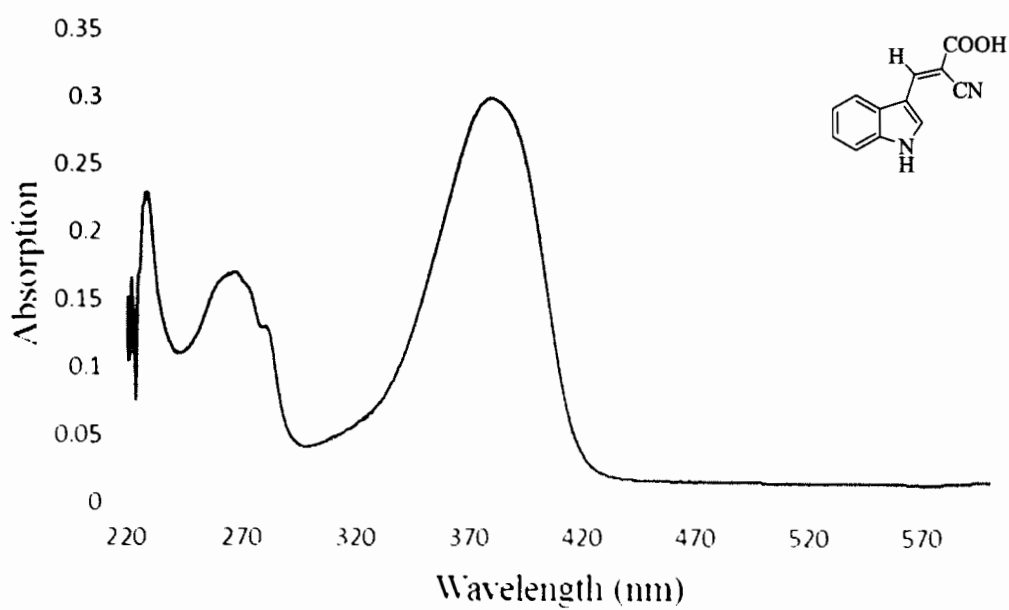


Figure A.30 UV-Vis absorption spectra of In3 in DCM at 1×10^{-5} M.

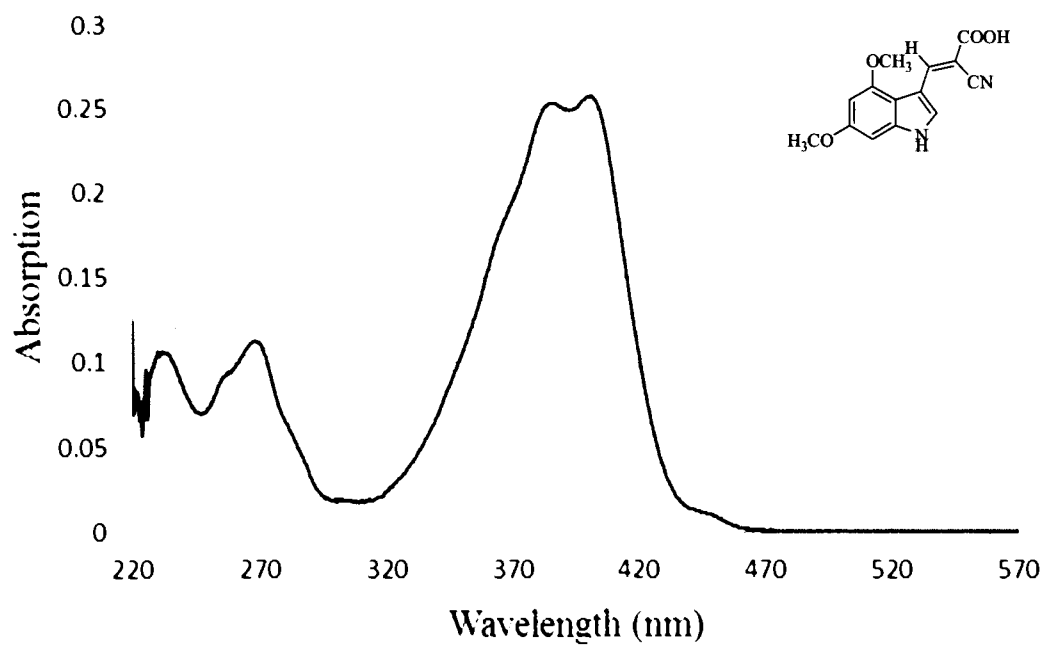


Figure A.31 UV-Vis absorption spectra of In4 in DCM at 5×10^{-6} M.

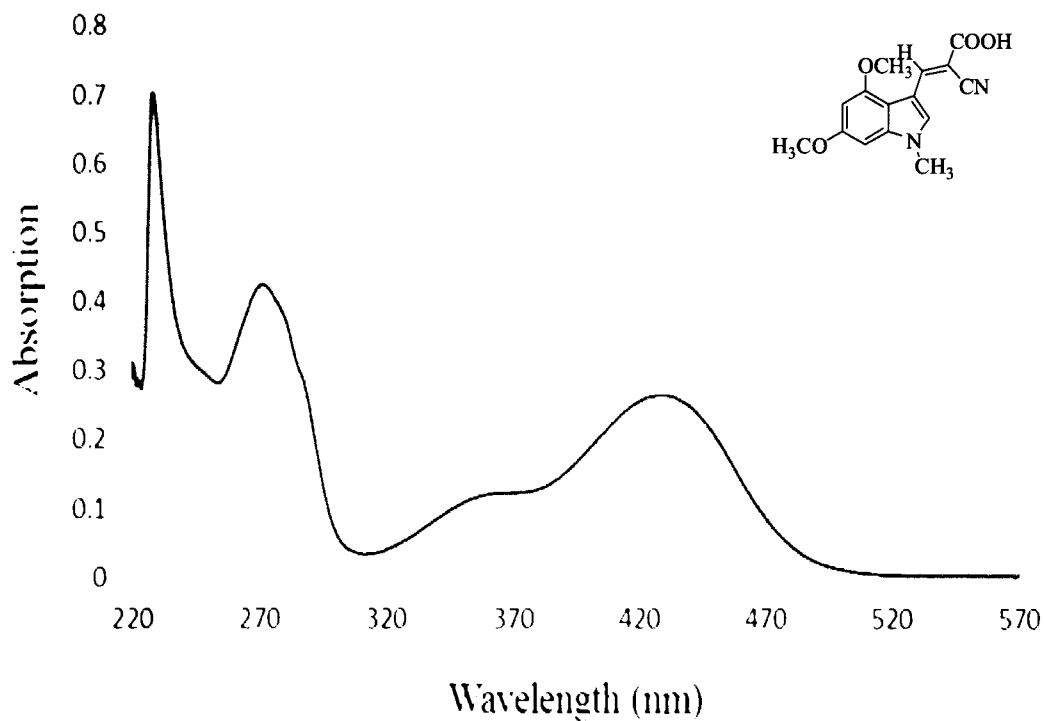


Figure A.32 UV-Vis absorption spectra of In5 in DCM at 5×10^{-6} M.

APPENDICES B

Publication



ประชุมวิชาการ มอบ. วิจัย ครั้งที่ 8

17 - 18 กรกฎาคม 2557

อาคารเทพรัตนสิริปภา มหาวิทยาลัยอุบลราชธานี

การสังเคราะห์และพิสูจน์เอกลักษณ์ของอนุพันธ์คาร์บาโซลเพื่อเป็นสารเรืองแสงสีน้ำเงิน
สำหรับอุปกรณ์ไดโอดเรืองแสงสารอินทรีย์

Synthesis And Characterization Of Carbazole Derivatives
As Blue Light-Emitters For Organic Light Emitting Diodes (OLEDs)

Thitima Siriroem¹, Tinnagon Keawin¹ and Vinich Promarak^{2*}

¹Center for Organic Electronics and Alternative Energy, Department of Chemistry and
Center of Excellence for Innovation in Chemistry, Faculty of Science,
Ubon Ratchathani University, Ubon Ratchathani, Thailand

²School of Chemistry and Center of Excellence for Innovation in Chemistry,
Institute of Science, Suranaree University of Technology, Nakhon Ratchasima, Thailand

*E-mail: t-mp_1989@hotmail.com

บทคัดย่อ

อนุพันธ์คาร์บาโซลที่มีหมู่ปิดท้ายด้วยโมเลกุลของไพรีนและแอนทราซีนถูกสังเคราะห์ขึ้นโดยใช้ปฏิกิริยาโบรมิเนชัน และปฏิกิริยา Suzuki cross-coupling และพิสูจน์เอกลักษณ์ด้วยเทคนิค ¹H NMR, UV-Vis, Fluorescence spectroscopy และ เทคนิค cyclic voltammetry โดย 9-Dodecyl-3,6-di(pyren-1-yl)carbazole (CP2) และ 9-Dodecyl-3,6-di (anthracen-1-yl) carbazole (CA2) ให้สเปกตรัมการคายแสงในช่วงสีน้ำเงินเข้มที่ 430 และ 442 nm และมีความเสถียรทางไฟฟ้าที่สูง สารเหล่านี้จึงน่าจะเป็นอีกทางเลือกหนึ่งสำหรับใช้เป็นสารเรืองแสงสีน้ำเงินในไดโอดเรืองแสงอินทรีย์

คำสำคัญ : คาร์บาโซล ไดโอดเรืองแสงที่มีชั้นสารเรืองแสงเป็นสารอินทรีย์ ปฏิกิริยา Suzuki cross-coupling

Abstract

Carbazole derivatives containing pyrene and anthracene substituents were synthesized using bromination and Suzuki cross-coupling reactions, and their chemical structure were characterized by ¹H NMR, UV-Vis, fluorescence spectroscopy and cyclic voltammetry. Compound 9-dodecyl-3,6-di (pyren-1-yl)carbazole (CP2) and 9-dodecyl-3,6-di (anthracen-1-yl)carbazole (CA2) showed the PL spectra in deep blue region at 430 and 442 nm and exhibited high electrochemical stability. These compounds could be alternative materials as blue light-emitters in organic light emitting diodes.

Keywords: Carbazole, Organic light-emitting diodes, Suzuki cross-coupling reaction

Introduction

Initially proposed by Ching W. Tang in 1987¹, organic light-emitting diodes (OLEDs) have attracted significant attention from the scientific community due to their potential for future flat-panel displays and lighting applications.² Today, the developments of OLED technologies mainly focus on the optimization of device structures and on developing new emitting materials. Clearly, new materials emitting pure colors

of red, green, and blue (RGB) with excellent emission efficiency and high stability, are the key point of OLED development for full-color flat displays. The performance of blue OLEDs is usually inferior to that of green and red OLEDs due to poor carrier injection into the emitters³ and electroluminescent (EL) properties of the blue OLEDs need to be improved. Therefore, one area of continuing research in this field is the pursuit of a stable-blue emitting material.⁴ Although many fluorescent blue emitters have been reported such as pyrene derivatives,⁵ carbazole derivatives,⁶ anthracene derivatives,⁷ fluorene derivatives, and aromatic hydrocarbon,⁹ there is still a clear need for further developments in terms of efficiency and color purity compared to red and green emitters.

Therefore, in this work, we reported the synthetic route and properties of 9-dodecyl-3,6-di(pyren-1-yl)carbazole (CP2) and 9-dodecyl-3,6-di(anthracen-1-yl)carbazole (CA2) (end-capped carbazole with pyrene and anthracene groups, respectively as solution processed blue emitters for OLEDs.

Objective

To synthesize and characterize the pyrene and anthracene-substituted carbazole derivatives as blue emitting materials for OLEDs.

Methodology and Experimental

1. General procedures

¹H NMR spectra were recorded on Bruker AVANCE (300 MHz) spectrometer. Chemical shifts (δ) are reported relative to the residual solvent peak in part per million (ppm). Coupling constants (J) are given in Hertz (Hz). UV-Visible spectra were recorded in CH₂Cl₂ on a Perkin-Elmer UV Lambda 25 spectrometer. Fluorescence spectra were recorded in CH₂Cl₂ on a Perkin-Elmer L S 50B Luminescence spectrometer. Analytical thin-layer chromatography (TLC) was performed with Merck aluminium plates coated with silica gel 60 F₂₅₄. Column chromatography was carried out using gravity feed chromatography Merck silica gel mesh, 60 Å. Solvent mixture were used and the portions are given by volume.

2. Synthetic procedures

2.1 Synthesis of 9-dodecylcarbazole (2)

To a solution of carbazole (10.0000 g, 59.80 mmol) in DMF (93 mL) was added NaH (2.1500 g, 89.58 mmol). Then, 1-Bromododecane (15.0000 g, 89.70 mmol) was added. The reaction mixture was stirred at 0°C-rt for 20 h. Water (100 mL) was added and the mixture was extracted with ethyl acetate (50 mL x 3). The combined organic phases were washed with a diluted HCl solution (50 mL x 2), water (100 mL), and brine (50 mL), dried over anhydrous Na₂SO₄, evaporated and purified by column chromatography to give a pale yellow viscous oil (25.3776 g, 97%); ¹H NMR (300 MHz, CDCl₃): δ 8.09 (2H, d, J = 2.4 Hz), 7.44 (4H, m), 7.25 (2H, d, J = 2.4 Hz), 4.3 (2H, t, J = 2.1 Hz), 1.88 (2H, t, J = 2.1 Hz), 1.33 (18H, m) and 0.89 (3H, t, J = 2.1 Hz)

2.2 Synthesis of 3,6-dibromo-9-dodecylcarbazole(3)

In the round bottom flask, covered with aluminum foil, a stirred solution of 9-dodecylcarbazole (2) (0.0700 g, 0.16 mmol) in THF (15 mL) was added NBS (0.0400 g, 0.19 mmol) in small portions. The reaction mixture was poured into ice-cold water. The mixture was allowed to warm to room temperature overnight. The mixture was extracted with methylene chloride (20 mL x 3), washed with water (20 mL x 3), dried over anhydrous Na_2SO_4 , evaporated and purified by column chromatography to give a white pearl solid (0.0719 g, 91%); $^1\text{H NMR}$ (300 MHz, CDCl_3) δ 8.15 (2H, d, $J = 1.5$ Hz), 7.56 (2H, dd, $J_1 = 0.9$ Hz, $J_2 = 0.6$ Hz), 7.26 (2H, d, $J = 0.9$ Hz), 4.24 (2H, t, $J = 0.9$ Hz), 1.82 (2H, t, $J = 0.9$ Hz), 1.43 (18H, m), 0.87 (3H, t, $J = 2.1$ Hz)

2.3 Synthesis of 9-dodecyl-3,6-di(pyren-1-yl)carbazole (CP2)

To a stirred solution of 3,6-dibromo-9-dodecyl carbazole (3) (0.4000 g, 0.81 mmol) and $\text{Pd}(\text{PPh}_3)_4$ (0.0400 g, 0.04 mmol) in tetrahydrofuran (30mL) was added pyrene-1-boronic acid (0.41g, 1.70mmol), and an aqueous Na_2CO_3 solution (0.8500 g, 8.10 mmol). The mixture was refluxed for 48 h. After cooling, the mixture was extracted with dichloromethane (30 mL x 3), washed with water(30mL x 3), dried over anhydrous, evaporated and purified by column chromatography to give a white pearl solids (0.3195 g, 53%); $^1\text{H NMR}$ (300 MHz, CDCl_3) δ 8.41 (2H, s), 8.34 (2H, d, $J = 9.30$ Hz), 8.25 (2H, d, $J = 7.80$ Hz), 8.20-8.10 (10H, m), 8.06-7.97 (4H, m), 7.80 (2H, d, $J = 8.4$ Hz), 7.64 (2H, d, $J = 7.64$ Hz), 4.47 (2H, t, $J = 7.2$ Hz), 1.10 (2H, t, $J = 6.9$ Hz), 1.57-1.30 (18H, m) and 0.91 (3H, t, $J = 6.9$ Hz)

2.4 Synthesis of 9-dodecyl-3,6-di(anthracen-1-yl)carbazole (CA2)

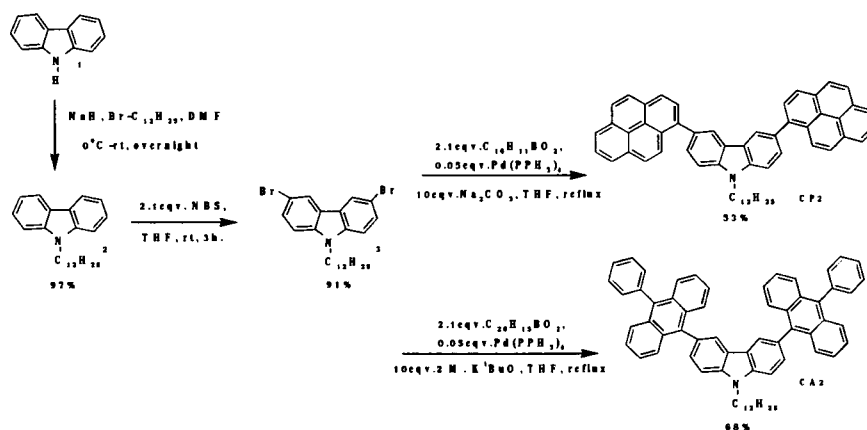
To a stirred solution of 3,6-dibromo-9-dodecyl carbazole (3) (0.2500g, 0.42 mmol) and $\text{Pd}(\text{PPh}_3)_4$ (0.02g, 0.05 mmol) in tetrahydrofuran (25 mL) were added 10-phenyl-9 anthraceneboronic acid (0.26g, 0.89 mmol), and an aqueous $^t\text{BuOK}$ solution (0.47 g, 4.26 mmol). The mixture was refluxed for 48 h. After cooling, the mixture was extracted with dichloromethane (30 mL x 3), washed with water (30mL x 3), dried over anhydrous, evaporated and purified by column chromatography to give a white pearl solids (0.2440 g, 68%); $^1\text{H NMR}$ (300 MHz, CDCl_3) δ 8.18 (2H, s), 7.83-7.80 (5H, m), 7.74-7.68 (7H, m), 7.63-7.50 (12H, m), 7.32-7.26 (12H, m), 4.56 (2H, t, $J = 6.9$ Hz), 2.15 (2H, t, $J = 7.5$ Hz), 1.57-1.28 (18H, m) and 0.86 (3H, t, $J = 6.3$ Hz)

Results and Discussion

1. Synthesis of CP2 and CA2

The target molecules CP2 and CA2 were successfully synthesized as shown in scheme 1. The 9-dodecylcarbazole was first synthesized by nucleophilic substitution reaction at the 9-position of carbazole (1) with 1-bromododecane. Then, selective bromination of compound 2 at 3 at the 6-position with NBS in THF afforded compound 3 in 91% yields. The target molecule CP2, dipyrene substituted carbazole, was synthesized by Suzuki cross coupling of 3 with pyrene-1-boronic acid using $\text{Pd}(\text{PPh}_3)_4$ as catalyst and Na_2CO_3 as base in THF at reflux for 48 h. Dianthracene substituted carbazole (CA2) was

synthesized by Suzuki cross coupling reaction of **3** and 10-phenyl-9-anthraceneboronic acid with $\text{Pd}(\text{PPh}_3)_4$ as a catalyst and $t\text{BuOK}$ as a base in THF at reflux for 48 h. (Scheme 1.) All compounds were characterized by ^1H NMR analysis. The data are presented in the experimental section.



Scheme 1. Synthesis of carbazole derivatives

2. Optical properties

The spectroscopic properties of CP2 and CA2 were measured in dichloromethane (CH_2Cl_2) as shown in Figure 1. The solution absorption spectra exhibited two major absorption bands. The first absorption bands at around 200-275 nm could be attributed to the $\pi\text{-}\pi^*$ transition of the carbazole moieties and the second absorption bands at longer wavelength around 350-400 nm corresponded to the $\pi\text{-}\pi^*$ transition of the carbazole-pyrene and carbazole-anthracene cores. These compounds in solution fluoresced in the blue region (430-442 nm) with featureless photoluminescence (PL) spectra. The emission spectra displayed maxima at 430 and 442 nm, for CP2 and CA2, respectively. From the substituted dipylene CP2 to substituted anthracene CA2, the PL spectra also showed red-shifted absorption and in PL spectra, concomitant with the increasing conjugation length (Figure 1).

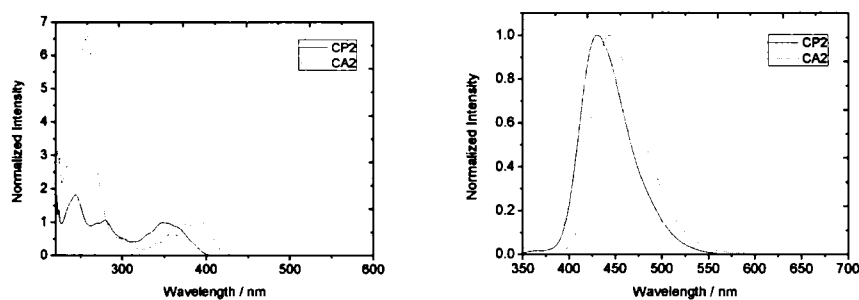


Figure 1. Normalized absorption spectra (left) and normalized emission spectra (right) of CP2 and CA2 in CH_2Cl_2

3. Electrochemical properties

Electrochemical behaviors of CP2 and CA2 were investigated by cyclic voltammetry (CV), and the results were shown in Figure 2. Multiple cyclic voltammetry (CV) scans of CA2 revealed identical cyclic voltammograms with no additional peak at lower potentials on the cathodic scan (E_{pc}). This suggested no electrochemical coupling at either the carbazole or anthracene peripheries, indicating electrochemically stable molecules.

The CV curve of CP2 showed three irreversible oxidation processes. The first oxidation is assigned to the removal of electrons from the carbazole moiety resulting in carbazole radical cations ($CBZ^{\cdot+}$). In the case of CP2, during additional peaks at lower potentials were observed during the cathodic scan indicating electrochemical coupling reactions of the radical cations. The generated $CBZ^{\cdot+}$ is stabilized by electron delocalization through 1,8-substituted electron rich pyrene rings to form a pyrene radical cation ($Py^{\cdot+}$) which is relatively less stable compared with the $CBZ^{\cdot+}$. The $Py^{\cdot+}$ readily undergoes a radical-radical dimerization coupling to form a stable neutral pyrene dimer as indicated by the presence of the cathodic peaks (E_{pc}) around 0.61–0.94 V in their first CV scan and an increasing change in the CV curves under the repeated CV scans (Figure 2).¹⁰ This might be the first example of pyrene derivatives that undertook an electrochemical oxidation coupling reaction. The HOMO energy levels were estimated to be -5.41 and -5.45 eV, respectively (Table 1).

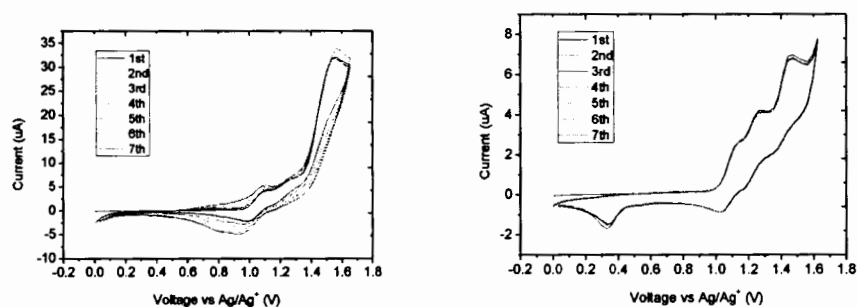


Figure 2. Cyclic voltammograms of CP2 (left) and CA2 (right) in dry CH_2Cl_2 with scan rate of 0.05 V/s and 0.1 M $n-Bu_4NPF_6$ as electrolyte

Table 1 Physical data of CP2 and CA2

Compound	$\lambda_{obs}(\log \epsilon)^a(\text{nm M}^{-1}\text{cm}^{-1})$	$\lambda_{em}^a(\text{nm})$	E_g^b (eV)	HOMO ^c (eV)	LUMO ^d (eV)
CP2	279 (5.37), 348 (2.35)	430	3.10	-5.41	-2.31
CA2	305 (3.93), 359 (4.09), 377 (4.24), 397 (4.23)	442	2.95	-5.45	-2.50

^aMeasured in dilute CH_2Cl_2

^b Calculated from the absorption edge, $E_g = 1240/\lambda_{onset}$

^cEstimated from HOMO = $-(4.44 + E_{onset}^{ox})$

^dEstimated from LUMO = HOMO + E_g

3. HOMO and LUMO frontier orbitals

To gain insights into the geometrical and electronic properties of these multiple substituted carbazoles, quantum chemical calculations were performed using the DFT/B3LYP/6-31G(d,p) method. The optimized structures of CP2 and CA2 revealed that the attached pyrene and anthracene units twisted out of the plane of the carbazole forming bulky substituents around the carbazole. This would facilitate the formation of amorphous morphology. In all cases for CP2 and CA2, π -electrons in the HOMO orbitals delocalized only over the carbazole and two substituents at the 3,6-positions substituted carbazole backbone, whereas after light irradiation (LUMO), the excited electrons were delocalized largely over the pyrene and anthracene plane.

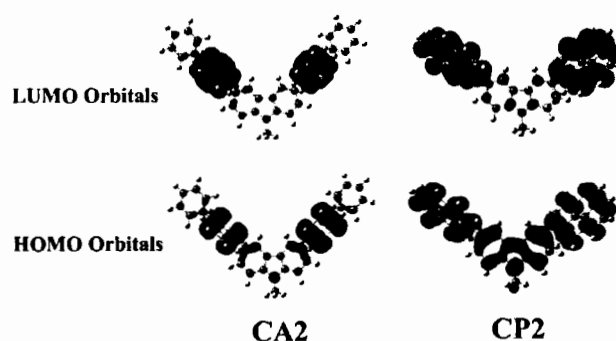


Figure 3. The HOMO (bottom) and LUMO (top) orbitals of CP2 and CA2 calculated by DFT/B3LYP/6-31G(d,p) method.

Conclusion

In conclusion, we have successfully synthesized pyrene and anthracene-substituted carbazole (CP2, CA2) by the Suzuki-cross coupling reaction of dibromo intermediates with pyrene-1-boronic acid and 10-phenyl-9-anthraceneboronic acid, respectively. The electronic and electrochemical properties of both compounds could be tuned by varying the substituents on carbazole ring. The substitution of dipyrrene CP2 by substituted anthracene in CA2 increased the conjugation length of compounds resulting in a red-shift and broad in absorption spectra. These compounds emitted blue light with high thermal stability, which is potentially useful for applications in electroluminescent devices. Optimize structures and electron density of HOMO and LUMO have been performed by DFT/B3LYP/6-31G(d,p) method.

Acknowledgement

This work was supported by Center of Excellence for Innovation in Chemistry (PERCH-CIC), and Faculty of science, UbonRatchathani University.

References:

- [1] C.W. Tang and S. A. VanSlyke, *Appl. Phys. Lett.*, 1987, 51, 913.

- [2] (a) C.-C. Wu, C.-W.Chen, C.-L.Lin and C.-J. Yang, *J. Disp. Technol.*, **2005**, 1, 248; (b) B. Geffroy, P. le Roy and C. Prat, *Polym. Int.*, **2006**, 55, 572; (c) F.So, J. Kido and P. L. Burrows, *MRS Bull.*, **2008**, 33, 663.
- [3] A. W. Grice, D. D. C. Bradley, M. T. Bernius, M. Inbasekaran, W. W. Wu and E. P. Woo, *Appl. Phys. Lett.*, **1998**, 73, 629.
- [4] (a) A. M. Thangthong, N. Prachumrak, S. Namuangruk, S. Jungsuttiwong, T. Keawin, T. Sudyoadsuk and V. Promarak, *Eur. J. Org. Chem.*, **2012**, 5263; (b) Q.-X. Tong, S.-L. Lai, M.-Y. Chan, Y.-C. Zhou, H.-L. Kwong, C.-S. Lee and S.-T. Lee, *Chem. Mater.*, **2008**, 20, 6310.
- [5] (a) T. Kumchoo, V. Promarak, T. Sudyoadsuk, M. Sukwattanasinitt and P. Rashatasakhon, *Chem.-Asian J.*, **2010**, 5, 2162; (b) T. M. Figueira-Duarte and K. Mllen, *Chem. Rev.*, **2011**, 111, 7260.
- [6] (a) Z. Yang, Z. Chi, L. Zhou, X. Zhang, M. Chen, B. Xu, C. Wang, Y. Zhang and J. Xu, *Opt. Mater.*, **2009**, 32, 398; (b) N. Agarwal, P. K. Nayak, F. Ali, M. P. Patankar, K. L. Narasimhan and N. Periasamy, *Synth. Met.*, **2011**, 161, 466.
- [7] (a) K.-R. Wee, W.-S. Han, J. -E. Kim, A.-L. Kim, S. Kwon and S. O. Kang, *J. Mater. Chem.*, **2011**, 21, 1115; (b) P.-I. Shih, C.-Y. Chuang, C.-H. Chien, E. W.-G. Diao and C.-F. Shu, *Adv. Funct. Mater.*, **2007**, 17, 3141; (c) S. Tao, Y. Zhou, C.-S. Lee, S.-T. Lee, D. Huang and X. Zhang, *J. Phys. Chem. C*, **2008**, 112, 14603; (d) G. Zhang, G. Yang, S. Wang, Q. Chen and J. S. Ma, *Chem.-Eur. J.*, **2007**, 13, 3630.
- [8] (a) A. L. Fischer, K. E. Linton, K. T. Kamtekar, C. Pearson, M. R. Bryce and M. C. Petty, *Chem. Mater.*, **2011**, 23, 1640; (b) M. C. Gather, M. Heeney, W. Zhang, K. S. Whitehead, D. D. C. Bradley, I. McCulloch and A. J. Campbell, *Chem. Commun.*, **2008**, 1079; (c) Y.-M. Jeon, J.-W. Kim, C.-W. Lee and M.-S. Gong, *Dyes Pigm.*, **2009**, 83, 66.
- [9] (a) T. Qin, W. Wiedemair, S. Nau, R. Trattnig, S. Sax, S. Winkler, A. Vollmer, N. Koch, M. Baumgarten, E. J. W. List and K. Mllen, *J. Am. Chem. Soc.*, **2011**, 133, 1301; (b) F. Liu, L.-H. Xie, C. Tang, J. Liang, Q.-Q. Chen, B. Peng, W. Wei, Y. Cao and W. Huang, *Org. Lett.*, **2009**, 11, 3850.
- [10] P. Kotchapradist, N. Prachumrak, R. Tarsang, S. Jungsuttiwong, T. Keawin, T. Sudyoadsuk and V. Promarak, *J. Mater. Chem. C.*, **2013**, 1, 4916-4924.

VITAE

- NAME** Miss.Thitima Siroem
- BORN** 16 January 1989, Ubon Ratchathani, Thailand
- EDUCATION** B. Sc. (Chemistry) Department of Chemistry, Faculty of Science,
Ubon Ratchathani University,
Ubon Ratchathani, Thailand, 2007-2010.
M. Sc. (Chemistry), Department of Chemistry, Faculty of
Science, Ubon Ratchathani University,
Ubon Ratchathani, Thailand, 2011-2015.
- SCHOLARSHIPS** Research Price from Center of Excellence for Innovation in
Chemistry, Office of the Higher Education Commission, Ministry
of Education: Postgraduate Education and Research Program in
Chemistry (PERCH-CIC), 2011-2012.

